NASA TECHNICAL MEMORANDUM

NASA TM X-73507
Volume I

NASA TM X-73507
Volume I

(NASA-TM-73507-Vol-1) EFFECT OF AIR TEMPERATURE AND RELATIVE HUMIDITY AT VARIOUS FUEL-AIR RATIOS ON EXHAUST EMISSIONS ON A PER-MODE BASIS OF AN AVCO LYCOMING 0-320 DIAD LIGHT AIRCRAFT ENGINE: VOLUME 1: G3/07

N78-29100

Unclas
27212

EFFECT OF AIR TEMPERATURE AND RELATIVE HUMIDITY AT VARIOUS FUEL-AIR RATIOS ON EXHAUST EMISSIONS ON A PER-MODE BASIS OF AN AVCO LYCOMING 0-320 DIAD LIGHT AIRCRAFT ENGINE

VOLUME I - RESULTS AND PLOTTED DATA

by Michael Skorobatckyi, Donald V. Cosgrove,
Phillip R. Meng and Erwin E. Kempke, Jr.
Lewis Research Center
Cleveland, Ohio 44135

July 1978

EFFECT OF AIR TEMPERATURE AND RELATIVE HUMIDITY AT VARIOUS FUEL-AIR RATIOS ON EXHAUST EMISSIONS ON A PER-MODE BASIS OF AN AVCO LYCOMING 0-320 DIAD LIGHT AIRCRAFT ENGINE

VOLUME I - RESULTS AND PLOTTED DATA

by Michael Skorobatckyi, Donald V. Cosgrove, Phillip R. Meng, and Erwin E. Kempke, Jr.

E-8916-2

SUMMARY

A carbureted four-cylinder air-cooled 0-320 DIAD Lycoming aircraft engine was tested to establish the effects of ambient air temperature and relative humidity at various fuel-air ratios on exhaust emissions on a per-mode basis (idle, taxi, takeoff, climb, and approach). The test conditions included carburetor leanout for each of the five modes, air temperatures of 50, 59, 80 and 100°F and relative humidities of 0, 30, 60, and 80%. Combinations of these parameters resulted in over 800 different test conditions.

Fuel-air ratio (calculated on the dry basis) showed the strongest single influence on CO, HC and NO_x exhaust emissions. The results agree well with known general characteristics of spark ignition piston engines operating over the same range of fuel-air ratio. Ambient conditions influence emissions in two ways. Change in air temperature and/or humidity induces a change in fuel-air ratio due to the variation of air density and displacement of air by water vapor. This results in a dependent change in emissions. In addition, for a constant fuel-air ratio, hot/humid ambient air conditions had a significant further influence on the HC and NO_x emissions due to chemical effects on the combustion process. At a rich fuel-air ratio and higher air temperature and relative humidity, the HC emissions increased by as much as 130% in the lower power modes and the NO_x emissions decreased by as much as 90% in the higher power modes; whereas the CO emissions were essentially independent of ambient conditions. For any fixed fuel-air ratio and zero humidity, higher air temperature had virtually no effect on CO, HC and NO_x emissions in any of the test modes, except for the 20% increase in CO emissions in climb.

The report is presented in two volumes. Volume I (herein) contains the results, plotted data, and microfiche film of the data taken at each of the individual test points. Volume II contains a compilation of the data taken at each of the individual test points. Volume II is included on microfilm at the back of this volume.

INTRODUCTION

NASA is involved in a research and technology program aimed at improving general aviation engines. One major objective of the program is to establish and demonstrate the technology which will safely reduce general-aviation piston-engine exhaust emissions to levels consistent with the EPA 1979 emissions standards.

One element of the above program was a joint FAA/NASA General Aviation Piston Engine Emissions Reduction effort. Funded studies have been completed by the two primary engine firms building general aviation piston engines: Avco-Lycoming and Teledyne-Continental. Each contractor tested five different engine models to experimentally characterize emissions and to determine the effects of variation in fuel-air ratio and spark timing on emissions levels and other operating characteristics such as cooling, misfiring, roughness, power, acceleration, etc. The FAA used its NAFEC facility to perform independent checks on each of the engines the contractors tested. It was recognized early in the program that the tests would be conducted under essentially uncontrolled induction air conditions at widely different geographical locations and that a better understanding of temperature and humidity effects would enhance the ability to make a correlation and better comparison of these data. It was also recognized that such understanding would be extremely useful in future emissions compliance testing. Therefore, NASA-Lewis Research Center has undertaken a series of aircraft engine tests to develop such a correlation. Two engines, models identical to ones in the FAA/NASA program, were selected for testing. The engines were: (1) Lycoming model 0-320 DIAD 4-cylinder, naturally-aspirated carbureted engine; and (2) a Teledyne Continental Model TSIO-360-C, a 6-cylinder turbocharged, fuel injected engine.

The exhaust emissions for the Lycoming 0-320 engine over the EPA emissions test cycle for a range of test conditions were reported in Reference 1. A summary of these baseline cycle test results can be best described by comparing the temperature and humidity results at 100°F and 80 percent humidity with those at 50°F and no humidity, and which shows that with the increased temperature and humidity, CO emissions increased by a factor of 1.6, HC emissions increased by a factor of 2.2, and NO_x emissions decreased by a factor of 3.5. Present-day aircraft engines do not use a tempertaure-density compensated fuel system. Hence, the cited changes in the exhaust emissions are primarily the result of richer-fuel-air ratios, which occur at the higher air temperatures and humidities.

Ambient conditions can also effect the induction vaporization and basic combustion process, thereby influencing the emissions. Therefore, a series of tests were performed to establish these direct effects for different engine operating conditions (load and fuel/air ratio) and ambient conditions. The results are reported herein. This report is printed in two volumes: Volume I contains the plotted test results and microfiche copies of all of the individual test points. Volume II contains the individual data test points in tabular form.

APPARATUS AND PROCEDURE

Test Facility

The aircraft engine is shown schematically in Figure 1 and photographically on the test stand in Figure 2. The engine was coupled to a 300 hp dynamometer through a fluid coupling in the drive shaft which was located under a safety shield. Engine cooling and induction air were both supplied by a laboratory air distribution system. The cooling and induction air system, as shown in Figure 3, can be controlled to deliver air to the engine over a temperature range of from 50° to 120° F and over a range of relative humidity from 0 to 80 percent. The cooling air was always at the same conditions as the induction air and was directed down over the engine by an air distribution hood. This hood was the same as that which was used by the engine manufacturer in their engine testing. The engine cooling air was removed from the test cell by a high capacity exhaust system which had the inlet located beneath the engine. An additional cell exhaust fan was used to maintain a slightly negative pressure in the test cell. This was done to vent off any combustible or toxic gases which may have been present in the test cell during engine operation.

The engine exhaust was manifolded together in a standard configuration with the emission sample probe located downstream of the manifold. The exhaust was then ducted out of the cell through the roof as shown in Figure 2. Care was taken to insure that the exhaust system was leak-proof. A leak-proof system was necessary to prevent air dilution of the gas sample which would result in erroneous emission measurements.

Engine Description. The 0-320 DIAD is a horizontally opposed, four cylinder, direct drive, air-cooled engine. The engine has a bore of 5.125 inches and a stroke of 3.875 inches with the resulting total piston displacement being 319.8 cubic inches. The compression ratio is 8.50:1. The engine is rated 160 bhp at 2700 rpm and 0.51 BSFC. Fuel metering is performed by a Marvel-Schebler MA4SPA carburetor using grade 100/130 aviation gasoline. A carburetor intake air box was used to insure uniform pressure distribution across the throat. The carburetor was calibrated for full-rich operation at the factory, typical of what might be expected as the rich limit of production engines. The carburetor, at this calibration, constituted the baseline for the engine. The fuel used was standardized reference fuel conforming to the requirements of the ASTM Committee on Aviation Reference Fuels and Certification. Ignition was supplied by a dual Bendix magneto timed to 25° BTDC. The engine is further described in AVCO Lycoming Specification 2283-C (Ref. 2).

Engine Exhaust System. There are two major areas of consideration that can affect the accuracy of emission measurements. These are the leak tightness of the engine exhaust system and the handling of the exhaust gas sample through the gas analyzer.

In order to obtain a representative exhaust gas sample for emissions analysis the individual cylinder exhaust tubes were brought together under the engine to a common header. Allowing for proper mixing, the gas sample probe was located approximately 5 ft.

downstream in the common header. Great care was taken in the design, fabrication and installation of the exhaust system so that it would not leak air into the exhaust gas upstream of the gas sample probe. It was found that the combination of exhaust gas temperature and engine vibration necessitated a number of changes in the exhaust system before an acceptable leak proof system was obtained.

Exhaust Gas Sample Handling. The criteria for exhaust gas analysis were twofold. The sample had to be representative of a complete mixing from all cylinders and the temperature of the gas sample at the analyzer had to be at least 300°F. The sample line from the exhaust gas manifold to the gas analyzer was heated to 300°F using an electrical tape type heater. The Scott analyzer (See Fig. 4) contained the following five analysis meters:

1. Beckman Model 864 Infrared CO Analyzer
2. Beckman Model 864 Infrared CO_2 Analyzer
3. Scott Model 125 Chemiluminescent NO/NO_x Analyzer. The Scott NO/NO_x Analyzer was modified at NASA-Lewis as discussed in reference 3.
4. Scott Model 415 Flame Ionization Detector for HC
5. Scott Model 250 Paramagnetic O_2 Detector.

Careful daily monitoring of these sen[illegible]e instruments indicated a need for frequent adjustments. It was [illegible]essary to zero and span calibrate these instruments with known gases at least once for each hour of operation. A complete console calibration was carried out at least once a month.

Instrumentation The engine instrumentation and contro[illegible] panel is shown in figure 5. The major measured parameters and estimated system accuracies for this investigation are listed below:

Parameter	Instrumentation	Accuracy
Fuel Flow	Hydraulic Wheatstone Bridge Flow Meter	$\pm$ 0.5%
Induction Air Flow	Turbine-type Flow Meter	$\pm$ 0.6%
Induction Air Press.	Absolute Transducer	$\pm$ 0.50%
Cooling Air Flow	Orifice ΔP Transducer	$\pm$ 1.5%
Cooling Air Press.	Absolute Transducer	$\pm$ 0.50%
Dew Point	Temp. Controlled Mirrored Photoelectric Sensor	$\pm$ 0.7°F
Engine Torque	Shaft Mounted Rotary Transformer Type	$\pm$ 0.5%
Dyno. Torque	Load Cell	$\pm$ 0.5%
Speed	Magnetic Pickup	$\pm$ 0.25%
Exh. Gas Temp.	Chrome-Alumel Thermocouple	$\pm$ 0.5%
Cyl. Hd. Temp.	Iron Constantan Thermocouple	$\pm$ 0.5%

All instrumentation was connected to the "CADDE" (Central Automatic Digital Data Encoder) Central Data Acquisition System and the data processed on an IBM 360/67 time-sharing computer.

TEST PROCEDURE

The engine leanout tests at various temperatures and relative humidities were conducted for the modes shown below:

Mode	Mode Description	Power Level	Speed	Time in Mode
1	Idle-Out	-----	600	1.0 min.
2	Taxi-Out	-----	1200	11.0 min.
3	Takeoff	(Full Power) 100%	2700	0.3 min.
4	Climb	80%	2430	5.0 min.
5	Approach	40%	2350	6.0 min.
6	Taxi-In	-----	1200	3.0 min.
7	Idle-In	-----	600	1.0 min.

These modes were divided into two distinct test operations. Takeoff, climb, and approach modes were run separately from the idle and taxi modes. In the takeoff, climb, and approach modes, cooling air flow was supplied across the engine at a differential pressure of three inches of water (approximately 2100 CFM). Approach and climb mode tests were run at a constant engine power over the matrix of variables. Takeoff mode tests were conducted at "wide-open throttle" position and consequently the engine power did vary at the various temperature, humidity and fuel-air ratio test conditions. Fuel flow to the engine was varied by adjusting the carburetor mixture control during these three modes.

The idle and taxi modes were conducted with no cooling air flow over the engine. During these two modes, the fuel-air ratio was varied by manually adjusting the "idle mixture screw" on the carburetor. Idle out, taxi out, taxi in, and idle-in were run sequentially at one setting of the carburetor "idle mixture screw". If abnormally rough operation appeared due to prolonged low power operation, the engine speed was increased to 2000 rpm at 150 ft-lbs torque for "clearing".

Emissions data was not recorded, in any of the modes, until the desired temperature and relative humidity was established in the induction and cooling air system and the engine achieved a stabilized operating condition for that mode.

Data Reduction

The LeRC emissions data reduction procedures are as specified by the EPA in the Federal Register (ref. 4). Shown in figure 6 is the flow diagram outlining the data reduction process. Some of the intermediate steps used in the raw emissions data reduction which are not explicitly defined in the Federal Register are summarized below and presented in Appendix A.

Five exhaust products are measured by the emissions analyzer. HC and NO_x are measured on a "wet" basis. The other three, CO, CO_2 and O_2, are measured on a "dry" basis and as a result their

volumetric percentages must be corrected for the water removal. The water correction factor (K_W) used for this conversion is defined as:

$$K_W = 1 - (H_2O)$$

where H_2O represents the total water vapor contained in the products of combustion. The water correction factor is based on a chemical reaction including water vapor, oxygen and carbon balance, measured fuel-air ratio and water-dry air mass ratio. This factor as used was obtained from Teledyne Continental Motors and is included in appendix A.

The Federal Register (ref. 4) states that the total engine exhaust volume flow rate is to be used in the computation of the pollutant emission rate. Appendix A contains the procedure used in obtaining the exhaust volume flow rate. Primarily, it is based on the total intake mass flow rate and the exhaust gas density. The exhaust gas density is calculated from the exhaust molecular weight, air molecular weight and air density at 68°F and 760 mm Hg pressure. The pollutant emission rate and mass per mode is then calculated per the Federal Register (ref. 4).

The time in mode value used in this calculation (lbs/mode emission rate) was stated in the test procedures. The idle out and idle-in emissions were plotted as separate points on the same plots after the calculated emissions values of lbs/mode for both idles were multiplied by a factor of two to normalize them to two minutes. The two minutes represents the total idle time of the emission test cycle. The taxi-out and taxi-in emissions values of lbs/mode for both taxis were normalized to fourteen minutes. The fourteen minutes represents the total taxi time of the emission test cycle. The remaining three modes takeoff, climb, and approach were plotted as calculated (per the Federal Register, ref. 4).

To verify the exhaust gas products concentrations, the Spindt procedure (ref. 5) was used. In this procedure, the fuel-air ratio is based on the measured exhaust gas products. This calculated fuel-air ratio, as presented in appendix A, is then compared to the measured fuel-air ratio. The percent difference between the measured to calculated is defined as:

$$\text{Percent Difference} = \frac{\text{Calculated fuel-air ratio} - \text{Measured fuel-air ra}}{\text{Measured fuel-air ratio}}$$

DATA AND RESULTS

As mentioned previously, higher air temperature and humidities affect emissions in two ways; (1) indirectly, by increasing the fuel-air ratio, (2) directly, by modifying the combustion process. The tests described herein were performed to establish the latter effort.

The leanout emissions data were taken for the following values of temperature and relative humidity:

Air temperature, °F: 50, 59, 80, 100
Relative humidity, %: 0, 30, 60, 80

Combinations of the above temperatures and humidities at various fuel-air ratios for the five modes tested (idle, taxi, takeoff, climb and approach) resulted in over 800 test conditions.

Comparison of Emissions Data Generated at the Two Extreme Test Conditions

The modal leanout exhaust emissions obtained at the two extreme ambient test conditions (50°F; 0% relative humidity and 100°F, 80% relative humidity) are compared in Figures 7a through 7o.

The CO, HC and NO_x emissions (lb/mode) are shown on the respective figures as solid lines for the 50°F, 0% relative humidity and as broken lines for the 100°F, 80% relative humidity over the various fuel-air ratios tested. At any one fuel-air ratio, the difference in the emissions values between the solid and broken lines represents ambient conditions direct effect on the emissions.

The two extreme ambient test condition effects on CO emissions are shown in figure 7a-e for each of the five engine test modes and various fuel-air ratios. The CO emissions showed some increase at the 100°F, 80% relative humidity condition in all the modes except takeoff. The takeoff mode (fig. 7c) shows a slight decrease in CO emissions. Figure 7f-7j are plots of HC emissions for each of the five test modes. The HC emissions were higher at the 100°F, 80% relative humidity conditions in all the modes except takeoff. The takeoff mode (fig. 7h) shows that the HC emissions were lower at the richer fuel-air ratio and higher in the leaner fuel-air ratio at the 100°F, 80% relative humidity as compared to the 50°F, 0% relative humidity test condition. The emissions in lbs/mode are directly related to the total mass flow through the engine (Appendix A). Therefore the decrease in emissions (CO and HC) in takeoff as temperature and humidity increases is in part attributed to the lower mass flow rate due to the elevated air temperatures at wide open throttle conditions.

The NO_x emissions (fig. 7k-7o) versus fuel-air ratio show a decreased in NO_x emissions at the 100°F, 80% relative humidity for all the modes and all fuel-air ratios tested. This decrease in NO_x emissions was more pronounced at leaner fuel-air ratios.

The data from figures 7a - 7o was used to quantify the variation in emissions (expressed as a % difference) as ambient conditions are changed from cool, dry to hot, moist and is presented as a function of engine operating mode and fuel-air ratio (figs. 8-10). For CO emissions (fig. 8) the climb mode had the largest percent difference with an increase of over 40% occurring at a fuel-air ratio of .07. The only mode showing a decrease in CO emissions was the takeoff mode. It showed a negative percent difference of 16% at a fuel-air ratio of .085.

The percent difference in HC emissions are shown in figure 9. The idle and taxi modes showed increases of over 130 percent difference in HC emissions at rich fuel-air ratios. The percent difference in HC at the approach mode showed the least sensitivity to fuel-air ratio. Again, only the takeoff mode resulted in negative percent differences of HC emissions. This occurred between fuel-air ratio of .080 - .085.

Figure 10 shows that the largest decrease in NO_x emissions as ambient conditions changed from cool, dry to hot, moist was obtained in the climb mode. It showed a fairly constant reduction of about 90% over all the fuel-air ratios tested. The taxi mode was also fairly insensitive to fuel/air reduction ratio. The other modes were strongly effected by fuel/air ratio, and of course, all five modes consistently exhibit negative percent differences.

Effects of Humidity on Modal Emissions at Four Temperatures

For the convenience of those having a further interest in ambient effects on emissions, the following sixty figures contain the emissions test data of over 800 test points. Figures 11 through 14 are divided into four sets by the inlet air temperatures of 50, 59, 80 and 100°F with relative humidities of 0,30,60 and 80%. Each set contains fifteen figures lettered "a through o" which show the lbs/mode of CO, HC and NO_x emissions at one temperature and four relative humidities for each of the five engine test mode conditions and at the fuel-air ratios tested.

All of the figures (11 through 14) each contain a list of the reading numbers of the test data plotted. The test data are divided into groups of identical ambient conditions with a symbol to the right of each group. The symbol not only defines the specific ambient test condition but also represents the emission value point plotted on the figure.

The CO emission appeared to be insensitive to humidity at each of the tested temperatures. At the lower air temperature of 50°F and 59°F, relative humidity had essentially no effect on the HC and NO_x emissions. The bulk of the effect of relative humidity on HC and NO_x emissions occur at the higher temperature.

Effects of Air Temperature for Zero Humidity Modal Emissions

To evaluate if temperature alone had any effect on emissions a comparison was made between the (fig. 11 and 14) emissions at 50°F and 100°F air temperature at 0% humidity. Air temperature had little effect on the formation of CO emissions for any given fuel-air ratio in the idle, taxi, takeoff and approach modes. In the climb mode, the test data results showed a constant 20% increase in CO emissions over the fuel-air ratios tested. The effect of air temperature on the formation of HC and NO_x emissions for the five test modes at any of the fuel-air ratios was insignificant.

Comparison of Modal Emissions

The variation in the mode time, exhaust volume flow, and the engine combustion process which occur throughout the EPA cycle, result in substantial differences in the contributions by mode to the total cycle emissions. Mode lean-out curves for the three emissions (CO, HC and NO_x) are graphically shown in figures 15-17 for 59°F air temperature and 60% relative humidity. (The EPA

standard day conditions). Each figure displays one of the emissions expressed in lb/mode versus fuel-air ratio for the five modes of engine operation. From each figure, it is evident that the climb, approach, and taxi modes are the highest contributors of emissions.

Comparison of Constructed Modal Cycle and Baseline Cycle Emissions

The comparison of the cycle emissions constructed from the modal emissions data with the experimental baseline full rich cycle test results (obtained from ref. 1) is shown in figure 18. Modal fuel-air ratio values corresponding to those of the baseline full rich cycle were used in the construction of the cycle emissions over the range of temperatures and humidities. The comparison of the CO emissions resulted in a relatively close agreement with the percent difference ranging from +8 to -13 percent. At the lower three operating temperatures of 50, 59 and 80° F and for all four of the humidities the percent difference between the constructed cycle and baseline cycle HC emissions (obtained from ref. 1) was less than ± 12 percent. This difference increased up to -24% at the 100°F temperature and 30% relative humidity conditions. The percent difference in NO_x emissions varied from -11 to +63 percent. The largest percent difference occurred at the test condition in which very low NO_x values were generated. Thus, the poor agreement is probably related to computing percent differences of small values having experimental inaccuracies. Overall, however, it was shown that leanout data can be used to construct optimum baseline cycles based on leaner fuel schedules and the data thereby provide a quick and simple method for assessing the benefit of tailored fuel schedules.

CONCLUDING REMARKS

A carbureted four-cylinder air-cooled 0-320-DIAD Lycoming aircraft engine was tested to establish the fuel vaporization and combustion effect of air temperature and humidity on exhaust emissions. The test conditions included carburetor leanout at four air temperatures and four values of relative humidity at each temperature for each of the five different engine operating modes. The following conclusions are based on the data obtained and the plots thereof presented in the report.

The general shape of the CO, HC and NO_x emissions vs. fuel-air ratio curves for a given mode is consistent with well known general emission characteristics for spark-ignition piston engines. From these curves, it is apparent that the exhaust emissions are strongly influenced by fuel-air ratio. In addition, hot/humid ambient inlet air conditions which affect the induction vaporization and basic combustion process are seen as significantly influencing the emissions. At a fixed fuel-air ratio with higher air temperatures and relative humidities, the HC emissions increased by as much as 130% and the NO_x emissions decreased by as much as 90% in certain modes.

Lean out curves for each of the emissions illustrated that the climb mode followed by the approach mode were the largest contributors of the CO and NO_x to the EPA cycle emissions, whereas the taxi mode was the largest contributor of the HC emissions. The comparison of the EPA cycle emissions (ref. 1) to the constructed seven mode cycle data resulted in reasonably good agreement. Thus, leanout data from these curves can be used to construct optimum cycle based on leaner fuel schedules and thereby provide a quick and simple method for assessing the benefits of tailored fuel schedules.

The results reported herein are based on tests conducted on one carbureted naturally-aspirated engine. A Continental turbocharged and fuel-injected TSIO-360-C engine has been investigated over the same range of test conditions as the Lycoming engine described herein. A least-squares regression technique of the data from each engine is being planned to study generalized representation of engine emission trends for ambient condition.

APPENDIX A

INTERMEDIATE EQUATIONS USED IN THE RAW EMISSIONS DATA REDUCTION

The basic computational procedures on emission data reduction are specified in the Federal Register (ref. 4). Presented are only those equations and calculations which are not explicitly defined in the Federal Register.

SYMBOLS

A	air flow, lb/hr
Ar	argon
a	moles of air
C_eH_b	molecular formula of the fuel
c	mass fraction of carbon in the fuel
D	density of exhaust products, lb/ft^3
E	exhaust molecular weight, lb/(lb-mole)
F	fuel flow, lb/hr
f	moles of fuel
h	mass fraction of hydrogen in fuel
M	molecular weight of air, 28.96 lb/(lb-mole)
m_n	mole fraction of the compound n
P	equals $(CO) + (CO_2)/[(CO) + (CO_2) + (HC)]$
Q	equals $(O_2)/(CO_2)$
R	equals $(CO)/(CO_2)$
V	exhaust volume flow rate, ft^3/hr
W	water flow rate, lb/hr
ρ	density of air at 68° F and 760 mm Hg pressure, 0.075 lb/ft^3

Subscripts:

b number of hydrogen atoms in one molecule of fuel

d measured on the "dry" basis water removed

e number of carbon atoms in one molecule of fuel

n identifies the individual constituent fraction

I. Water Correction Factor

The chemical reaction including water vapor in the air may be written as:

$$fC_eH_b + a(O_2 + 3.72744\ N_2 + 0.04451\ A_r)$$
$$+ wH_2O \rightarrow m_1H_2O + m_2CO_2 + m_3CO + m_4NO + m_5O_2$$
$$+ m_6HC + m_7H_2 + m_8N_2 + m_9Ar$$

An oxygen balance results in equation (1).

$$m_1 = 2a + w - 2m_2 - m_3 - m_4 - 2m_5 \qquad (1)$$

A carbon balance results in equation (2).

$$f = \frac{m_2 + m_3 + m_6}{e} \qquad (2)$$

The fuel-air mass ratio may be defined as

$$\frac{F}{A} = \frac{f(12.01\ e + 1.008\ b)}{a(138.2689)} \qquad (3)$$

The water - dry air mass ratio may be defined as

$$\frac{W}{A} = \frac{w(18.016)}{a(138.2689)} \qquad (4)$$

Substituting equations (2) to (4) into equation (1) and rearranging

$$m_1 = \left(2.0 + 7.67478\ \frac{W}{A}\right)\left[\frac{(m_2 + m_3 + m_6)\left(12.01 + 1.008\ \frac{b}{e}\right)}{138.2689\ \frac{F}{A}}\right]$$
$$-2m_2 - m_3 - m_4 - 2m_5 \qquad (5)$$

For clarity equation (5) may be written using chemical symbols to represent the mole fraction for each constituent

$$(H_2O) = \left(2.0 + 7.67478\ \frac{W}{A}\right)\left[\frac{(CO_2) + (CO) + (HC)\left(12.01 + 1.008\ \frac{b}{e}\right)}{138.2648\ \frac{F}{A}}\right]$$

$$-2(CO_2) - (CO) - (NO) - 2(O_2) \qquad (6)$$

The above equation (6), represents the total water vapor contained in the products of combustion with each constituent measured on a "wet" basis. Since CO, CO_2, and O_2 are measured dry and since the water correction factor is defined as

$$K_w = 1.0 - (H_2O) \qquad (7)$$

equation (6) may be written in terms of dry measurements as

$$\frac{H_2O}{1 - (H_2O)} = \left(2.0 + 7.67478\ \frac{W}{A}\right)$$

$$\times \left\{\frac{\left[(CO_2)_d + \frac{(HC)}{1 - (H_2O)}\right]\left[\left(12.01 + 1.008\ \frac{b}{e}\right)\right]}{138.2648\ \frac{F}{A}}\right\}$$

$$- 2(CO_2)_d - (CO)_d - \frac{NO}{1 - (H_2O)} - 2(O_2)_d \qquad (8)$$

The solution to equation (8) for H_2O is an iteration process since HC and NO are measured wet. The water correction factor is then calculated using equation (7).

II. Exhaust Volume Flow Rate

The exhaust volume flow rate can be equated as:

$$V = \frac{A + W + F}{D}$$

The exhaust density can be expressed as

$$D = \frac{PXE}{M}$$

Figure A1 shows the relation between the exhaust molecular weight and F/A ratio obtained from "computer program for calculation of complex chemical equilibrium composition" NASA SP-273 (ref. 6). The pollution production rate is then calculated as specified in the Federal Register (ref. 4).

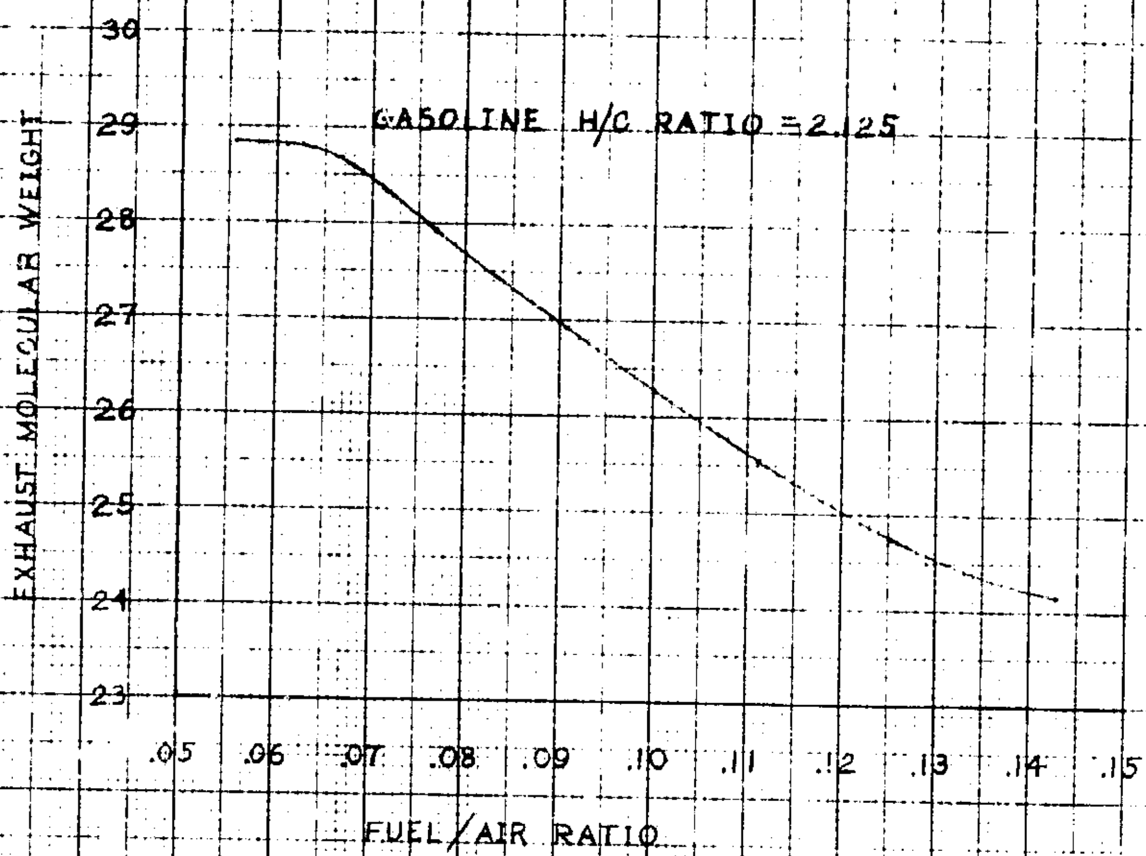

FIGURE A1 - EXHAUST MOLECULAR WEIGHT AS A FUNCTION OF FUEL AIR RATIO FOR AVIATION GASOLINE

III. Fuel Air Ratio Based on Exhaust Gas Components and Procedure of Spindt (ref. 5)

The F/A ratio can be expressed as:

$$\frac{F}{A} = \frac{1}{P\left[11.492\ c\left(1.0 + \frac{\frac{R}{2} + Q}{1 + R}\right) + \left(\frac{120h}{3.5 + R}\right)\right]}$$

APPENDIX B

TEST DATA

The data from individual test points, which were taken on a carbureted, four-cylinder, 0-320 DIAD Lycoming light-aircraft engine, have been microfilmed and are contained in the pocket at the back of this volume. These data points represent all of the environmental and engine conditions tested in the individual seven modes in the EPA emissions test cycle as discussed in Volume I. The test data presented herein, representing over 800 data points (readings), were taken at air temperatures of 50°, 59°, 80°, and 100° F at values of 0, 30, 60, and 80 percent relative humidity over a range of fuel-air ratios from 0.06 to 0.113. The data points included in this appendix are all of those for which the exhaust emissions are plotted on a per-mode basis in Volume I of this report. Data point reading number listings are included in tabular form for each series of test conditions and the data symbols which were used for the curves plotted in Volume I. Because of the large number of data points, the data points are arranged numerically by reading number for easy reference.

REFERENCES

1. Meng, Phillip R., et al.. Emissions of an Avco Lycoming 0-320-DIAD Air Cooled Light Aircraft Engine as a Function of Fuel-Air Ratio, Timing, and Air Temperature and Humidity. NASA TM X-73500, 1976.

2. Detailed Specification for Engine, Aircraft, Model 0-320-DIA, -D2A, -D1B, -D2B, -D1C, -D2C, -D2G. 160 Horsepower, Direct Drive. Spec. No. 2283C, Avco-Lycoming, 1974.

3. Summers, Robert: NO_x Destruction by CO in NO_x to NO Converters of Chemiluminescence NO Analyzers. NASA TM X-73480, 1976.

4. Control of Air Pollution from Aircraft and Aircraft Engines Emission Standards and Test Procedures for Aircraft. Federal Register, vol. 38, no. 136, Pt. II, Tuesday, July 17, 1973, pp. 19088-19103.

5. Spindt, R. S.: Air Fuel Ratio from Exhaust Gas Analysis. SAE Paper 650507, May 1965.

6. Gordon, Sanford; and McBride, Bonnie J.: Computer Program for Calculation of Complex Chemical Equilibrium Compositions, Rocket Performance, Incident and Reflected Shocks and Chapman-Jonguet Detonations. NASA SP-273, 1971.

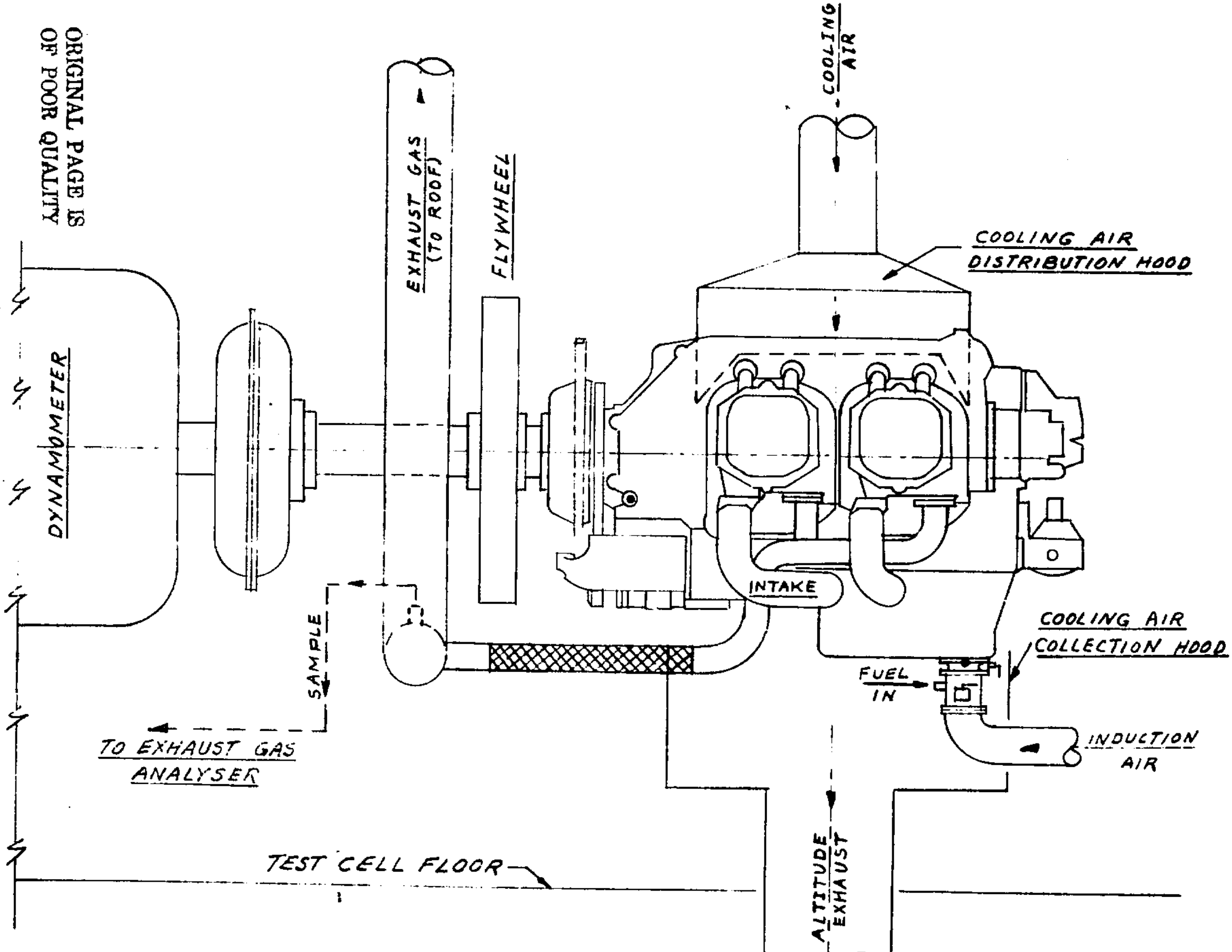

FIG. 1 - LYCOMING O-320-D ENGINE

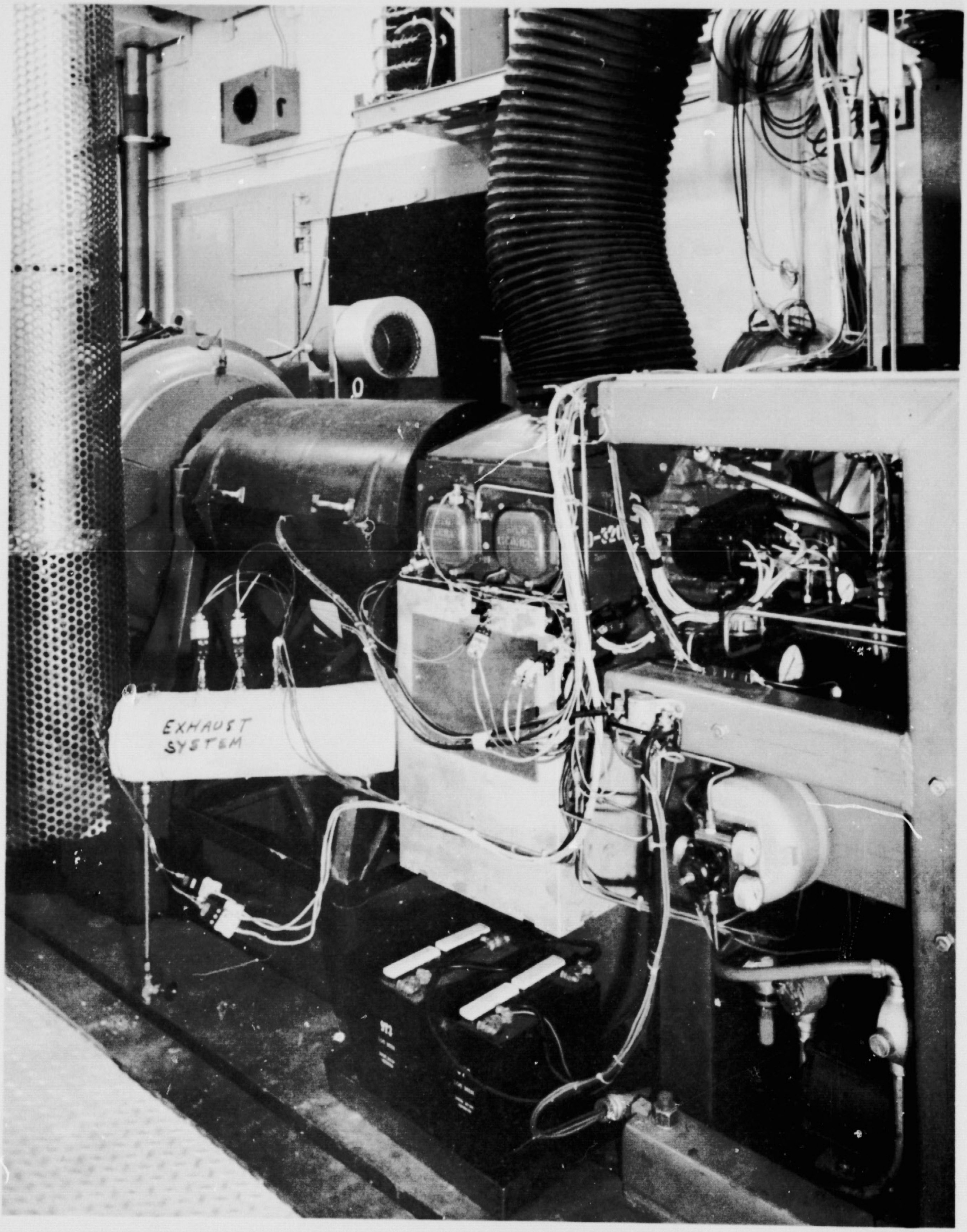

FIGURE 2. ENGINE DYNAMOMETER TEST STAND

ORIGINAL PAGE IS
OF POOR QUALITY

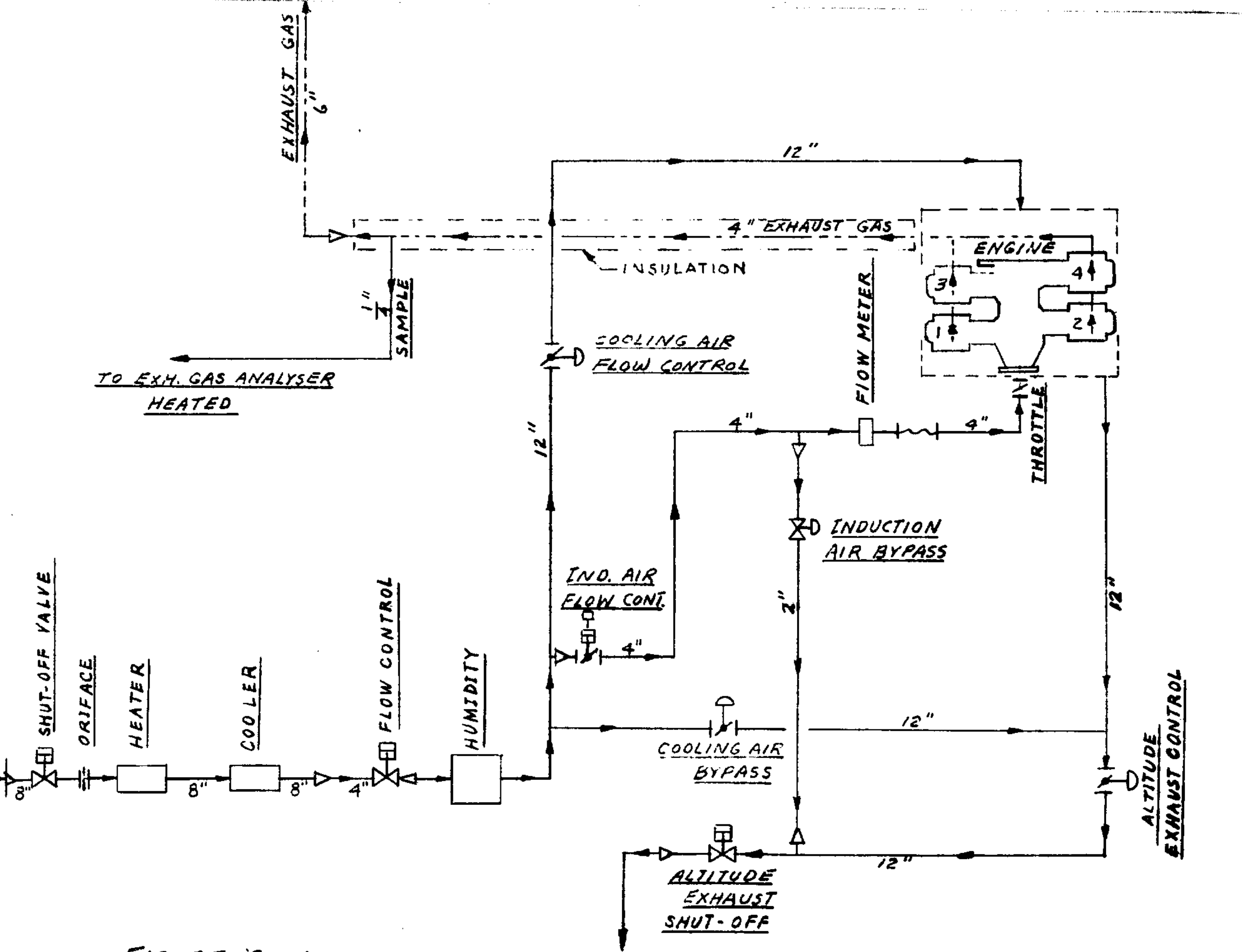

FIGURE 3. ENGINE TEST STAND FACILITY SYSTEMS

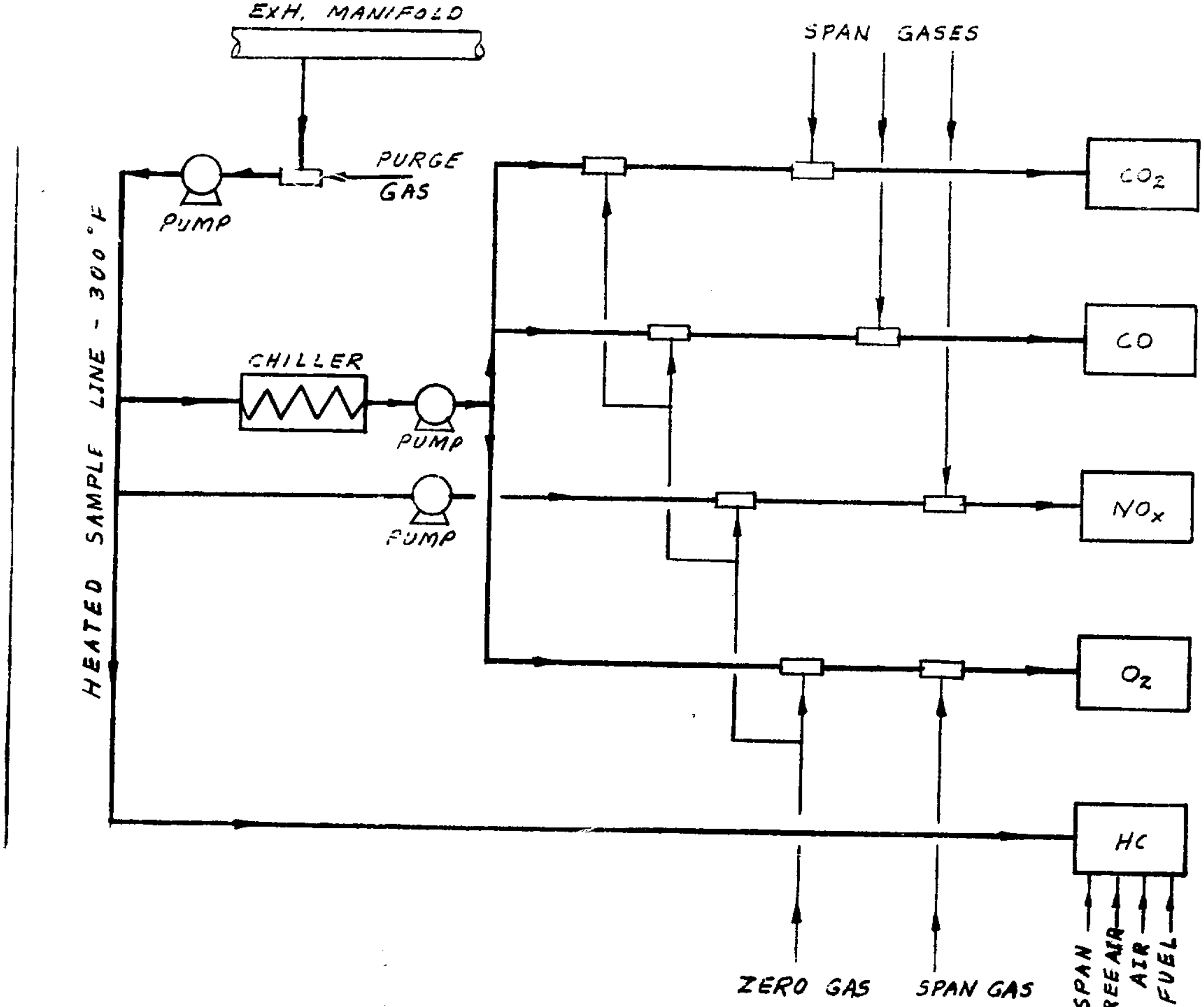

FIG. 4 EXHAUST GAS ANALYZER

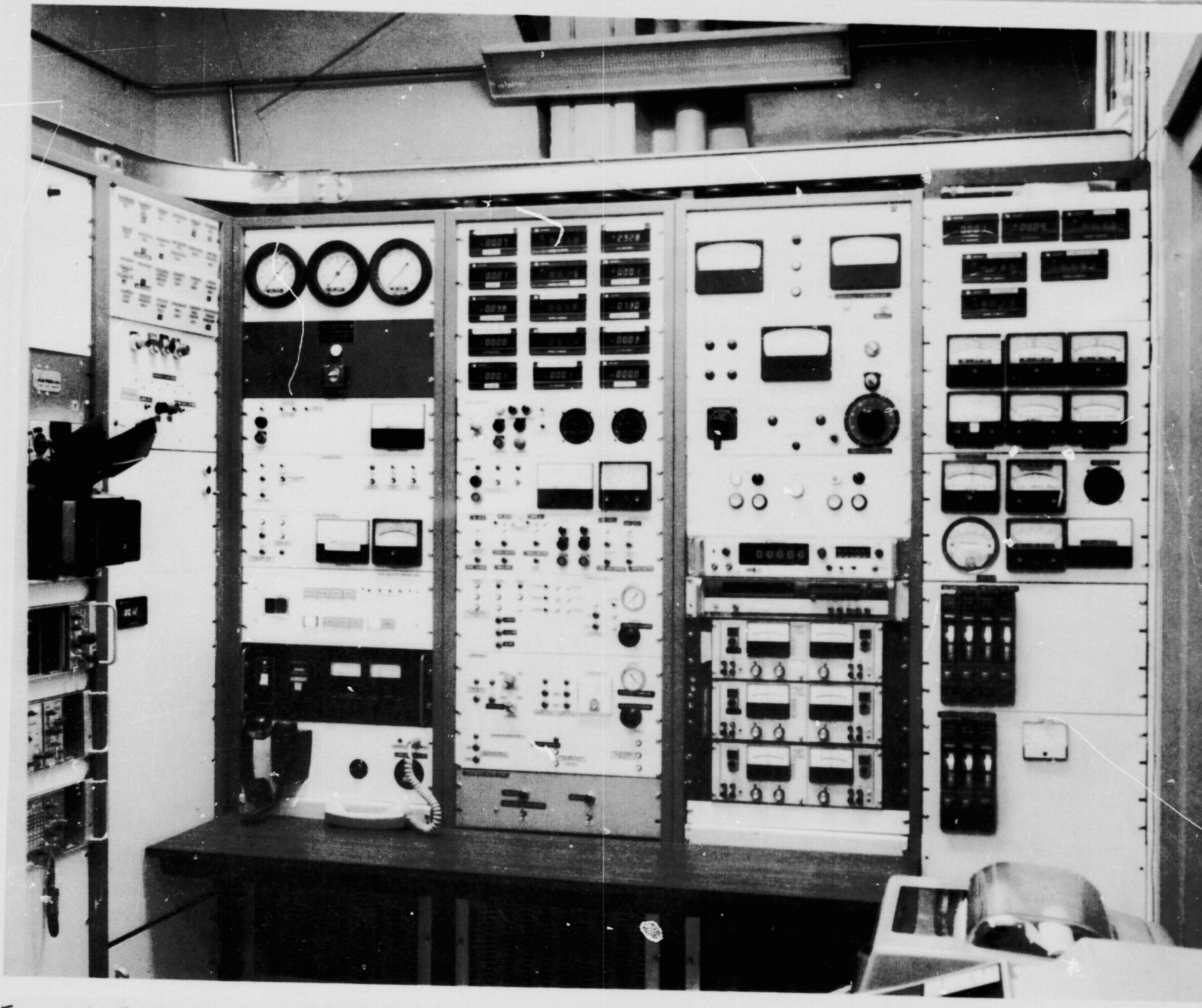

FIGURE 5. ENGINE INSTRUMENTATION AND CONTROL PANEL

ORIGINAL PAGE IS
OF POOR QUALITY

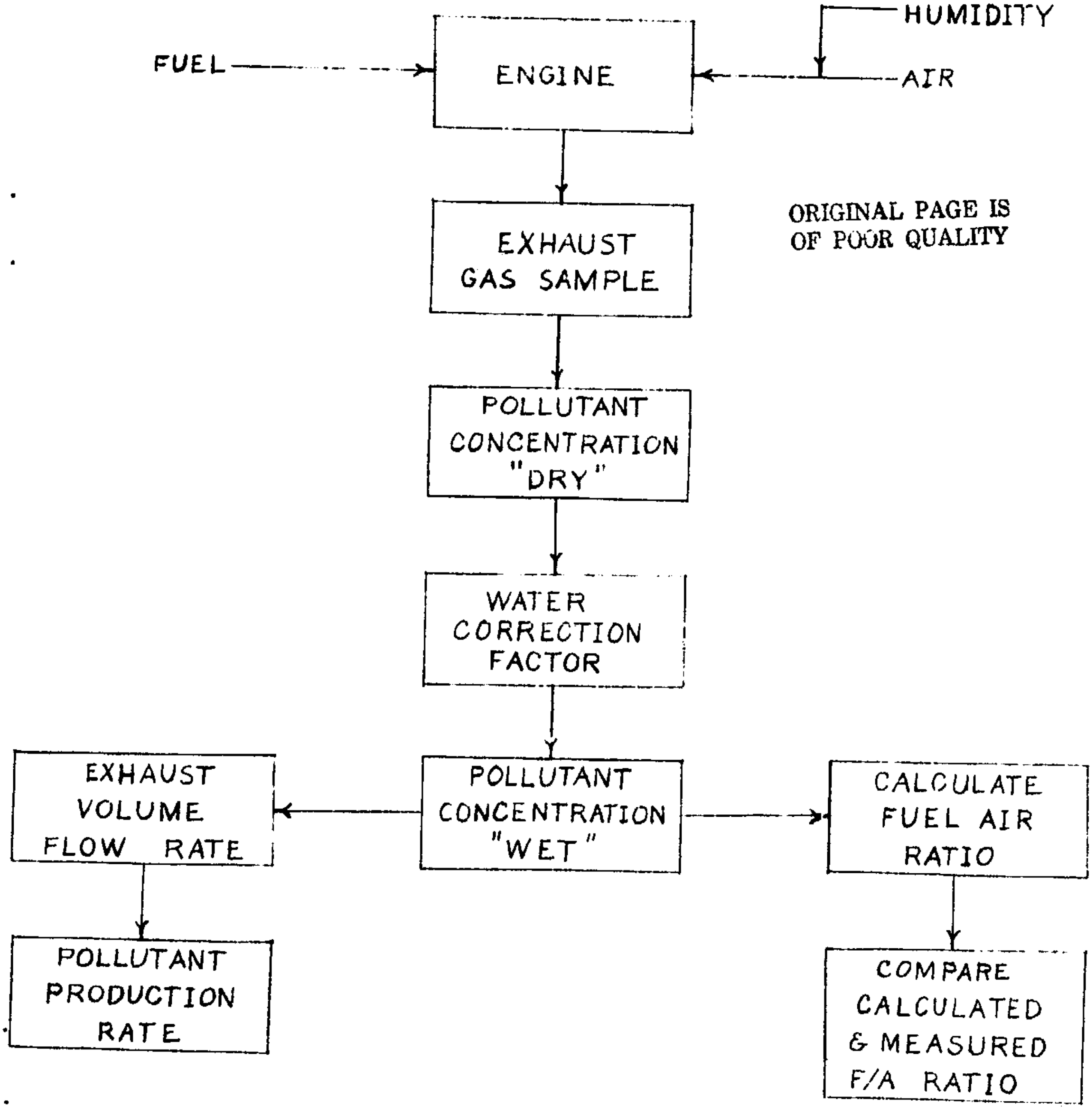

EXHAUST EMISSION
DATA REDUCTION FLOW CHART

FIGURE 6

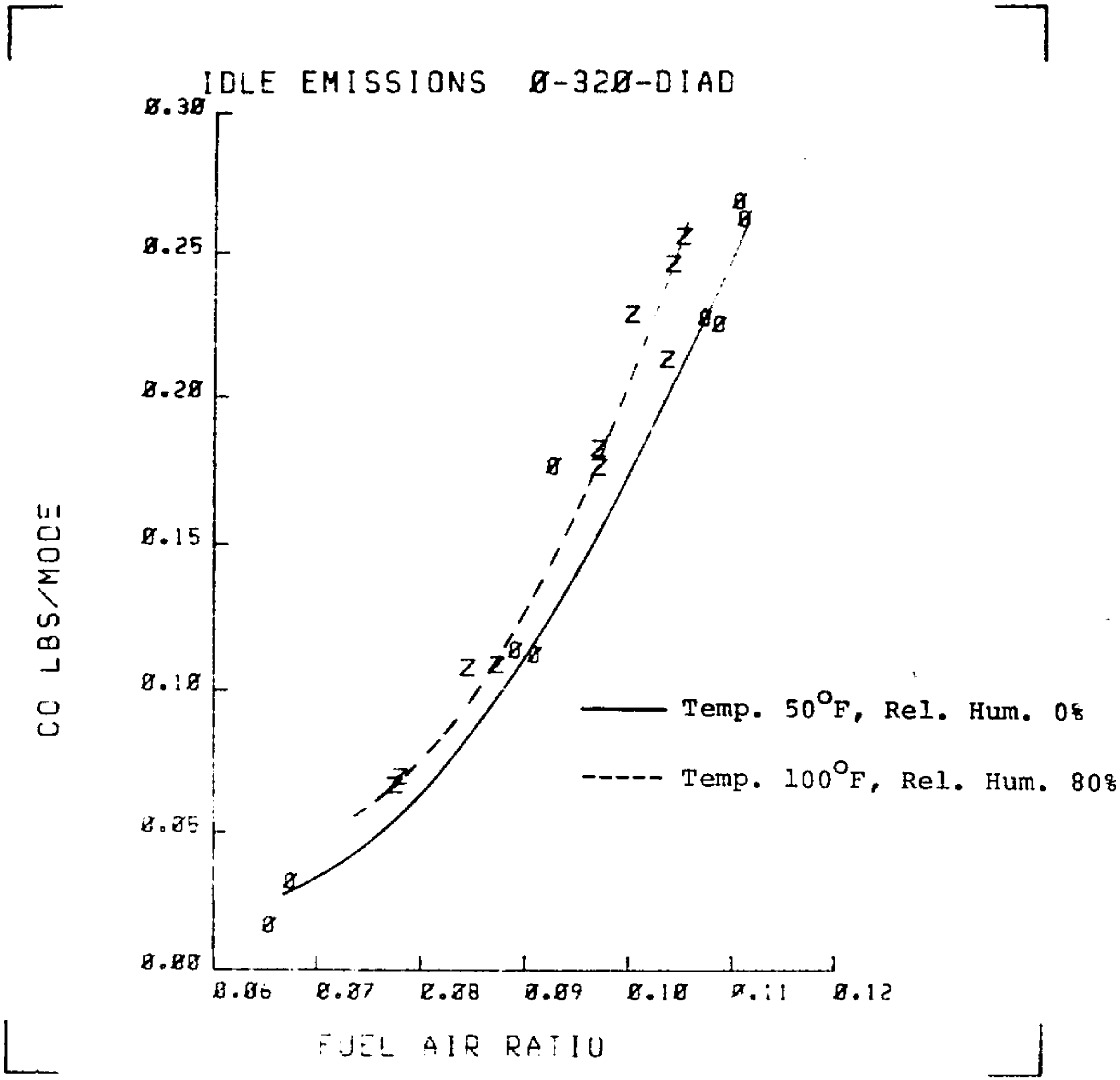

IDLE EMISSIONS Ø-32Ø-DIAD
CO LBS/MODE
Ø.3Ø
Ø.25
Ø.2Ø
Ø.15
Ø.1Ø
Ø.Ø5
Ø.ØØ
Ø.Ø6
Ø.Ø7
Ø.Ø8
Ø.Ø9
Ø.1Ø
Ø.11
Ø.12
FUEL AIR RATIO
Temp. 50°F, Rel. Hum. 0%
Temp. 100°F, Rel. Hum. 80%

FIGURE 7 a

TAXI EMISSIONS Ø-32Ø-DIAD

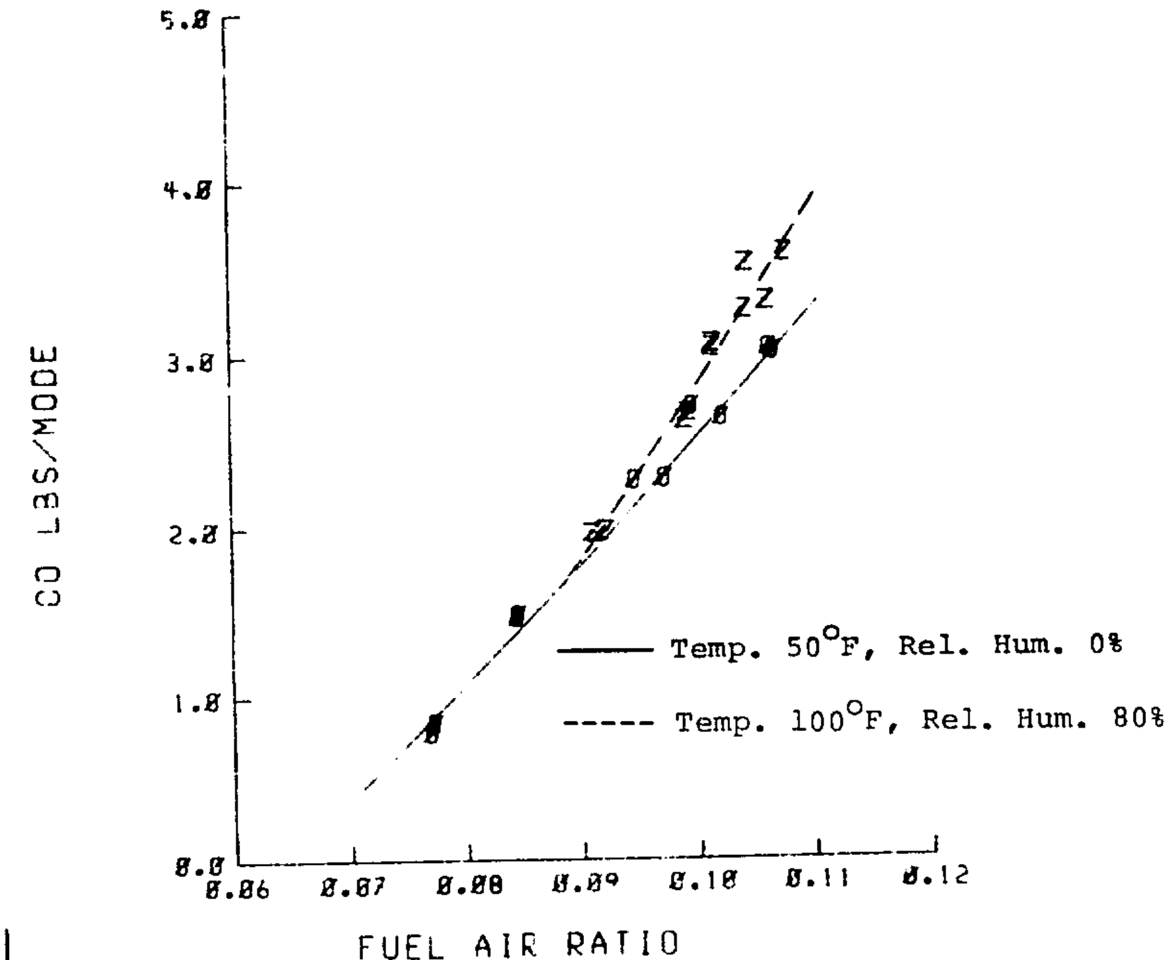

FIGURE 7b

ORIGINAL PAGE IS OF POOR QUALITY

TAKE OFF EMISSIONS Ø-32Ø-DIAD

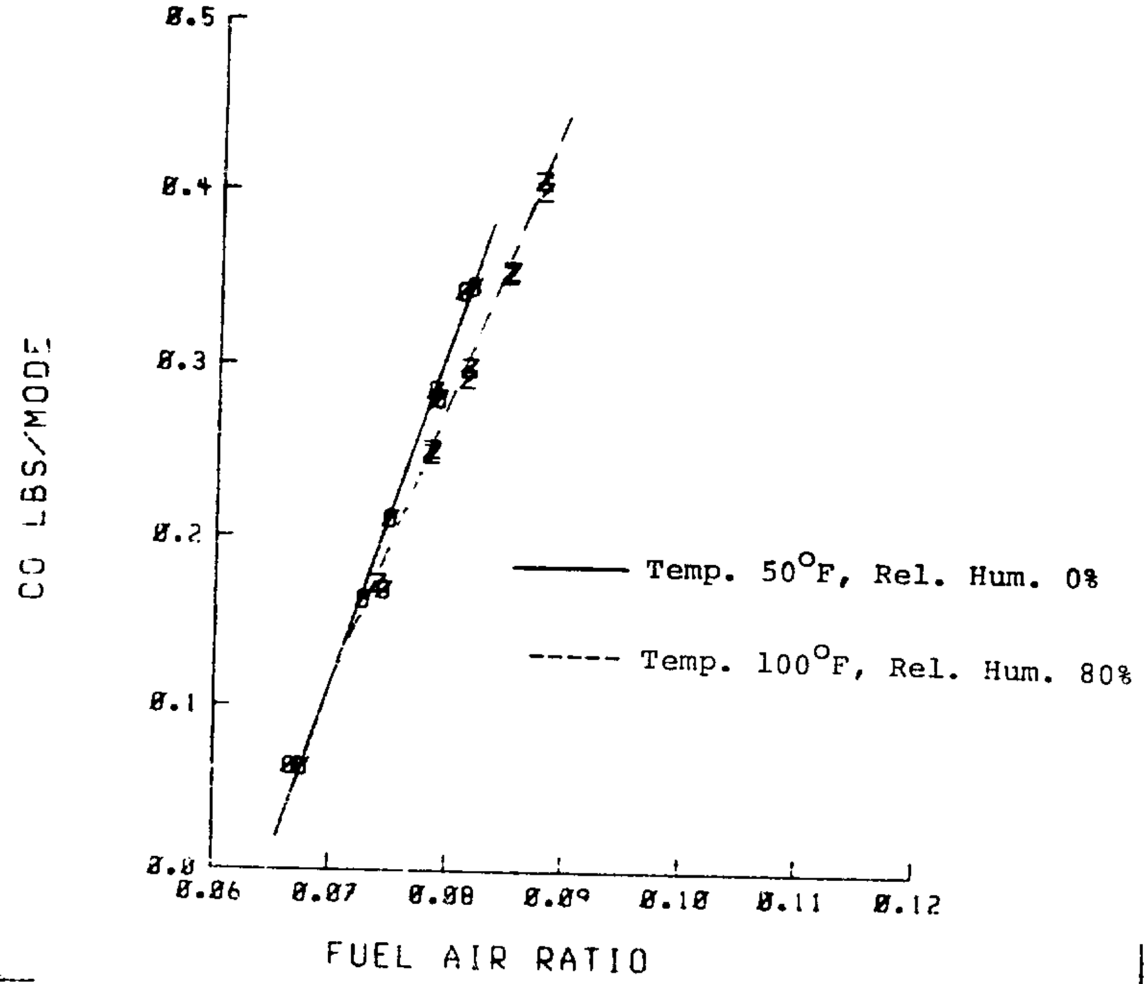

FIGURE 7c

CLIMB EMISSIONS Ø-32Ø-DIAD

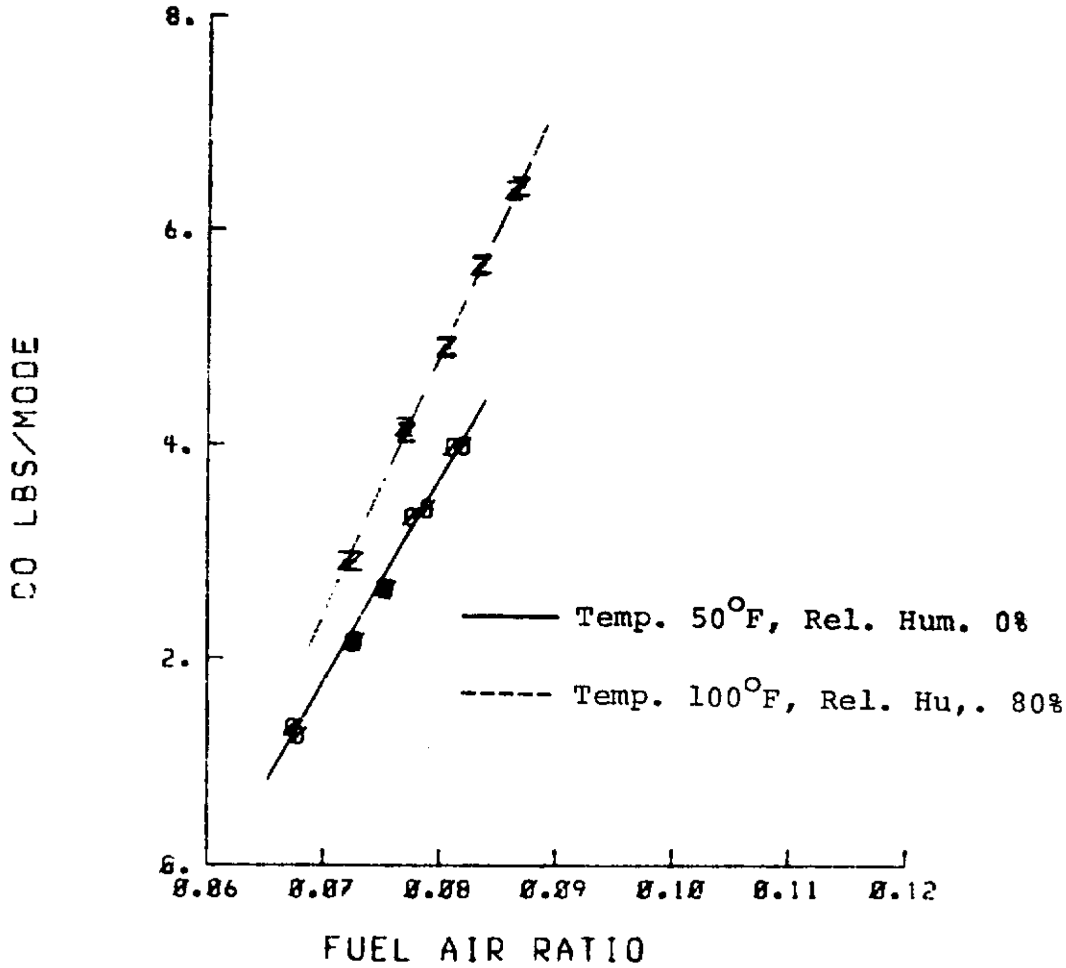

FIGURE 7 d

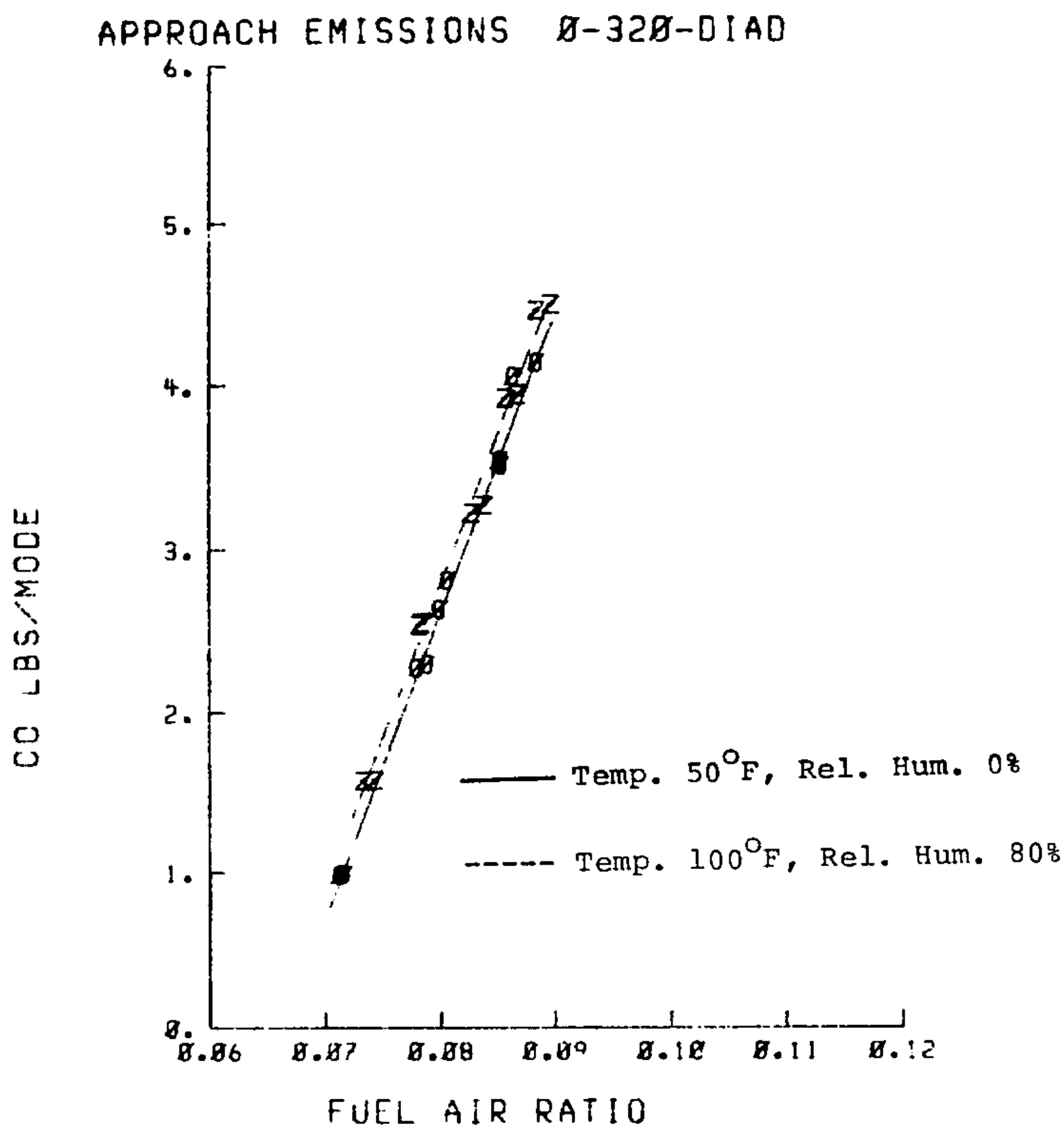
APPROACH EMISSIONS Ø-32Ø-DIAD
6.
5.
4.
3.
2.
1.
Ø.
Ø.Ø6
Ø.Ø7
Ø.Ø8
Ø.Ø9
Ø.1Ø
Ø.11
Ø.12
CO LBS/MODE
FUEL AIR RATIO
Temp. 50°F, Rel. Hum. 0%
Temp. 100°F, Rel. Hum. 80%

FIGURE 7e

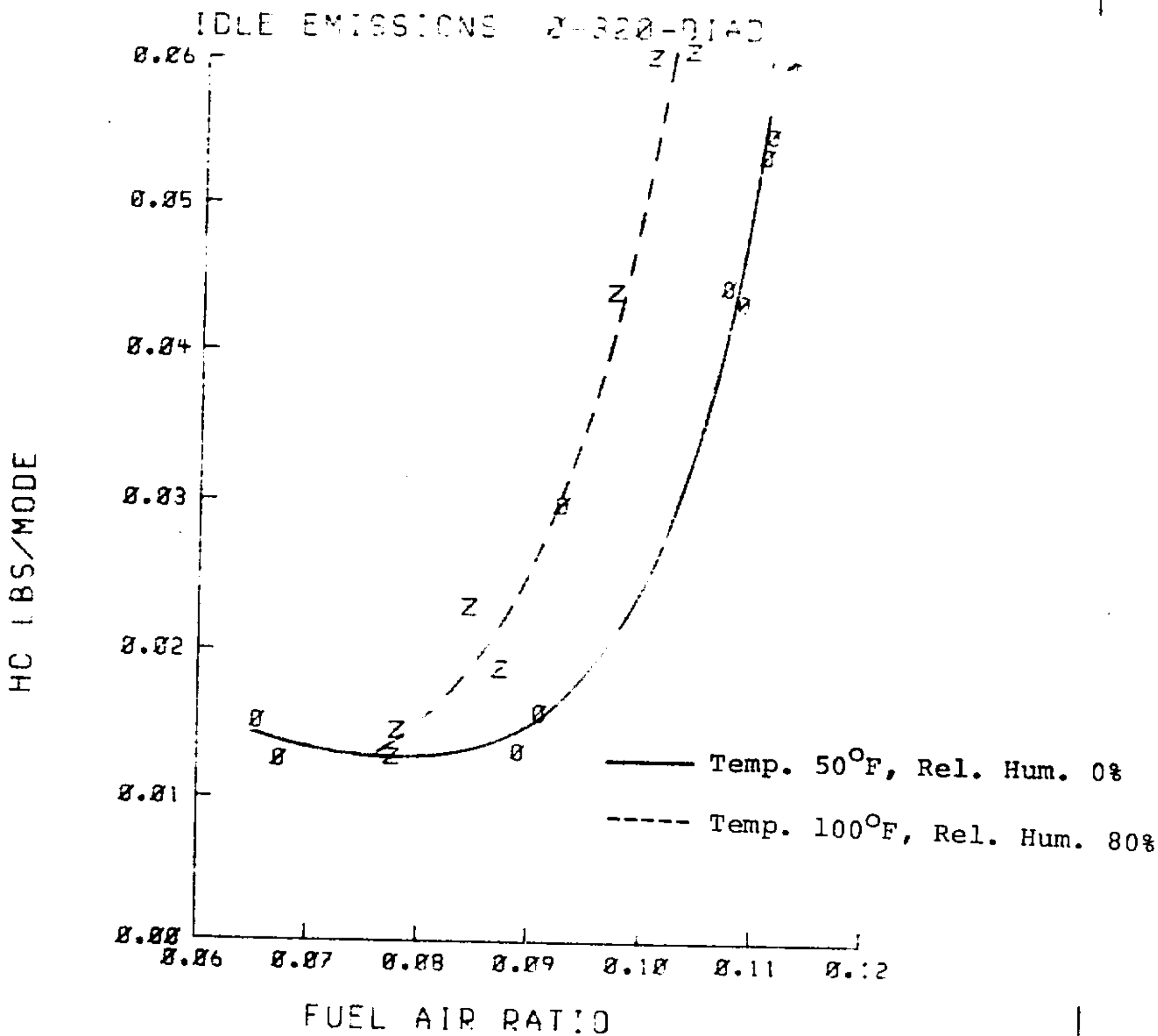
IDLE EMISSIONS O-320-DIAD
HC LBS/MODE
0.00
0.01
0.02
0.03
0.04
0.05
0.06
FUEL AIR RATIO
0.06
0.07
0.08
0.09
0.10
0.11
0.12
Temp. 50°F, Rel. Hum. 0%
Temp. 100°F, Rel. Hum. 80%

FIGURE 7f

TAXI EMISSIONS Ø-32Ø-DIAD

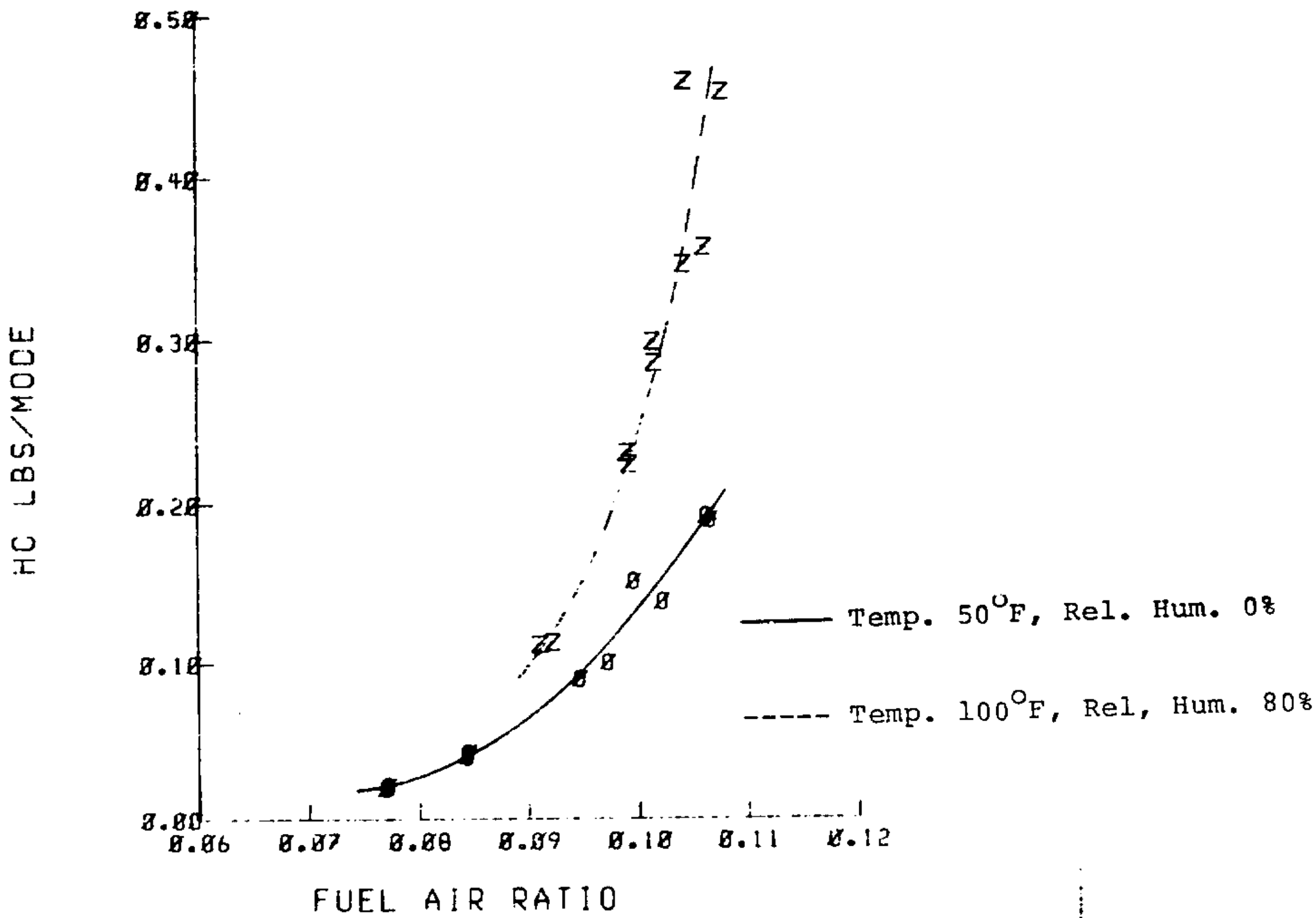

FIGURE 7 g

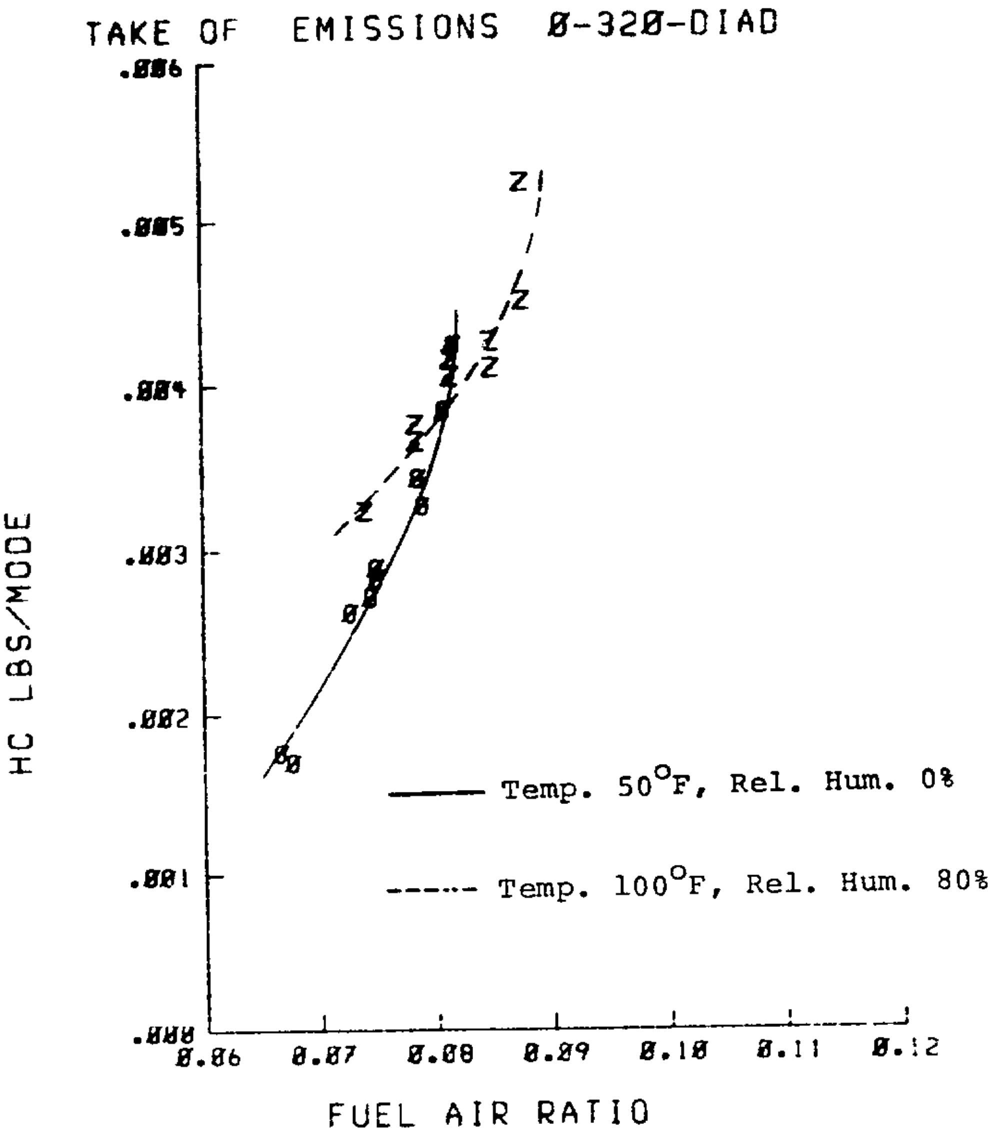

FIGURE 7h

ORIGINAL PAGE IS
OF POOR QUALITY

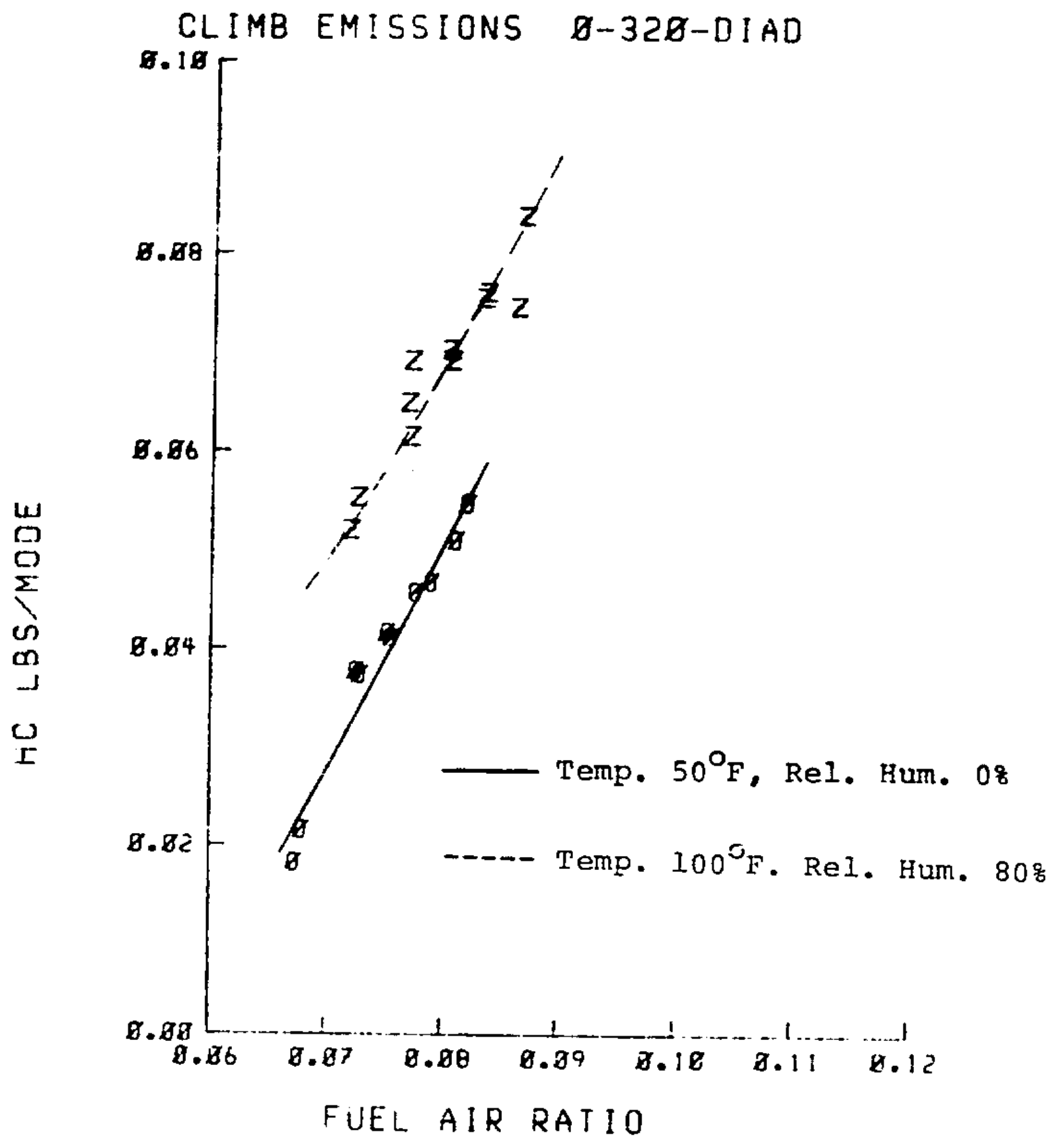
CLIMB EMISSIONS Ø-32Ø-DIAD
HC LBS/MODE
Ø.1Ø
Ø.Ø8
Ø.Ø6
Ø.Ø4
Ø.Ø2
Ø.ØØ
Ø.Ø6
Ø.Ø7
Ø.Ø8
Ø.Ø9
Ø.1Ø
Ø.11
Ø.12
FUEL AIR RATIO
Temp. 50°F, Rel. Hum. 0%
Temp. 100°F. Rel. Hum. 80%

FIGURE 7i

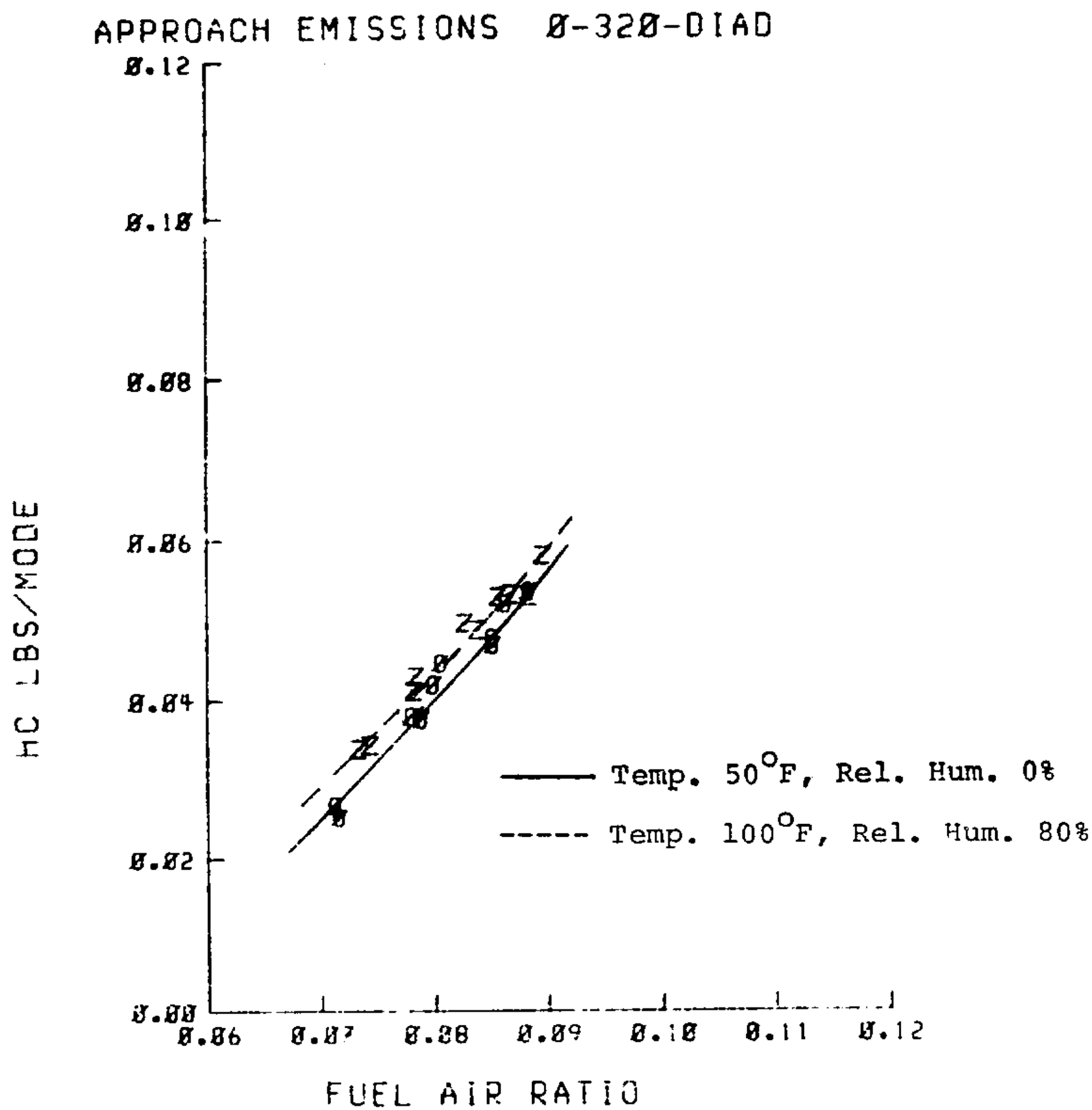

FIGURE 7 j

ORIGINAL PAGE IS OF POOR QUALITY

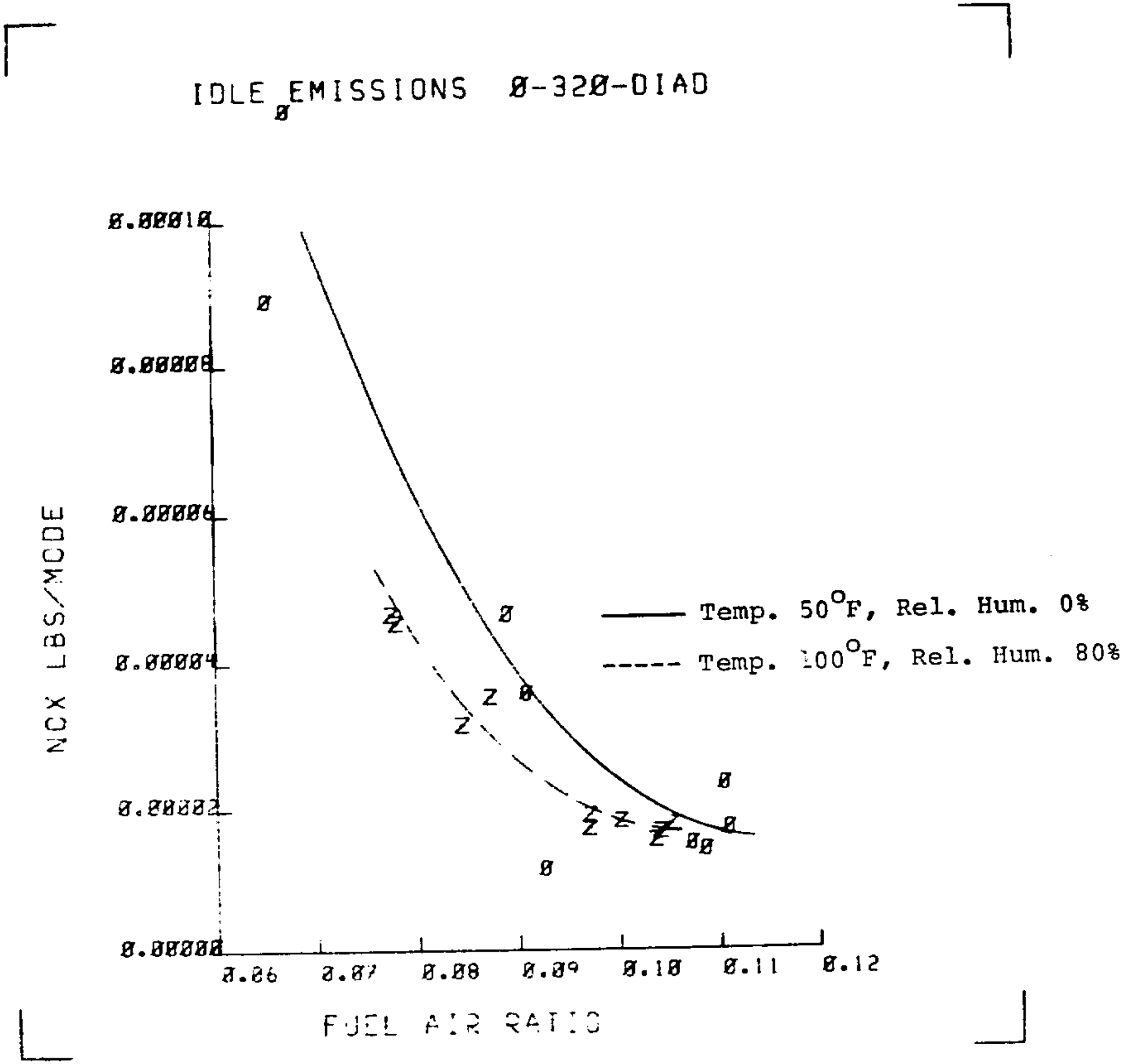

IDLE EMISSIONS Ø-320-DIAD
Ø.ØØØ1Ø
Ø.ØØØØ8
Ø.ØØØØ6
Ø.ØØØØ4
Ø.ØØØØ2
Ø.ØØØØØ
NOX LBS/MODE
Ø.Ø6
Ø.Ø7
Ø.Ø8
Ø.Ø9
Ø.1Ø
Ø.11
Ø.12
FUEL AIR RATIO
Temp. 50°F, Rel. Hum. 0%
Temp. 100°F, Rel. Hum. 80%

FIGURE 7k

TAXI EMISSIONS Ø-32Ø-DIAD

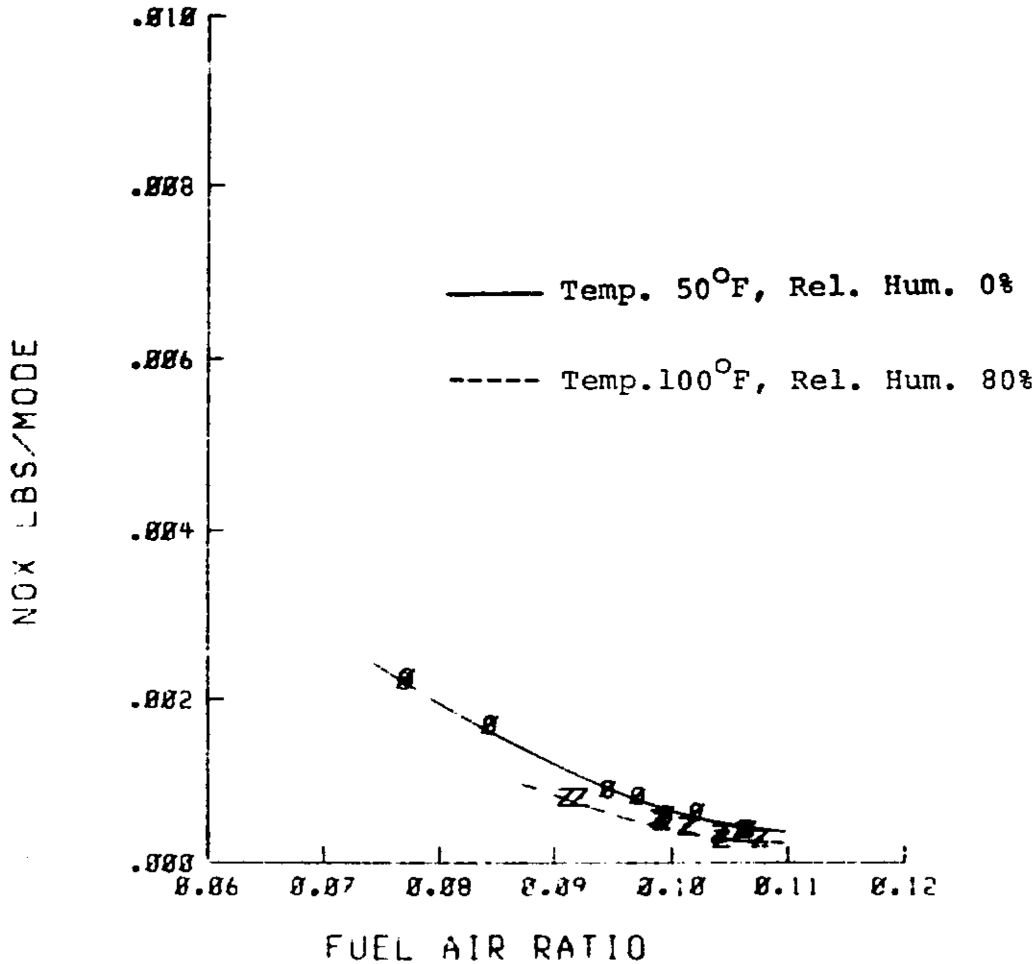

FIGURE 71

TAKE OFF EMISSIONS Ø-320-DIAD

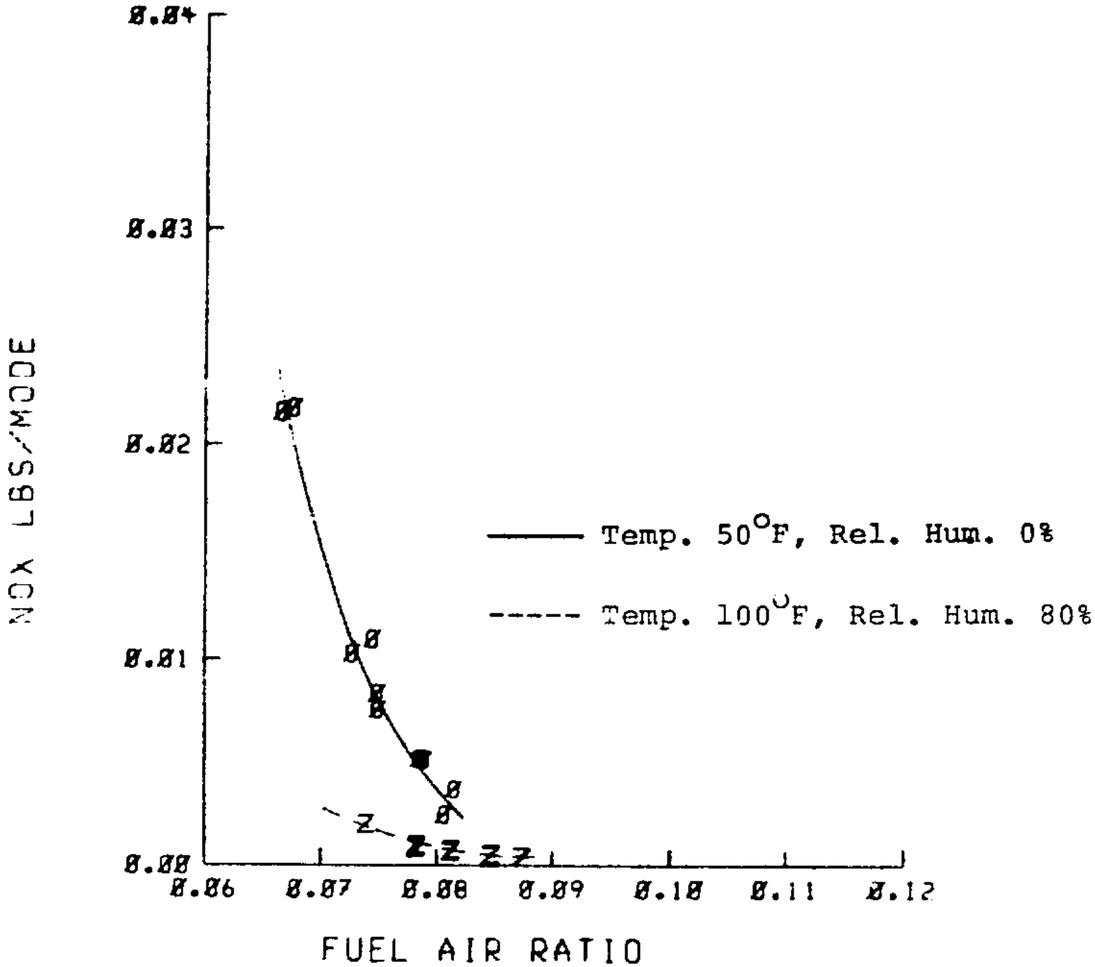

FIGURE 7m

CLIMB EMISSIONS Ø-32Ø-DIAD

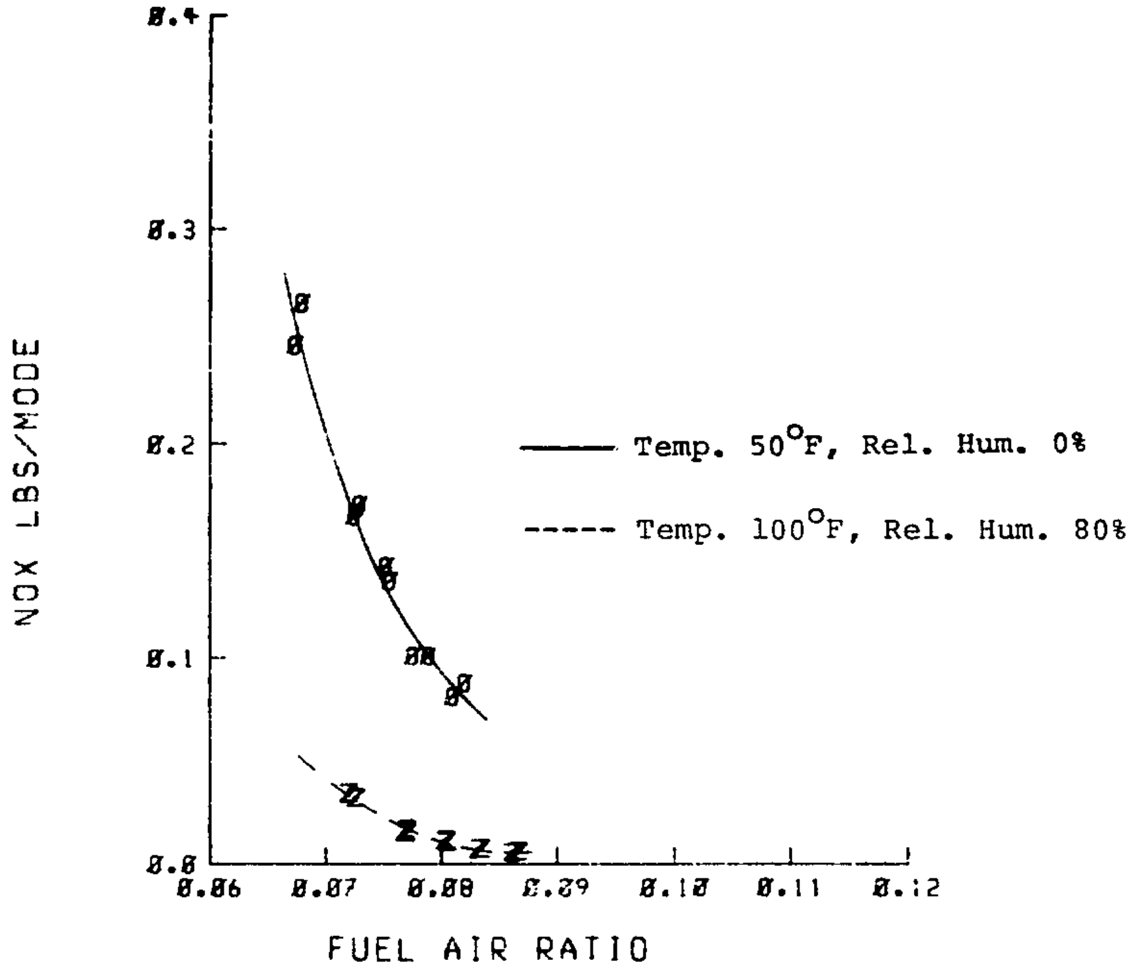

FIGURE 7n

APPROACH EMISSIONS Ø-32Ø-DIAD

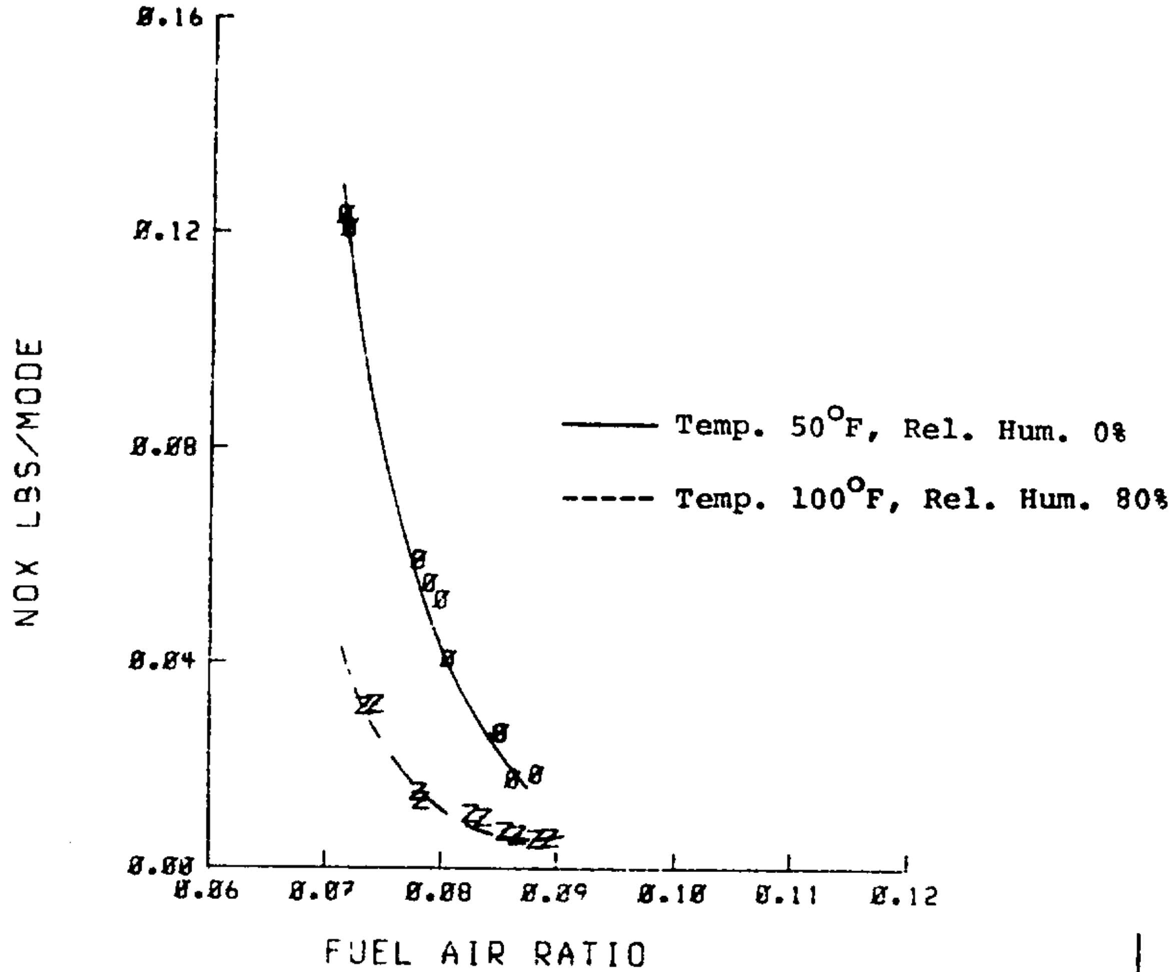

FIGURE 7o

CO EMISSIONS
(PERCENT DIFFERENCE BETWEEN 50°F, 0% R.H. AND 100°F, 80% RH)
FOR VARIOUS FUEL-AIR RATIOS AND ENGINE OPERATING MODES

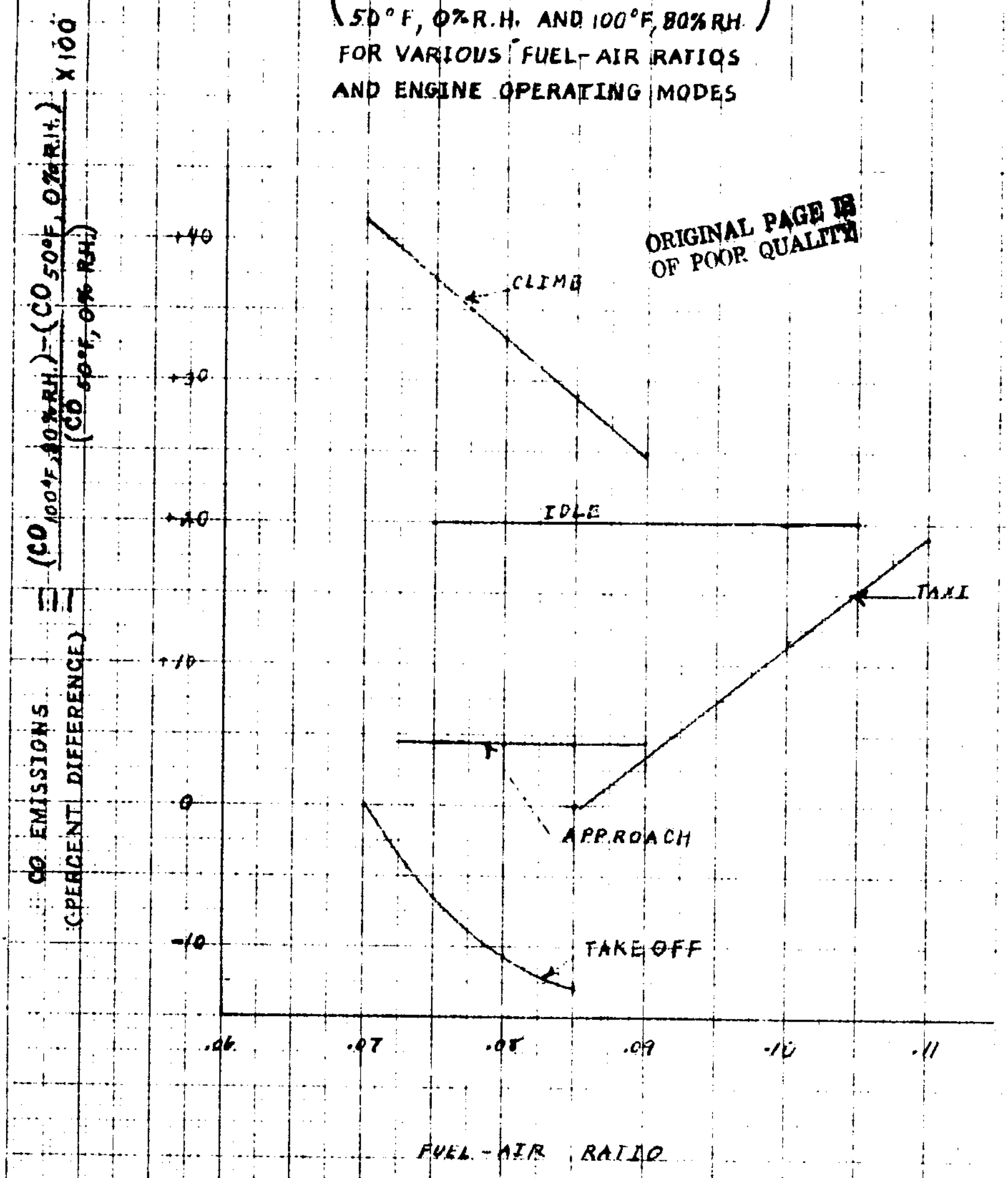

FIGURE 8

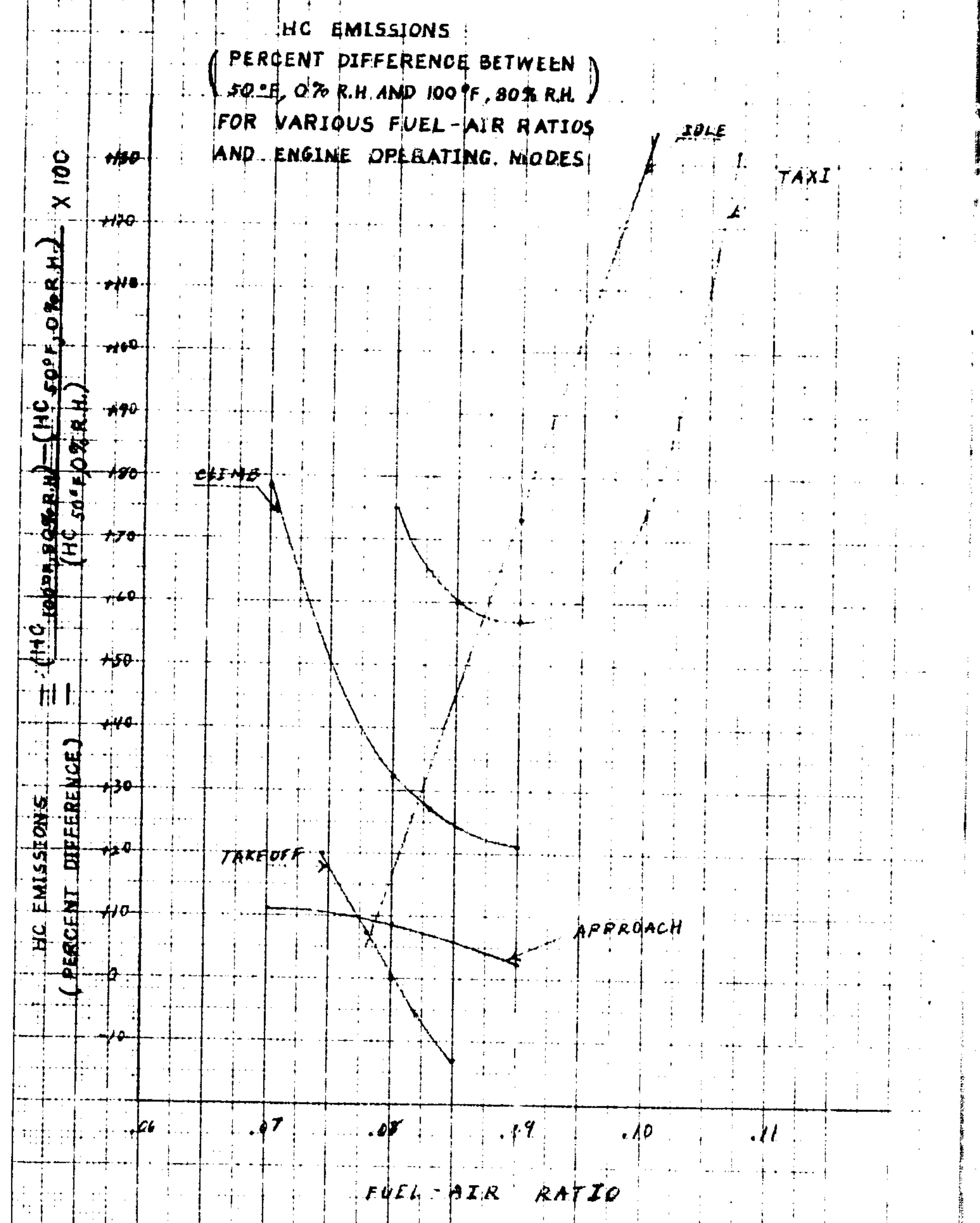

HC EMISSIONS
(PERCENT DIFFERENCE BETWEEN 50°F, 0% R.H. AND 100°F, 80% R.H.)
FOR VARIOUS FUEL-AIR RATIOS AND ENGINE OPERATING MODES
HC EMISSIONS (PERCENT DIFFERENCE) = ((HC 100°F, 80% R.H.) − (HC 50°F, 0% R.H.)) / (HC 50°F, 0% R.H.) X 100
IDLE
TAXI
CLIMB
TAKEOFF
APPROACH
+180
+170
+110
+100
+90
+80
+70
+60
+50
+40
+30
+20
+10
0
-10
.06
.07
.08
.09
.10
.11
FUEL-AIR RATIO

FIGURE 9

NO_x EMISSIONS
(PERCENT DIFFERENCE BETWEEN 50°F, 0% R.H. AND 100°F, 80% R.H.) FOR VARIOUS FUEL-AIR RATIOS AND ENGINE OPERATING MODES

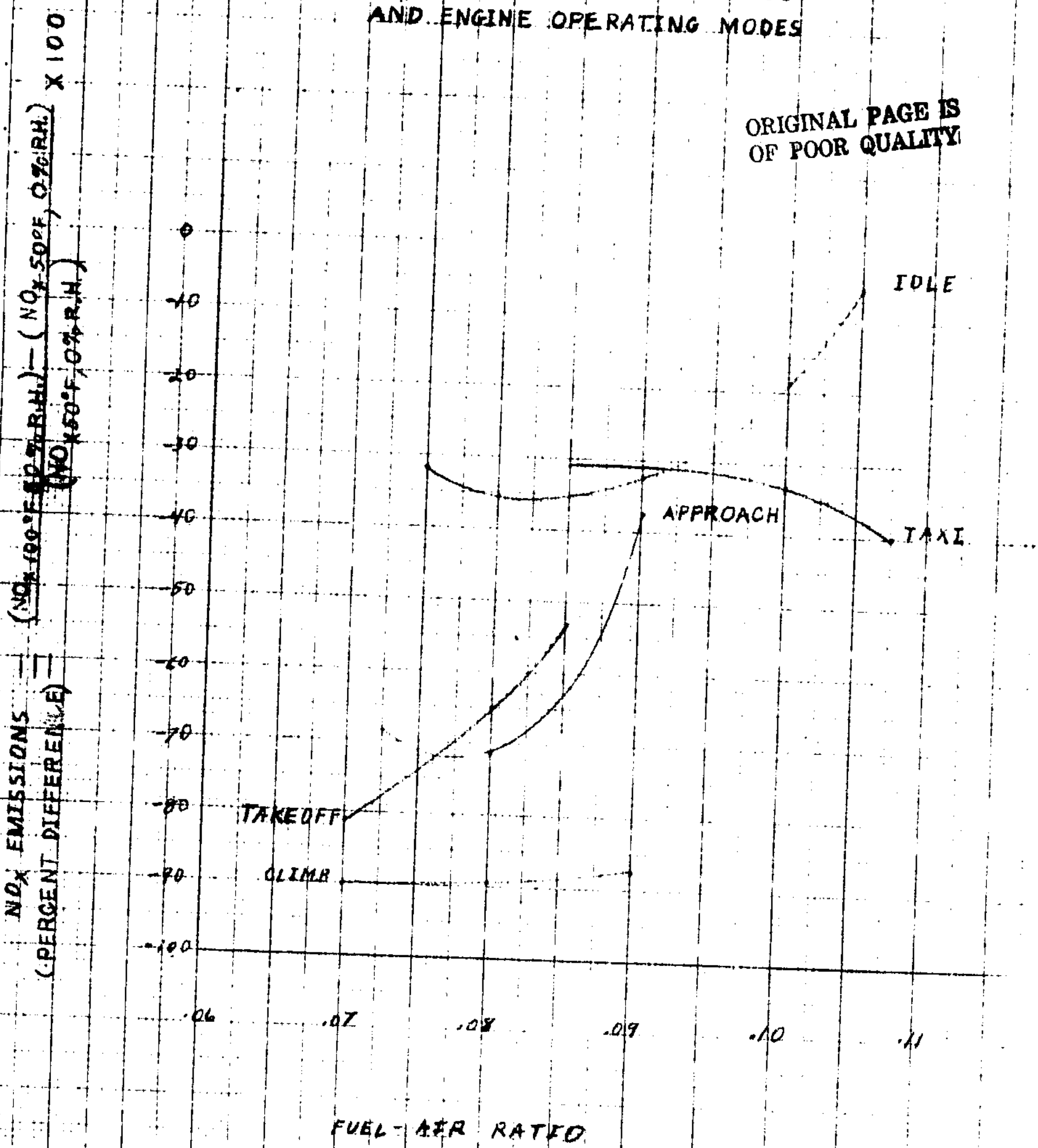

FIGURE 10

NASA LEAN-OUT DATA

TEMP. 50^{0}F REL. HUM. 0, 30, 60, 80%

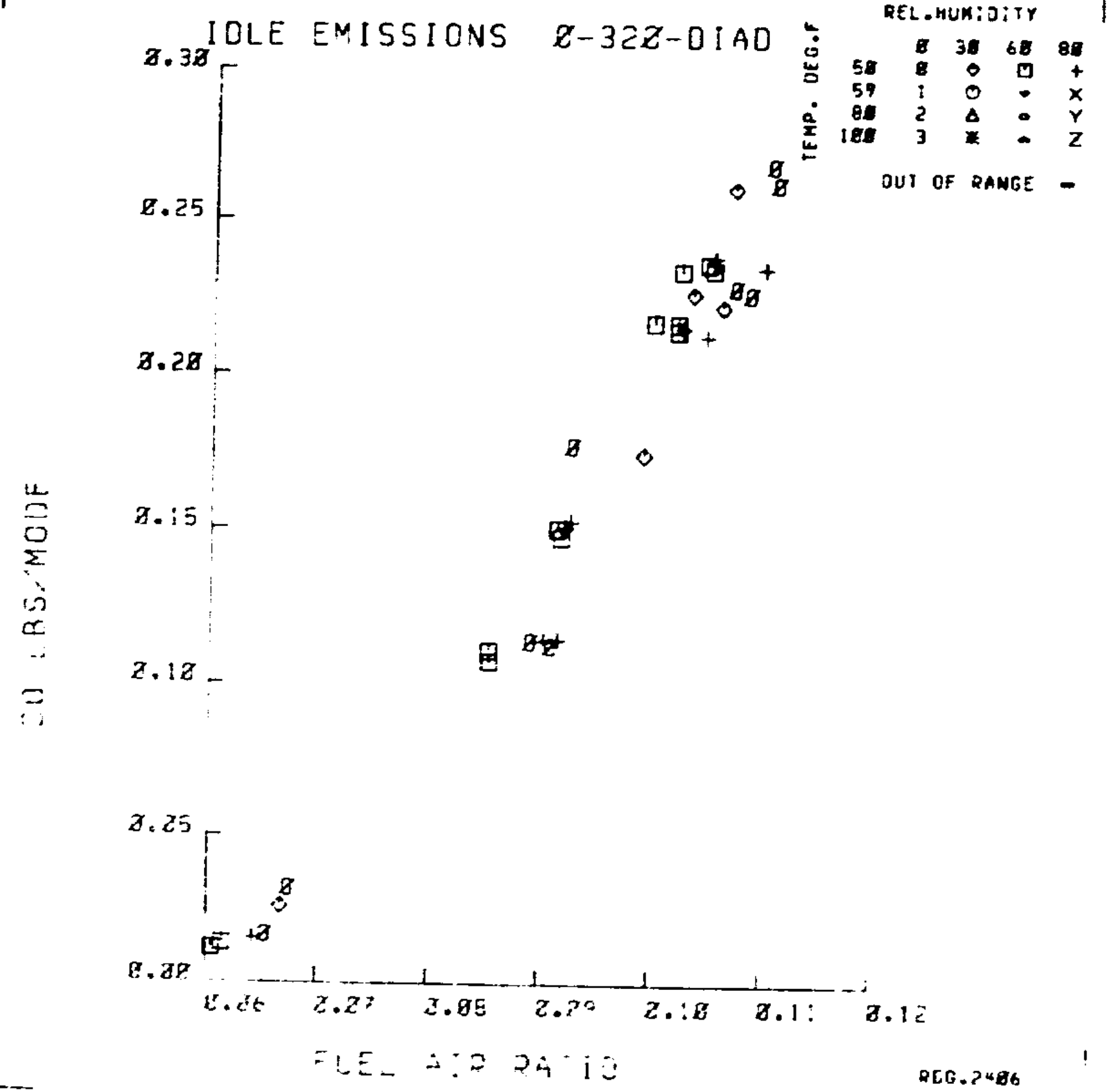

IDLE		IDLE	
2406		2412	
2413		2414	
2418	ϕ	2424	ϕ
2425		2426	
2430		2464	
2477		2487	◇
2488	◇	2489	
3576		3579	
3583		3584	
3585	□	3586	
3589		3593	□
3594		3605	
3607		3608	
3611		3618	
3619		3624	
3625	+	3628	+
3629		3632	
3633			

FIGURE 11a

NASA LEAN-OUT DATA

TEMP. 50°F REL. HUM. 0, 30, 60, 80%

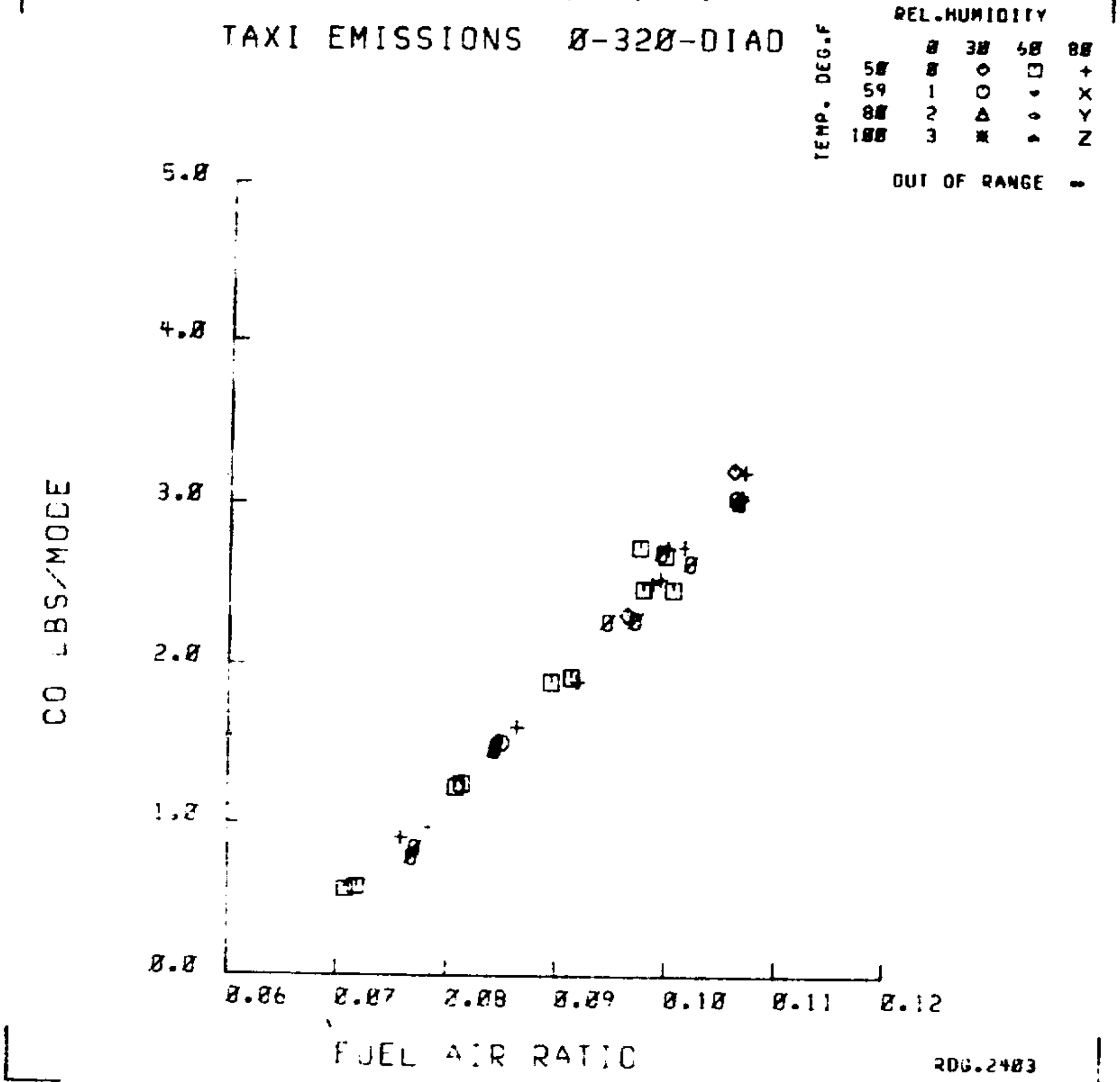

TAXI		TAXI	
2403		2405	
2409		2411	Ø
2415	Ø	2417	
2420		2423	
2427		2429	
2465	◇	2469	◇
2490		3577	
3578		3581	
3582		3587	□
3588	□	3591	
3592		3609	
3610		3613	
3614		3620	
3623		3626	+
3627	+	3630	
3631		3634	
3635			

FIGURE 11b

ORIGINAL PAGE IS OF POOR QUALITY

NASA LEAN-OUT DATA

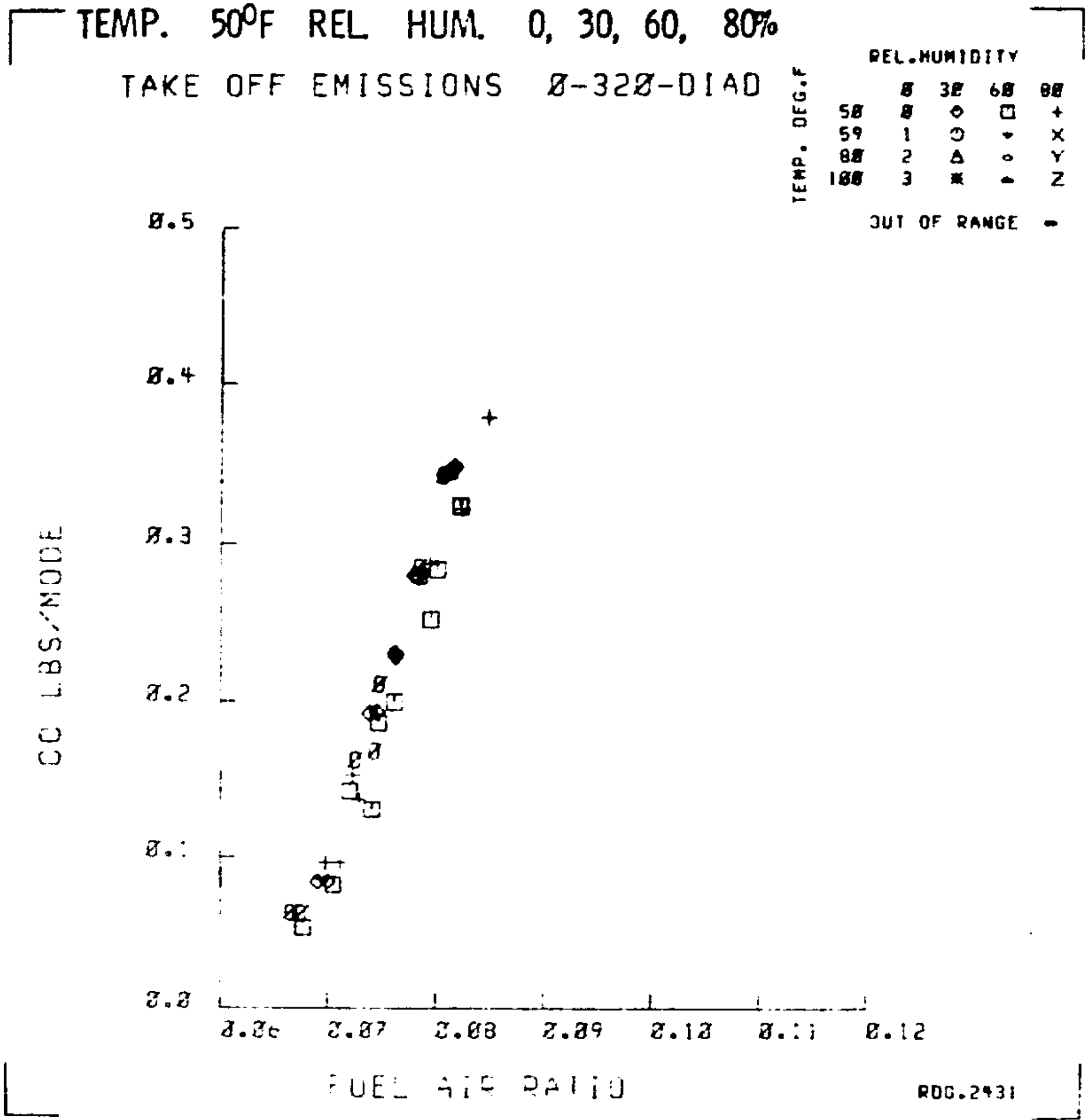

FIGURE 11c

TAKE-OFF		TAKE-OFF	
2431		2435	
2438		2442	
2445	Ø	2448	Ø
2452		2455	
2458		2461	
2494		2498	
2501		2504	
2507	◇	2511	◇
2514		2517	
2521		2524	
3639		3640	
3643		3649	
3652	□	3655	□
3658		3661	
3664		3667	
3668		3671	
3674		3680	
3686	+	3689	+
3692		3695	

NASA LEAN-OUT DATA

TEMP. 50°F REL. HUM. 0, 30, 60, 80%

CLIMB EMISSIONS Ø-32Ø-DIAD

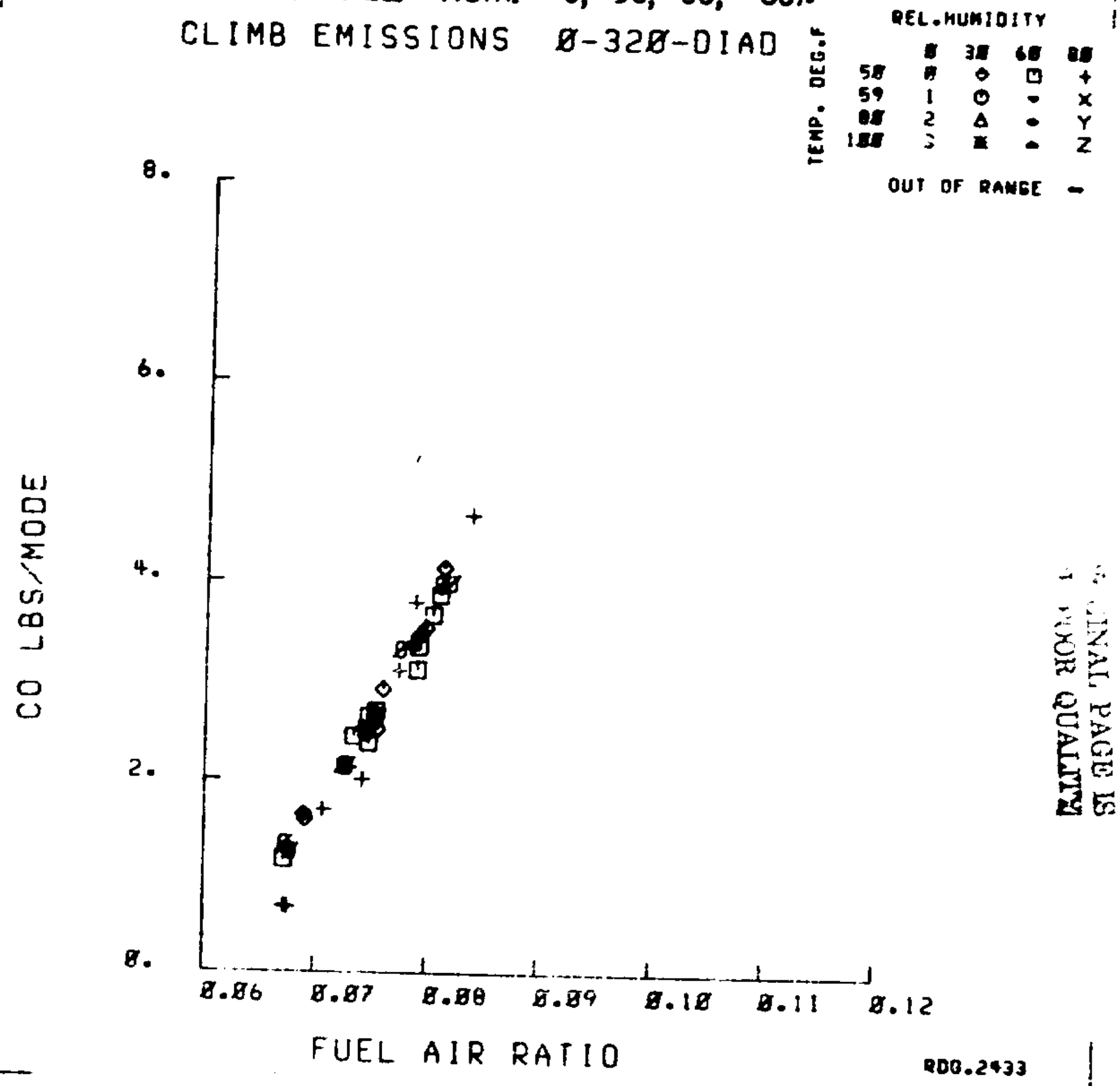

ORIGINAL PAGE IS OF POOR QUALITY

CLIMB
2433
2439
2446 ϕ
2453
2459
2495
2502
2512 ◇
2519
2525
3641
3647
3653 □
3659
3665
3672
3678
3684 +
3690
3696

CLIMB
2436
2443
2449 ϕ
2456
2462
2499
2505
2515 ◇
2522
3637
3644
3650 □
3656
3662
3669
3675
3681 +
3687
3693

FIGURE 11a

NASA LEAN-OUT DATA

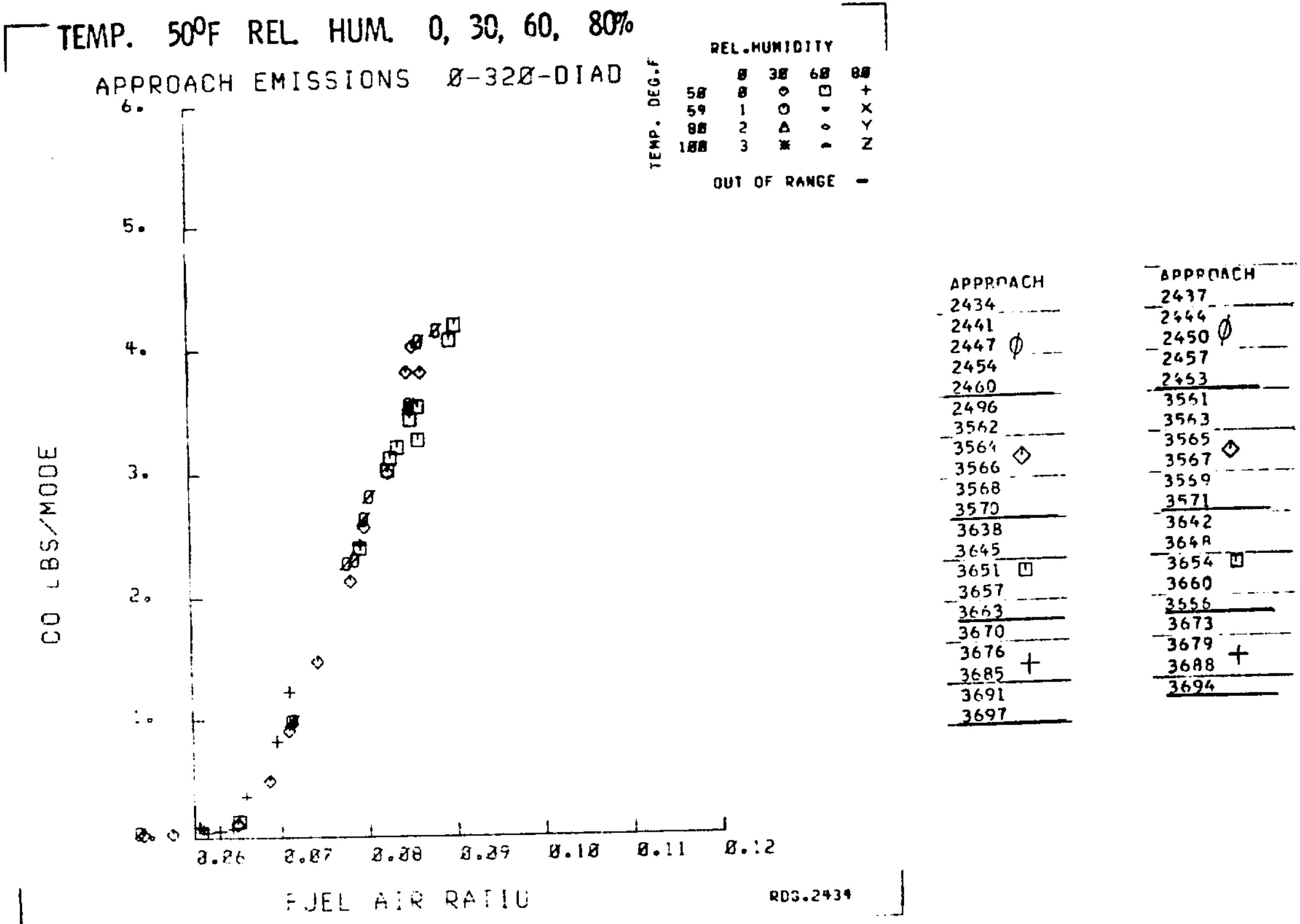

FIGURE 11e

NASA LEAN-OUT DATA

TEMP. 50°F REL. HUM. 0, 30, 60, 80%

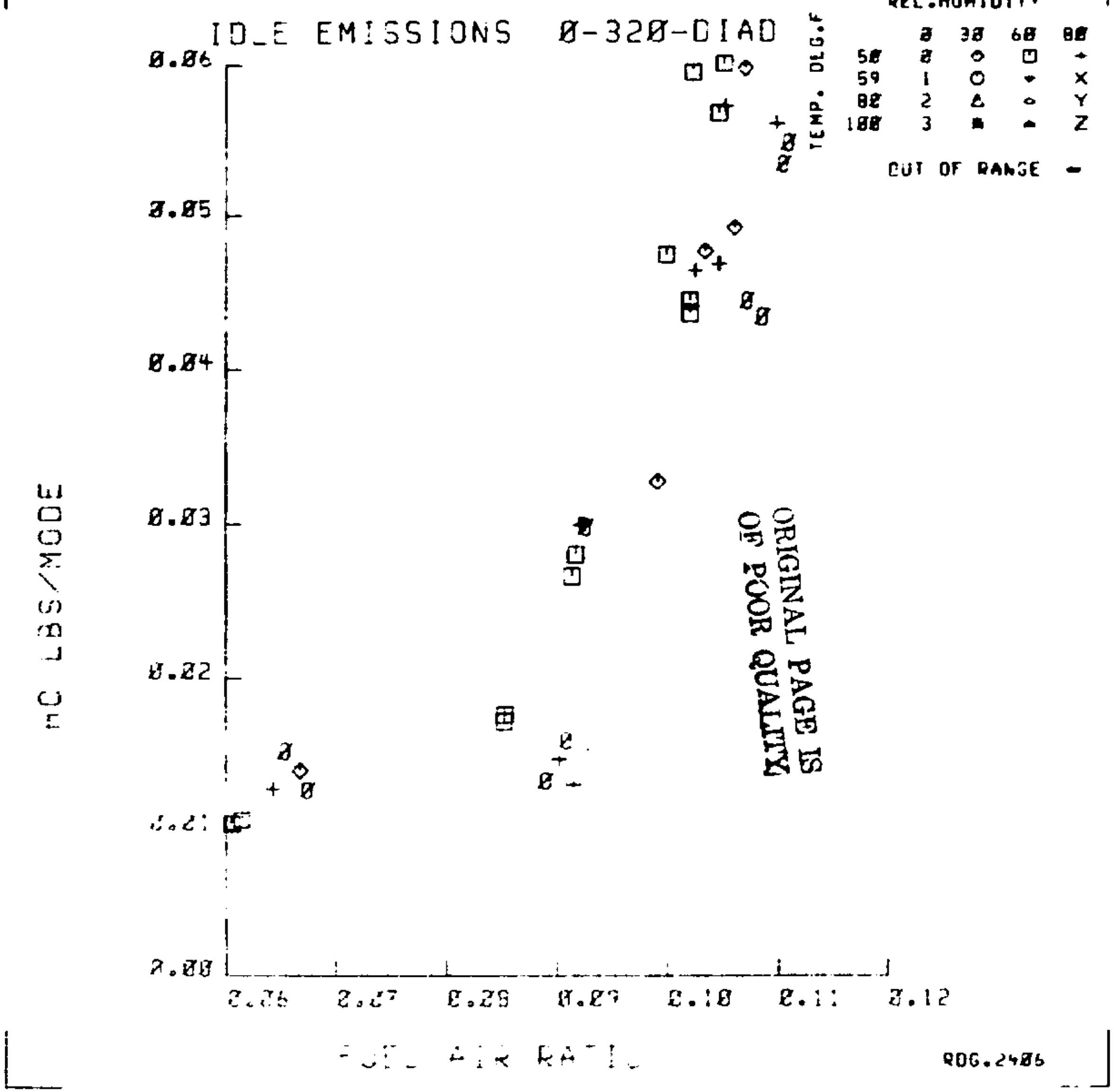

FIGURE 11f

IDLE	IDLE
2406	2412
2413	2414 ∅
2418 ∅	2424
2425	2426
2430	2464
2477	2487 ◇
2488 ◇	2489
3576	3579
3583	3584
3585 ⊡	3586
3589	3593 ⊡
3594	3605
3607	3608
3611	3618
3619	3624 +
3625 +	3628
3629	3632
3633	

NASA LEAN-OUT DATA

TEMP. 50°F REL. HUM. 0, 30, 60, 80%

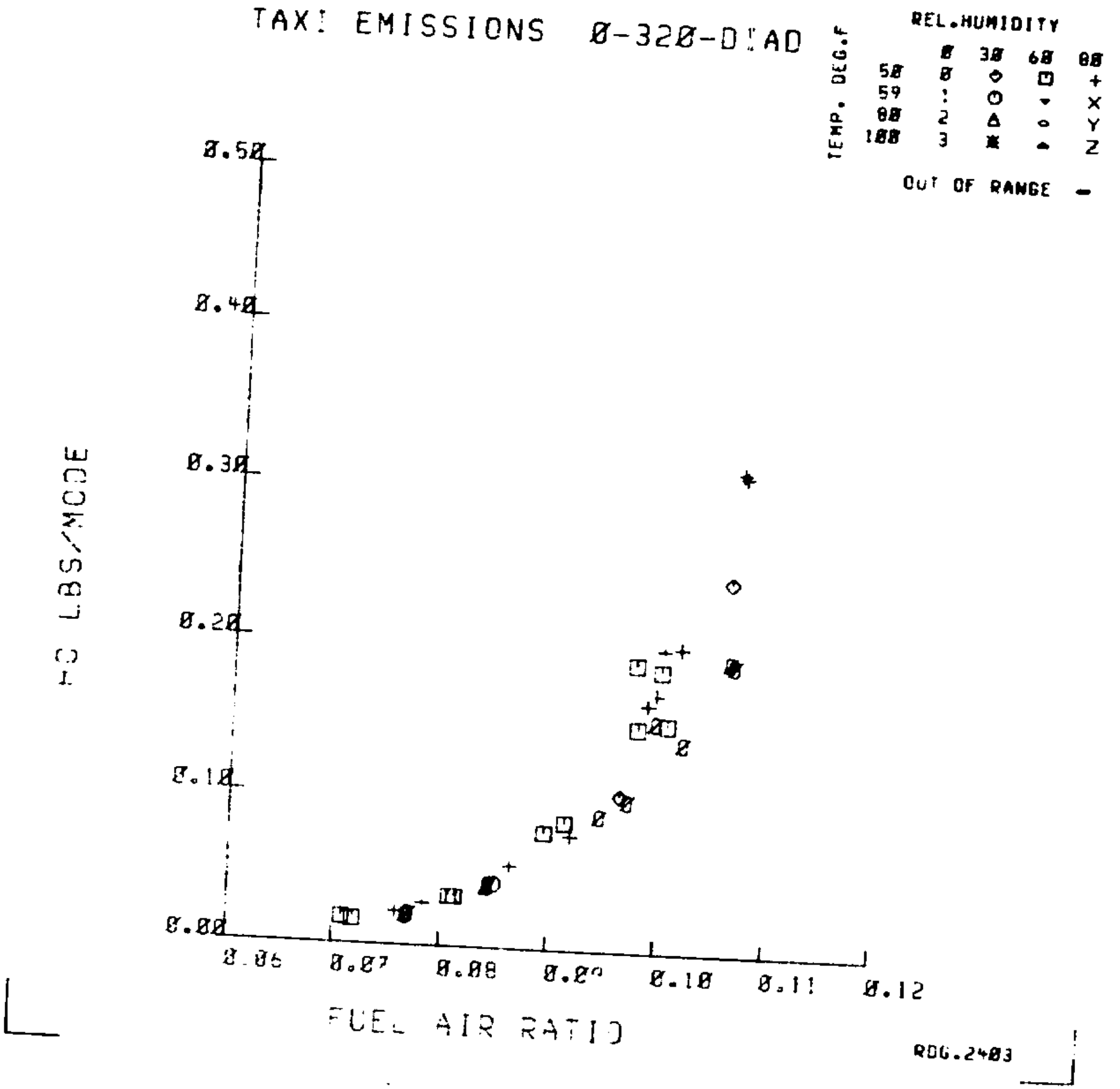

TAXI	
2403	
2409	
2415	Ø
2420	
2427	
2465	◇
2490	
3578	
3582	
3588	⊡
3592	
3610	
3614	
3623	
3627	+
3631	
3635	

TAXI	
2405	
2411	Ø
2417	
2423	
2429	
2459	◇
3577	
3581	
3587	⊡
3591	
3609	
3613	
3620	
3626	+
3630	
3634	

FIGURE 11g

NASA LEAN-OUT DATA

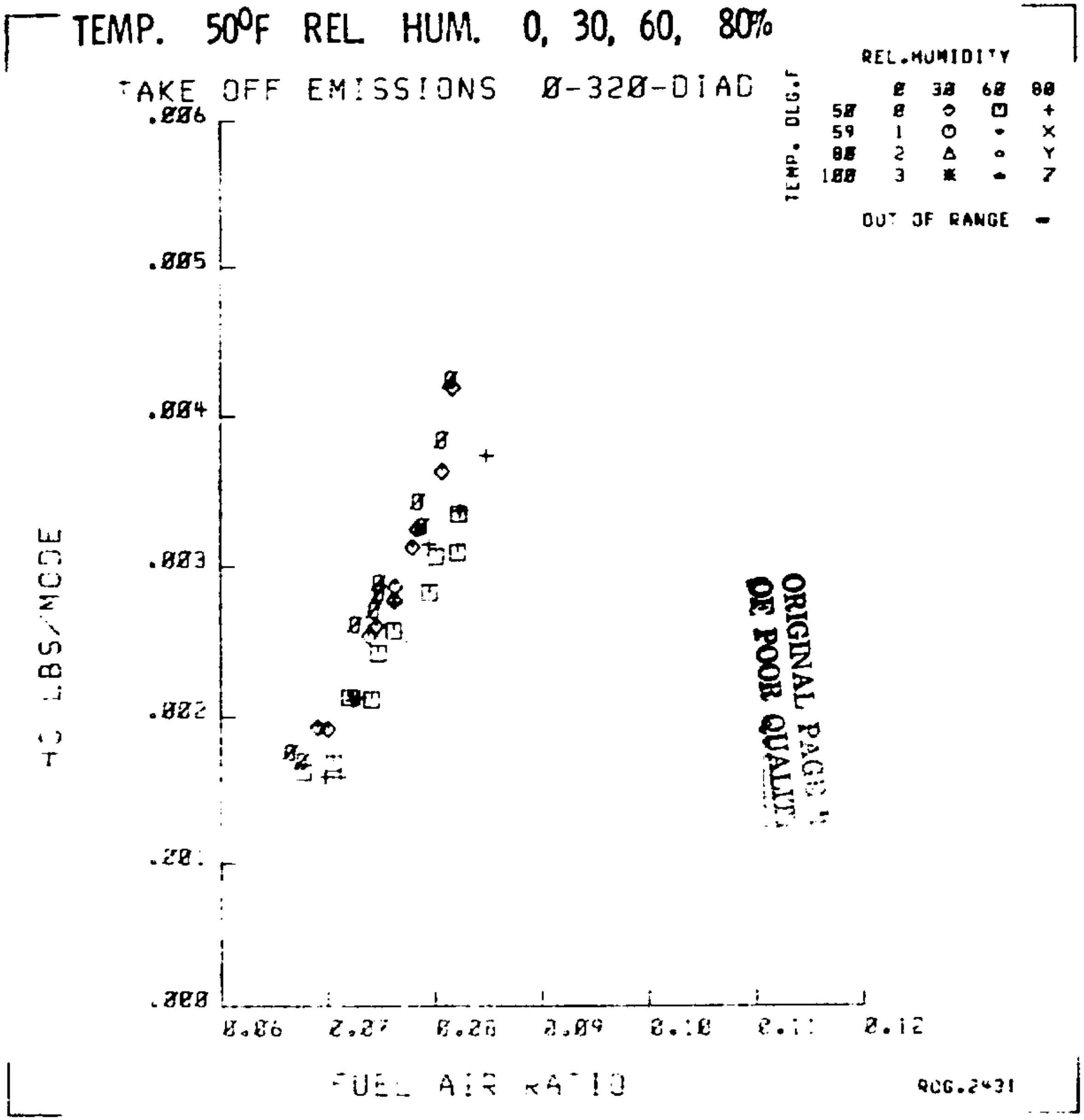

TAKE-OFF		TAKE-OFF	
2431		2435	
2438		2442	Ø
2445	Ø	2448	
2452		2455	
2459		2461	
2494		2498	
2501		2504	
2507	◇	2511	◇
2514		2517	
2521		2524	
3639		3640	
3643		3649	
3652	◻	3655	◻
3658		3661	
3664		3667	
3668		3671	
3674	+	3680	+
3686		3689	
3692		3695	

ORIGINAL PAGE IS OF POOR QUALITY

FIGURE 11h

NASA LEAN-OUT DATA

TEMP. 50^0F REL. HUM. 0, 30, 60, 80%

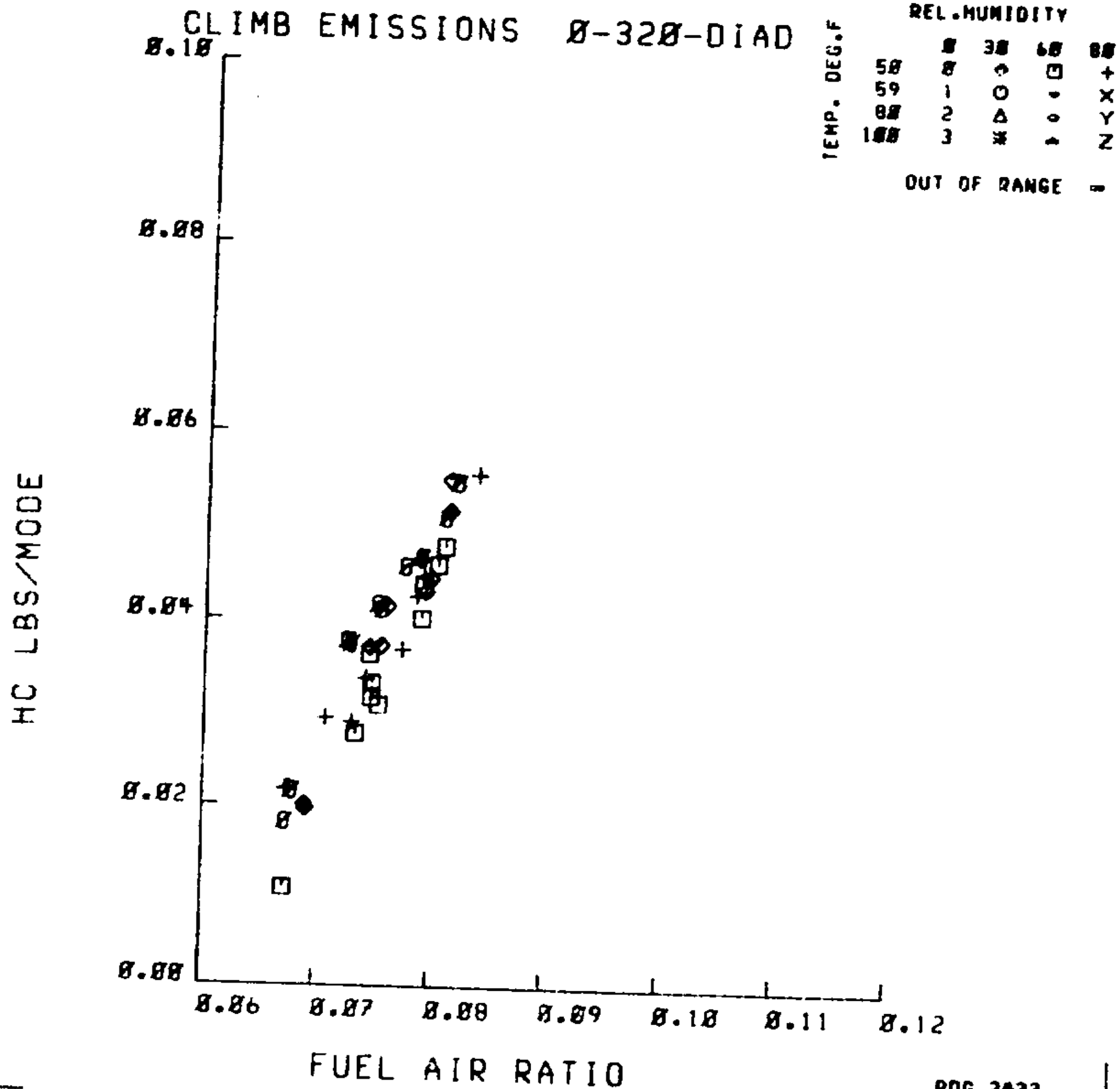

CLIMB
2433
2439
2446 ϕ
2453
2459
2495
2502
2512 ◇
2519
2525
3641
3647
3653 □
3659
3665
3672
3678
3684 +
3690
3696

CLIMB
2436
2443
2449 ϕ
2456
2462
2499
2505 ◇
2515
2522
3637
3644
3650 □
3656
3662
3669
3675
3681 +
3687
3693

FIGURE 11i

NASA LEAN-OUT DATA

TEMP. 50°F REL. HUM. 0, 30, 60, 80%

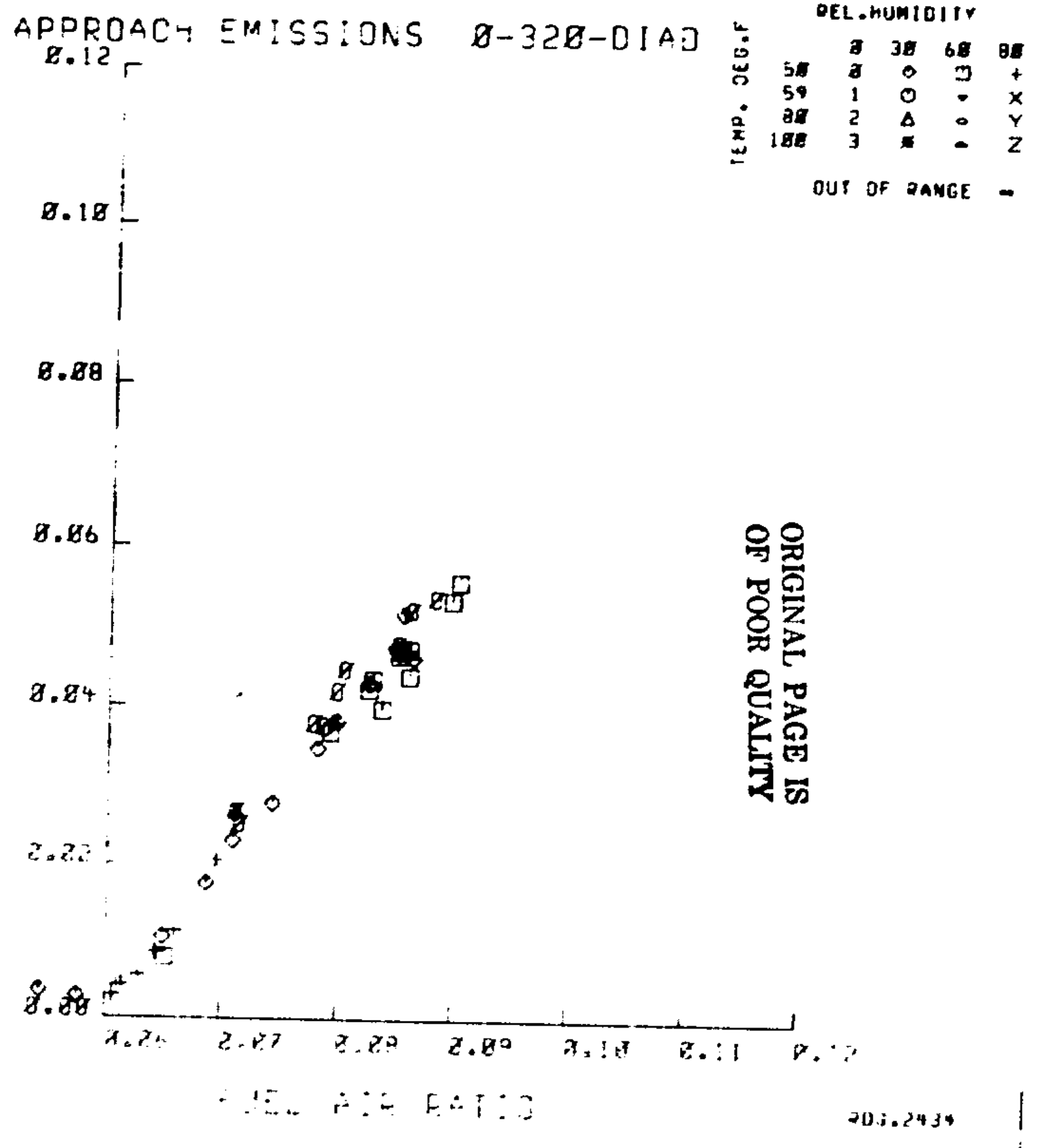

APPROACH
2434
2441
2447 ∅
2454
2460
2496
3562
3564 ◇
3566
3568
3570
3638
3645
3651 □
3657
3663
3670
3676 +
3685
3691
3697

APPROACH
2437
2444
2450 ∅
2457
2463
3561
3563
3565 ◇
3567
3569
3571
3642
3648
3654 □
3660
3666
3673
3679 +
3688
3694

FIGURE 11j

NASA LEAN-OUT DATA

TEMP. 50°F REL. HUM. 0, 30, 60, 80%

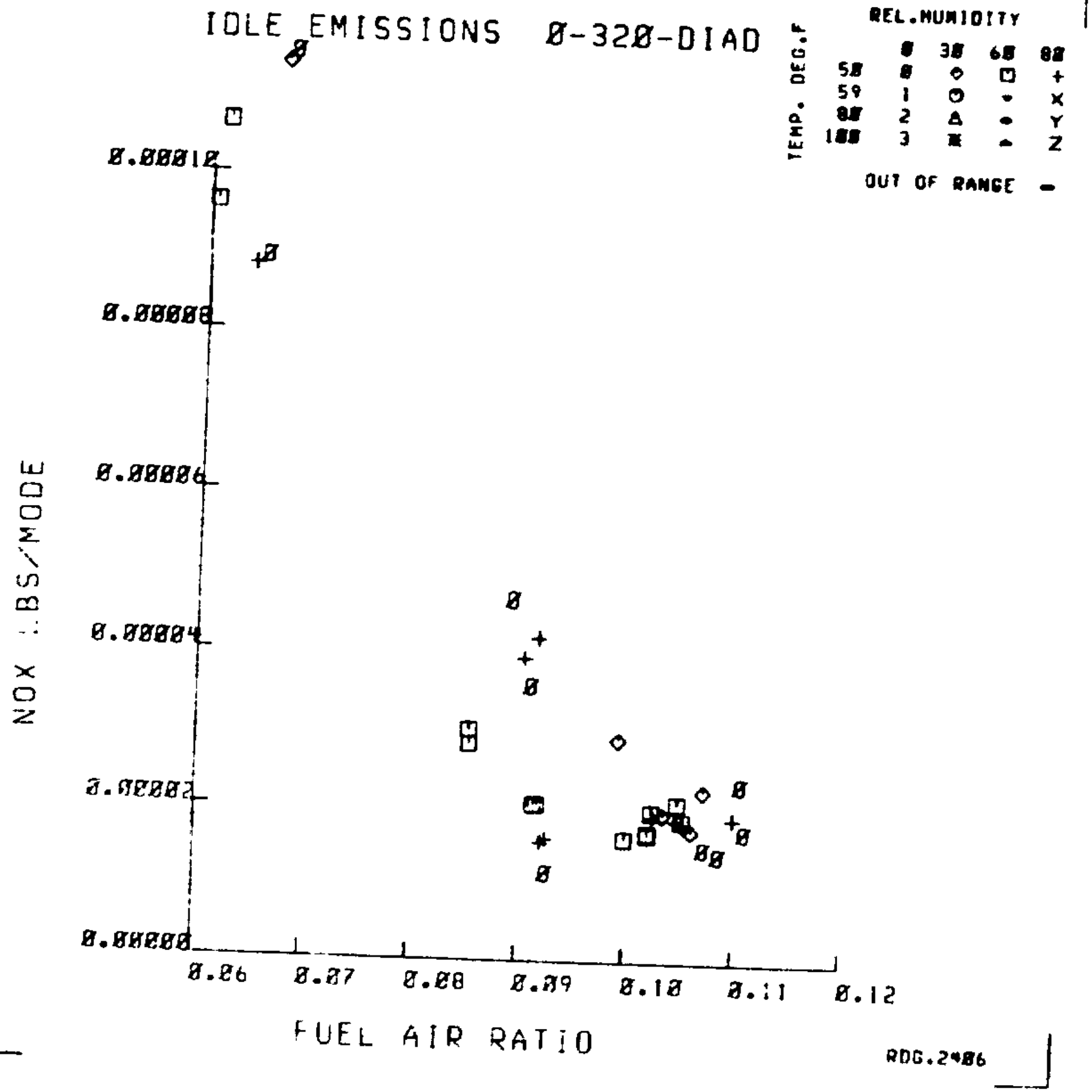

IDLE		IDLE	
2406		2412	
2413		2414	ϕ
2418	ϕ	2424	
2425		2426	
2430		2464	
2477	◇	2487	◇
2488		2489	
3576		3579	
3583		3584	
3585	□	3586	
3589		3593	□
3594		3605	
3607		3608	
3611		3618	
3619		3624	
3625	+	3628	+
3629		3632	
3633			

FIGURE 11k

NASA LEAN-OUT DATA

TEMP. 50°F REL. HUM. 0, 30, 60, 80%

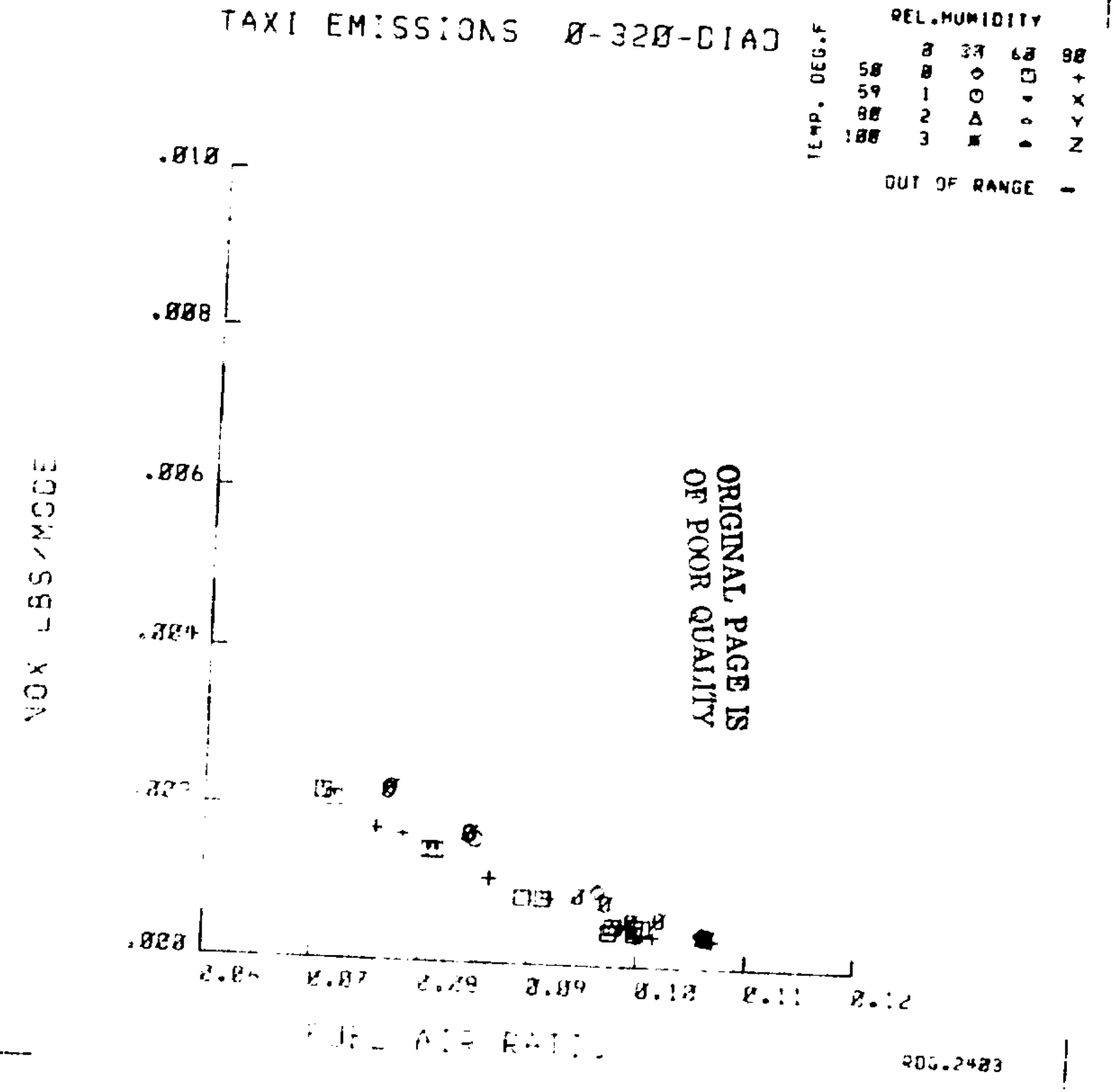

TAXI		TAXI	
2403		2405	
2409		2411	Ø
2415	Ø	2417	
2420		2423	
2427		2429	
2465	◇	2459	◇
2490		3577	
3578		3581	
3582		3587	⊡
3588	⊡	3591	
3592		3609	
3610		3613	
3614		3620	
3623		3626	+
3627	+	3630	
3631		3634	
3635			

FIGURE 11

NASA LEAN-OUT DATA

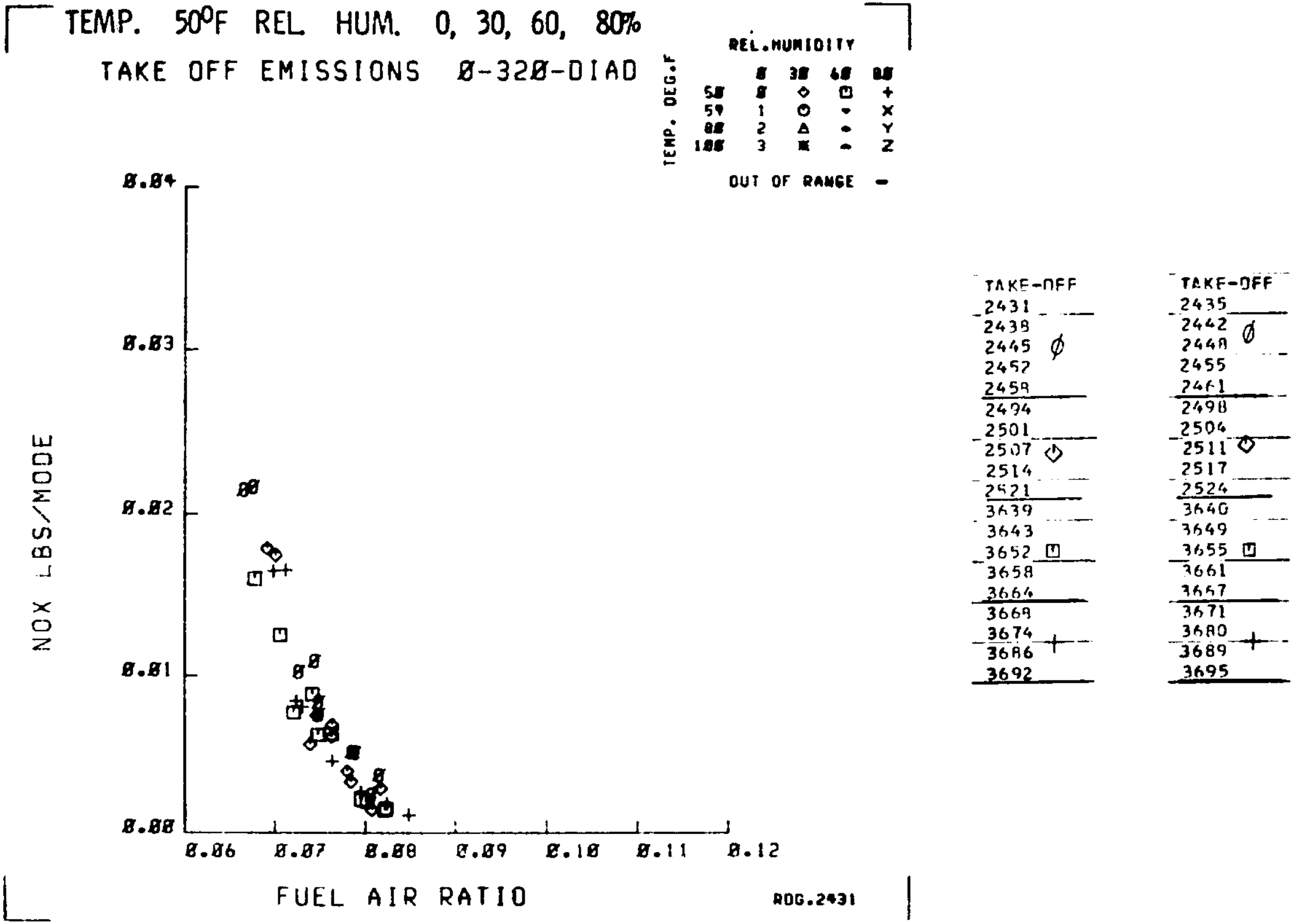

FIGURE 11m

NASA LEAN-OUT DATA

TEMP. 50°F REL. HUM. 0, 30, 60, 80%

CLIMB EMISSIONS Ø-32Ø-DIAD

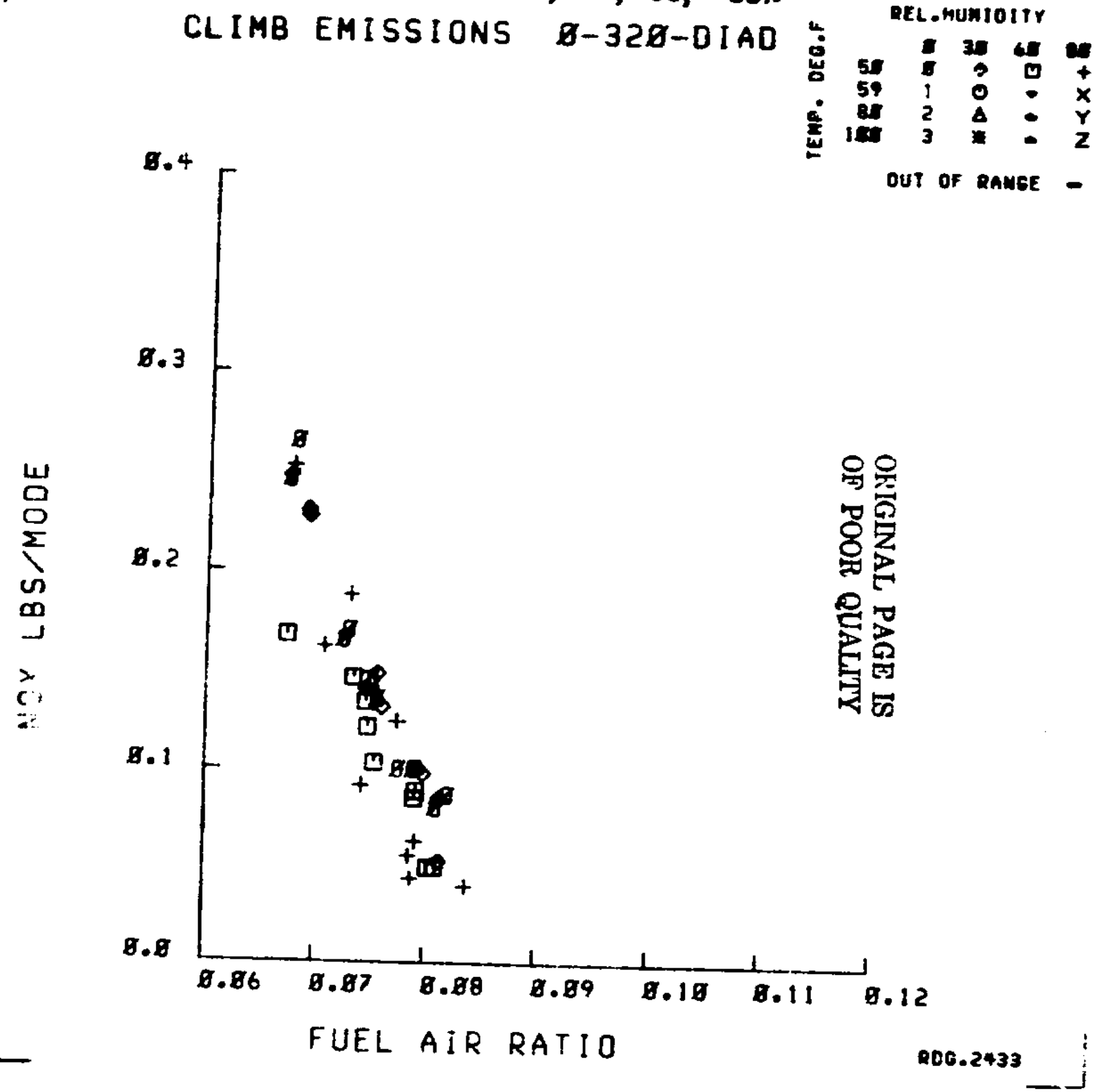

CLIMB	
2433	
2439	
2446	Ø
2453	
2459	
2495	
2502	
2512	◇
2519	
2525	
3641	
3647	
3653	□
3659	
3665	
3672	
3678	
3684	+
3690	
3696	

CLIMB	
2436	
2443	
2449	Ø
2456	
2462	
2499	
2505	
2515	◇
2522	
3637	
3644	
3650	□
3656	
3662	
3669	
3675	
3681	+
3687	
3693	

FIGURE 11n

NASA LEAN-OUT DATA

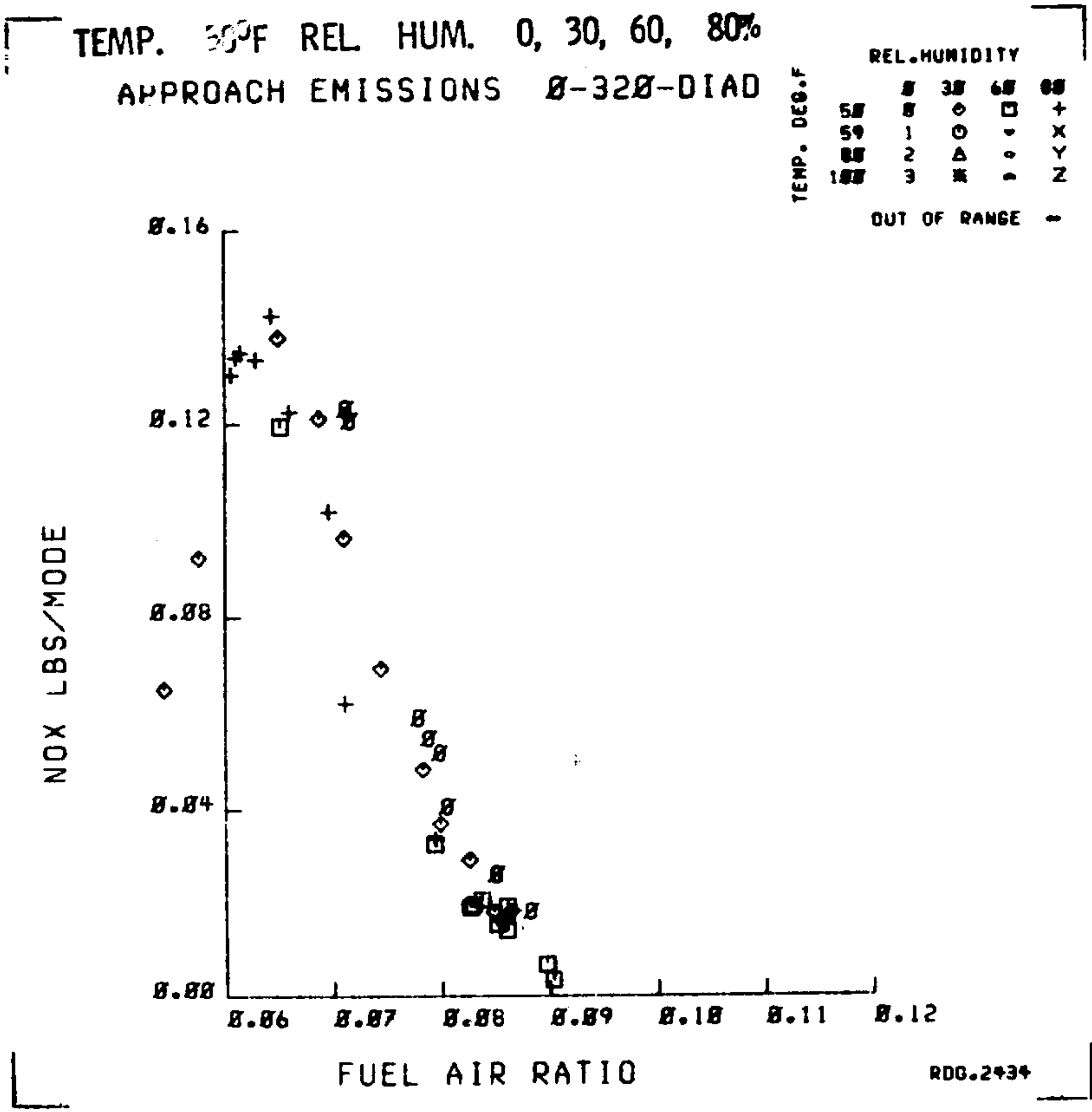

APPROACH	
2434	
2441	
2447	Ø
2454	
2460	
2496	
3562	
3564	◇
3566	
3568	
3570	
3638	
3645	
3651	□
3657	
3663	
3670	
3676	+
3685	
3691	
3697	

APPROACH	
2437	
2444	
2450	Ø
2457	
2453	
3561	
3563	
3565	◇
3567	
3569	
3571	
3642	
3648	
3654	□
3660	
3656	
3673	
3679	+
3688	
3694	

FIGURE 11c

NASA LEAN-OUT DATA

TEMP. 59°F REL. HUM. 0, 30, 60, 80%

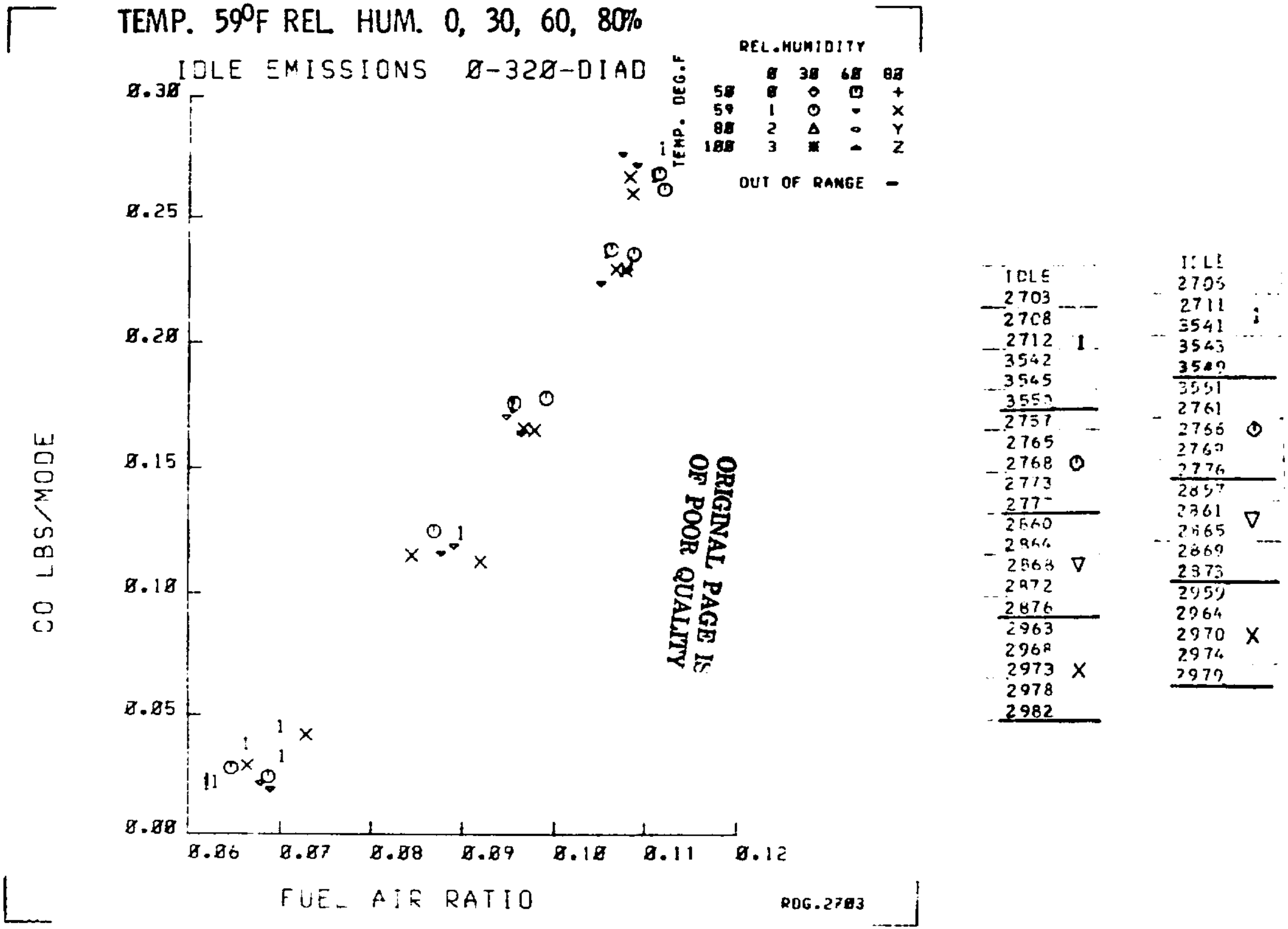

FIGURE 12a

NASA LEAN-OUT DATA

TEMP. 59°F REL. HUM. 0, 30, 60, 80%

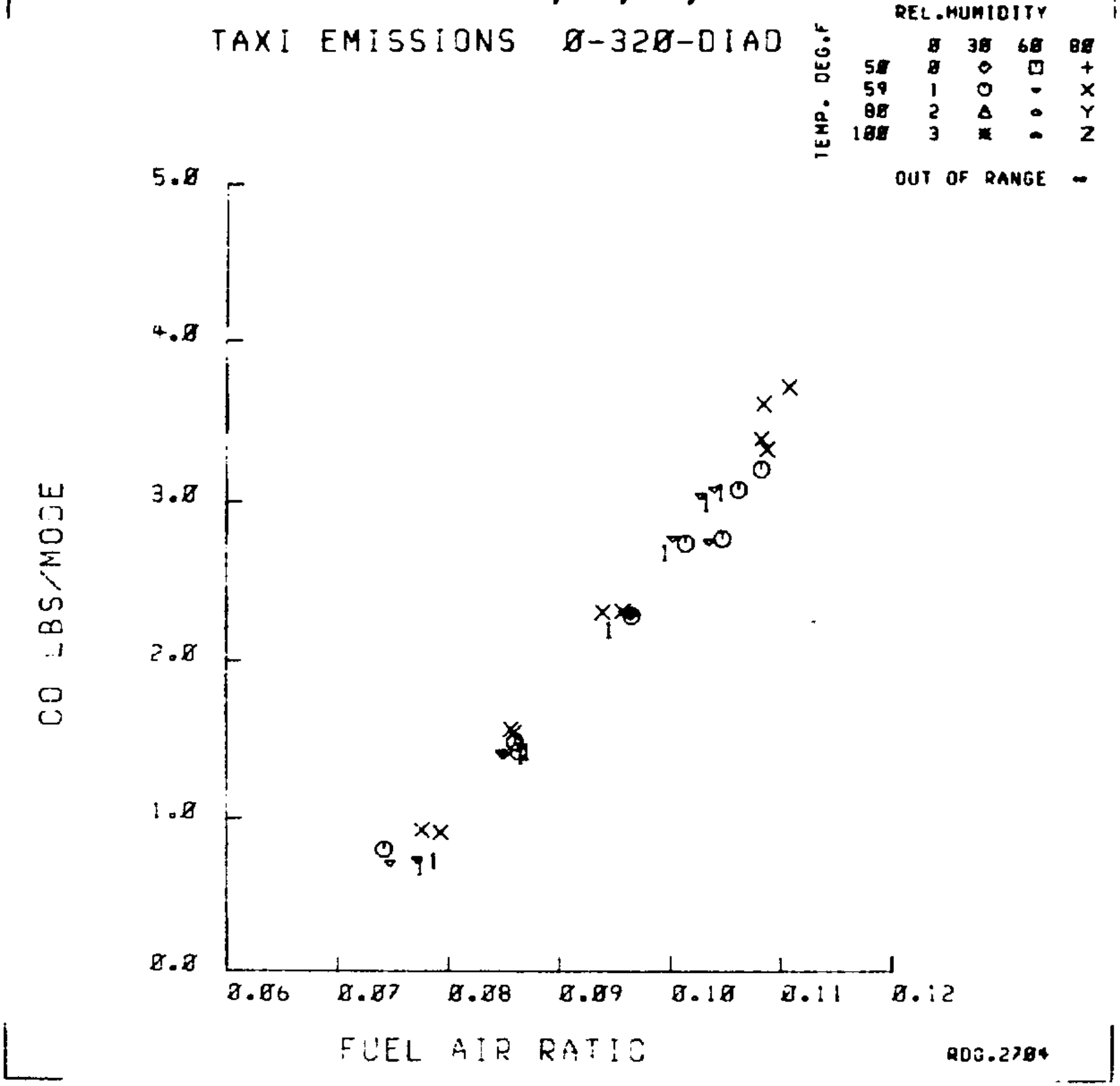

TAXI		TAXI	
2704		2705	
2710	1	2714	1
2717		2718	
2721		2722	
2758		2759	
2763		2764	O
2767	O	2770	
2771		2774	
2775		2858	
2859		2862	
2863		2866	∇
2867	∇	2870	
2871		2874	
2875		2960	
2961		2965	
2967		2971	X
2972	X	2975	
2976		2980	
2981			

FIGURE 12b

NASA LEAN-OUT DATA

TEMP. 59°F REL. HUM. 0, 30, 60, 80%

TAKE OFF EMISSIONS Ø-32Ø-DIAD

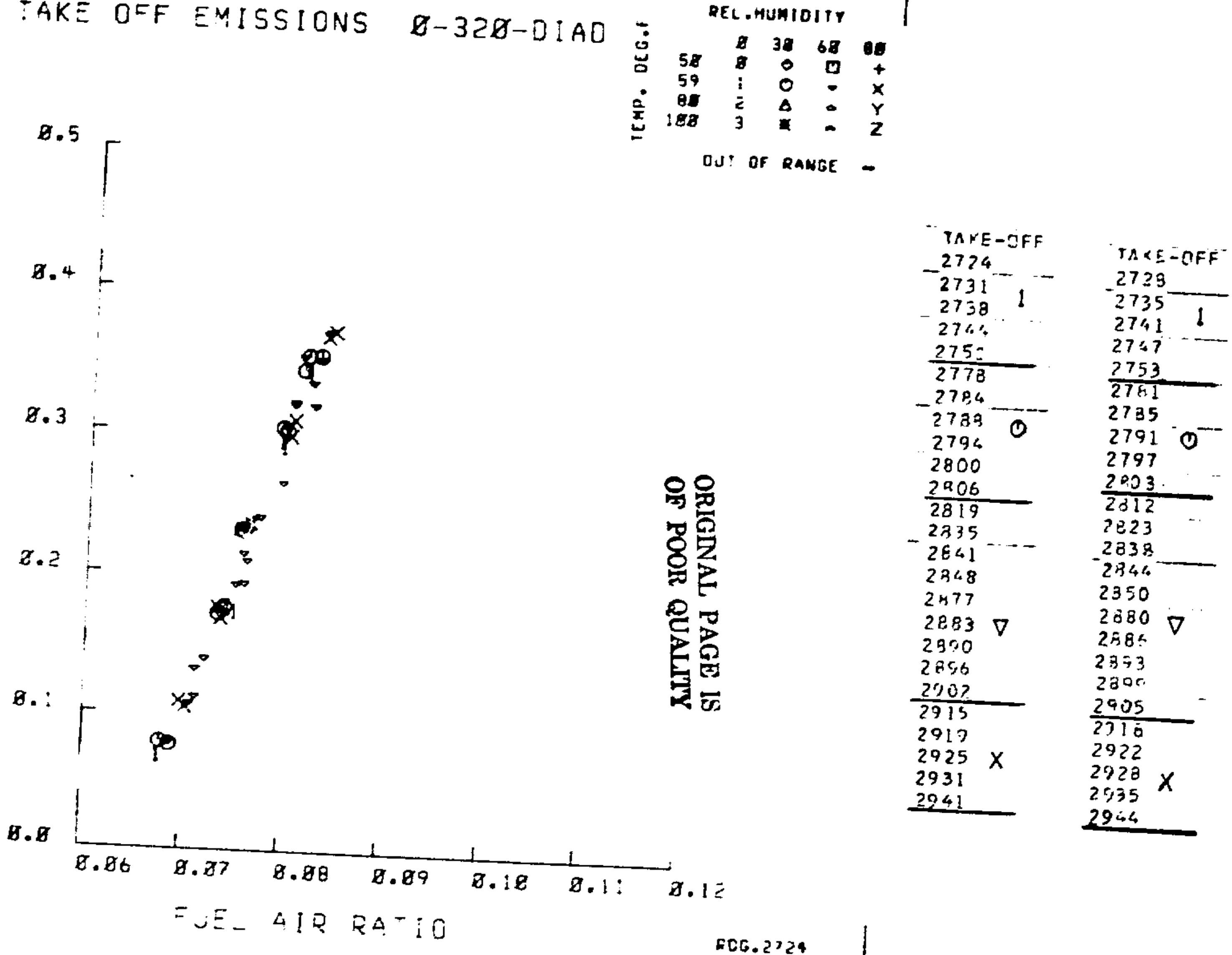

ORIGINAL PAGE IS OF POOR QUALITY

FIGURE 12c

NASA LEAN-OUT DATA

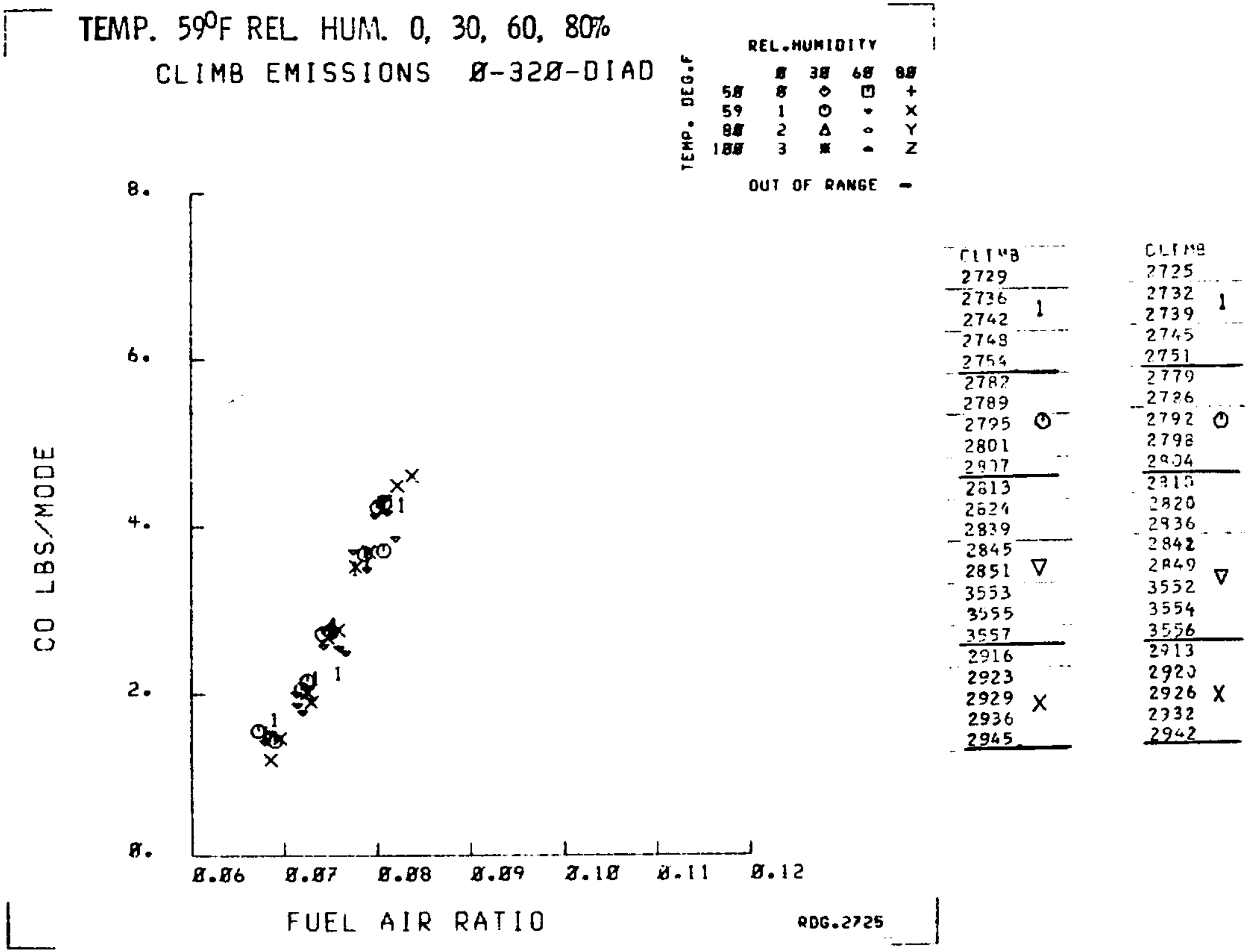

FIGURE 12a

NASA LEAN-OUT DATA

TEMP. 59°F REL. HUM. 0, 30, 60, 80%

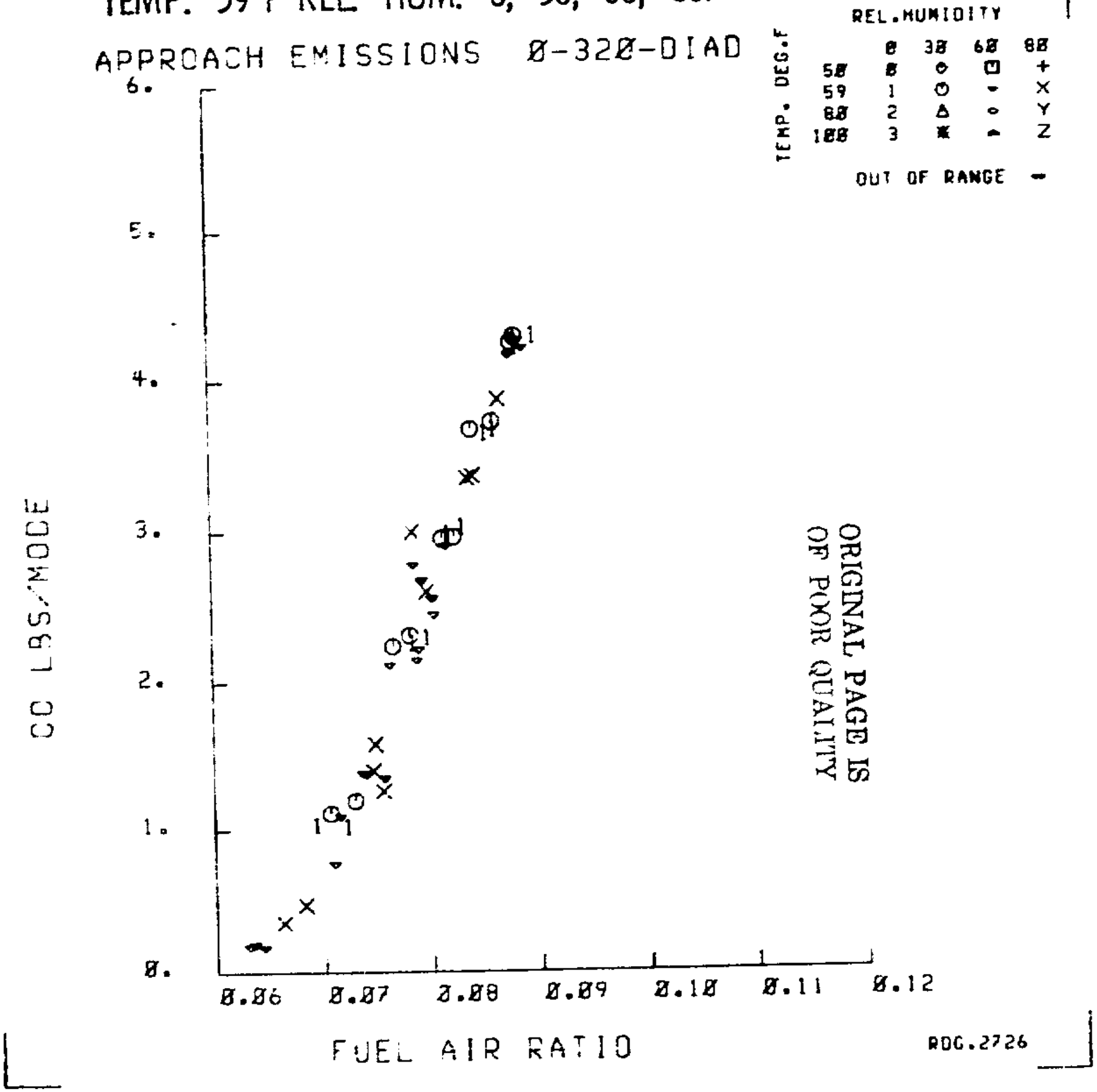

APPROACH		APPROACH	
2726		2730	
2733	1	2737	1
2740		2743	
2746		2749	
2752		2755	
2780		2783	
2787		2790	
2793	⊙	2796	⊙
2799		2802	
2805		2808	
2811		2814	
2822		2825	
2837		2840	
2843		2846	
2847		2852	
2879	▽	2882	▽
2885		2889	
2892		2895	
2898		2901	
2904		2908	
2914		2917	
2921		2924	
2927	X	2930	X
2934		2940	
2943		2946	

FIGURE 12e

NASA LEAN-OUT DATA

TEMP. 59°F REL. HUM. 0, 30, 60, 80%

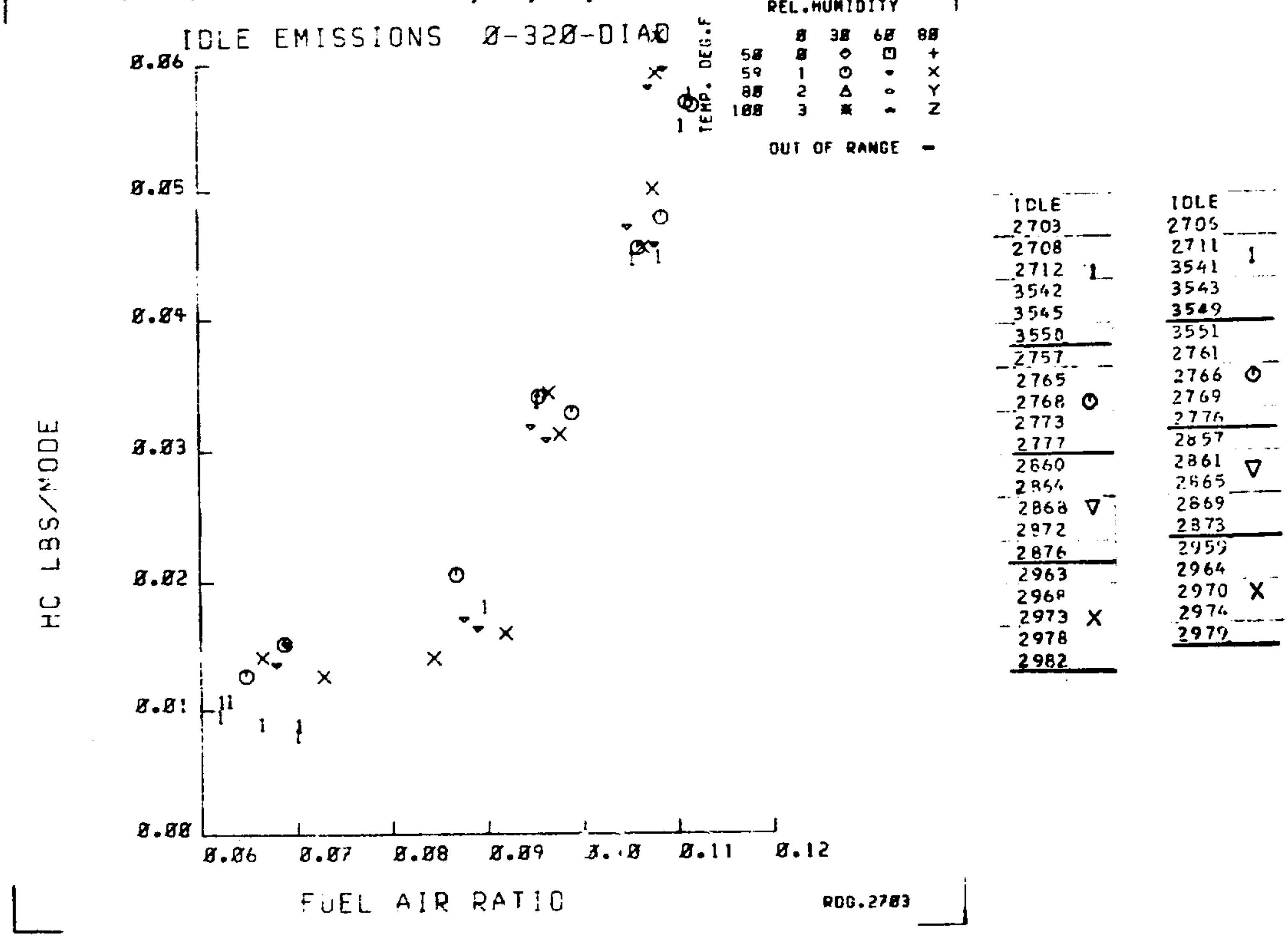

FIGURE 12f

NASA LEAN-OUT DATA

TEMP. 59°F REL. HUM. 0, 30, 60, 80%

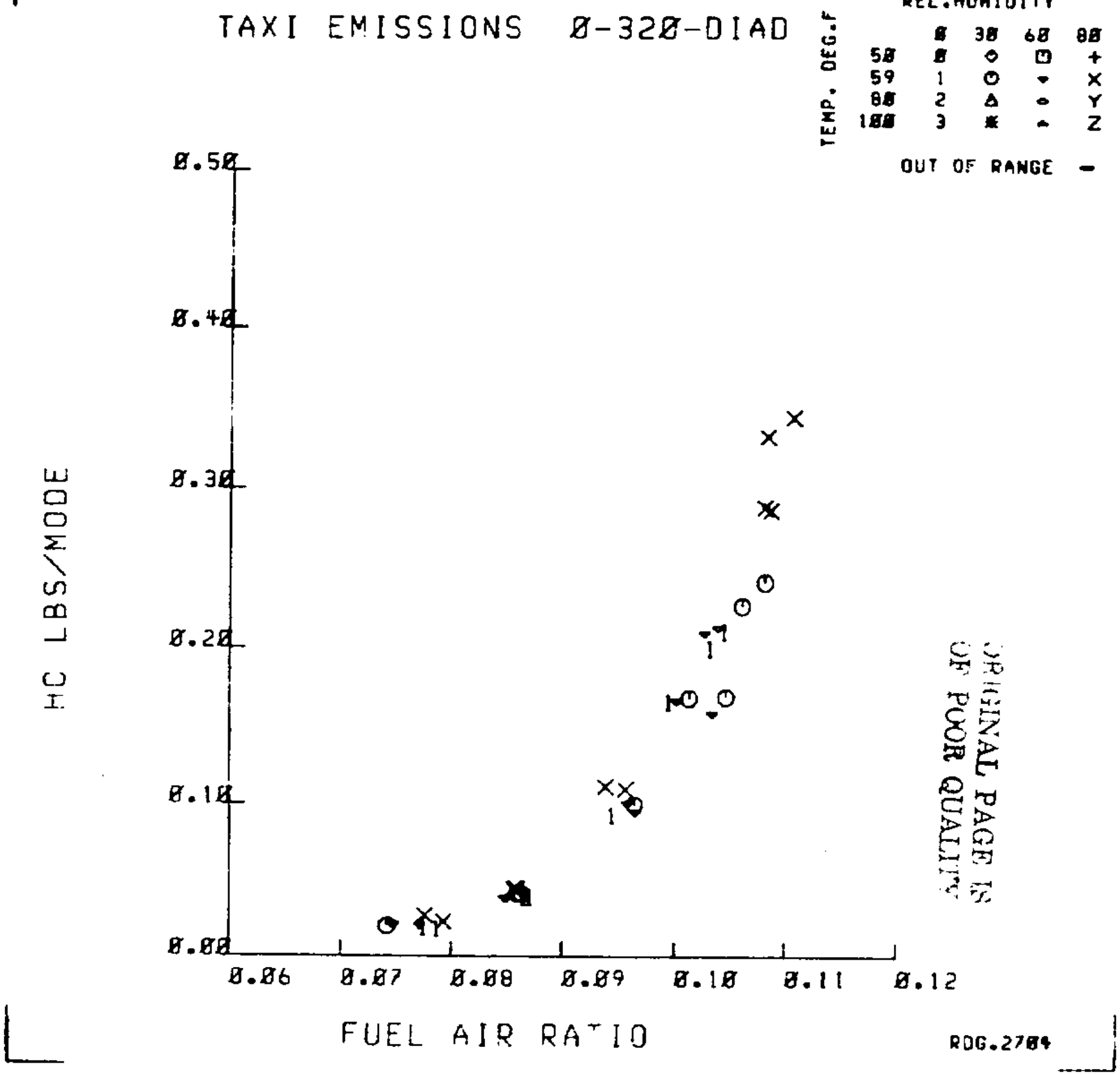

TAXI	
2704	
2710	1
2717	
2721	
2758	
2763	
2767	O
2771	
2775	
2859	
2863	
2867	∇
2871	
2875	
2961	
2967	
2972	X
2976	
2981	

TAXI	
2705	
2714	1
2718	
2722	
2759	
2764	O
2770	
2774	
2858	
2862	
2866	∇
2870	
2874	
2960	
2965	
2971	X
2975	
2980	

FIGURE 12g

NASA LEAN-OUT DATA

TEMP. 59°F REL. HUM. 0, 30, 60, 80%

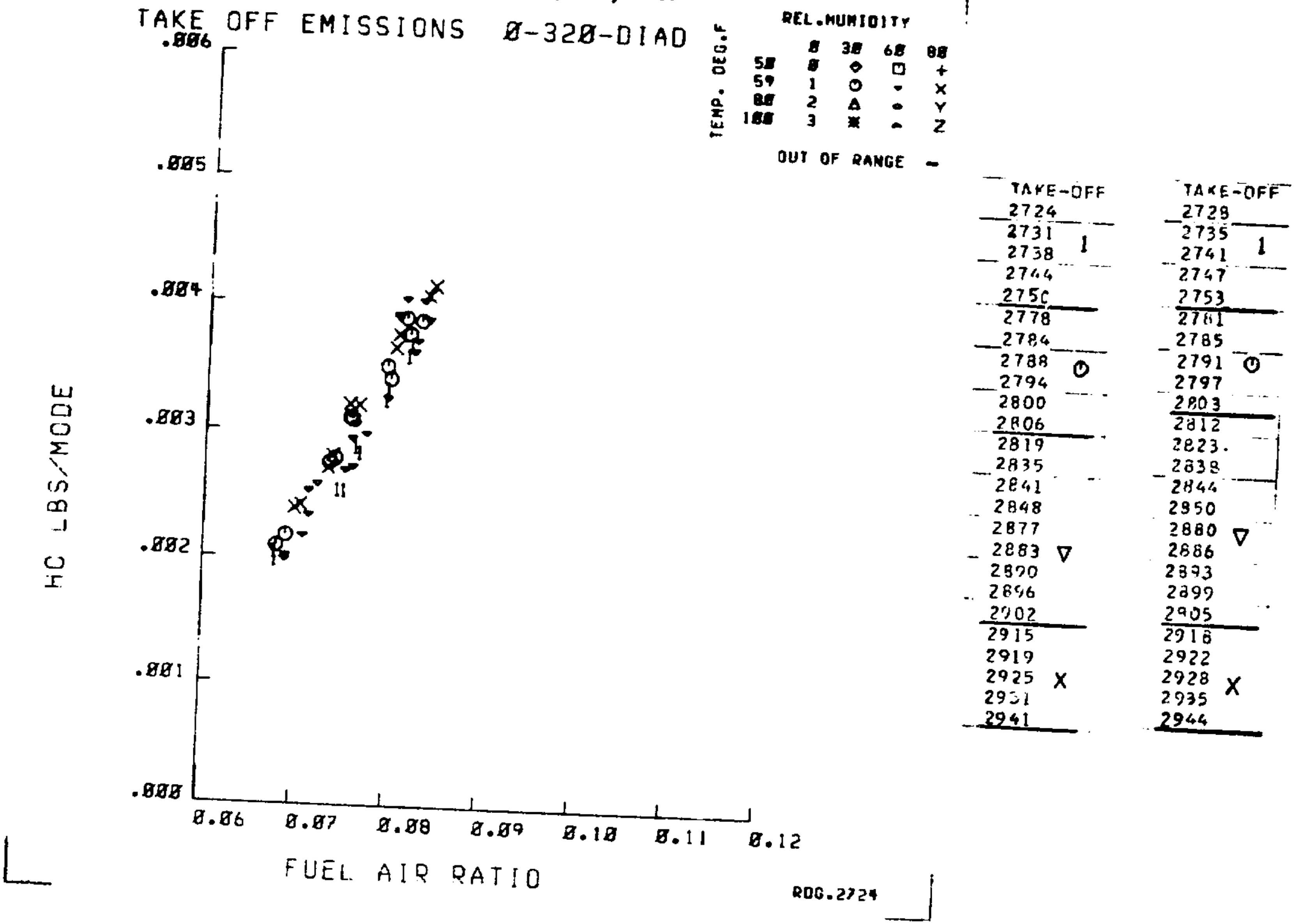

FIGURE 12h

NASA LEAN-OUT DATA

TEMP. 59°F REL. HUM. 0, 30, 60, 80%

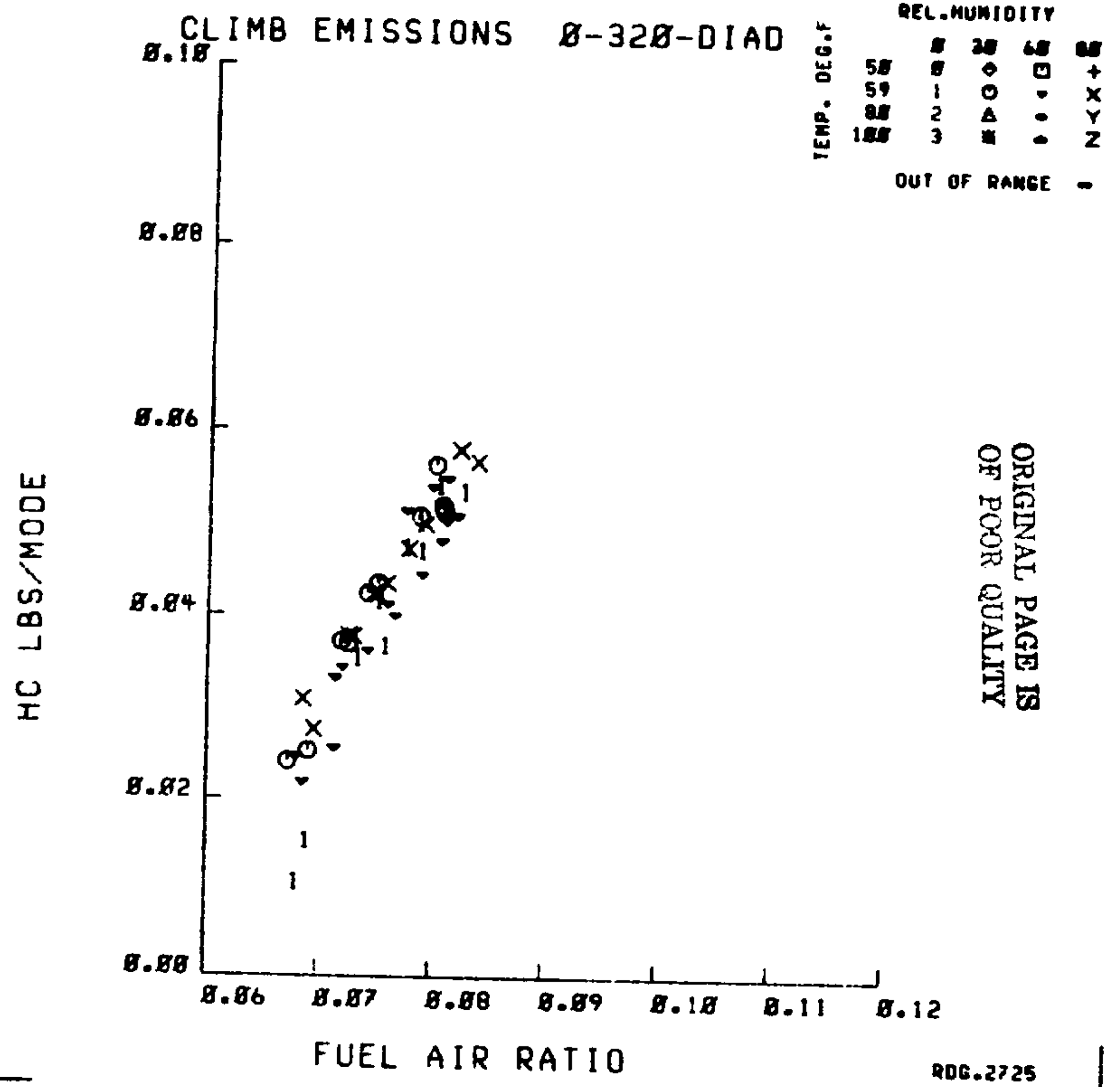

CLIMB	
2725	
2732	1
2739	
2745	
2751	
2779	
2786	
2792	O
2798	
2804	
2810	
2820	
2836	
2842	
2849	∇
3552	
3554	
3556	
2913	
2920	
2926	X
2932	
2942	

CLIMB	
2729	
2736	1
2742	
2748	
2754	
2782	
2789	
2795	O
2801	
2807	
2813	
2824	
2839	
2845	
2851	∇
3553	
3555	
3557	
2916	
2923	
2929	X
2936	
2945	

ORIGINAL PAGE IS OF POOR QUALITY

FIGURE 12i

NASA LEAN-OUT DATA

TEMP. 59^{0}F REL. HUM. 0, 30, 60, 80%

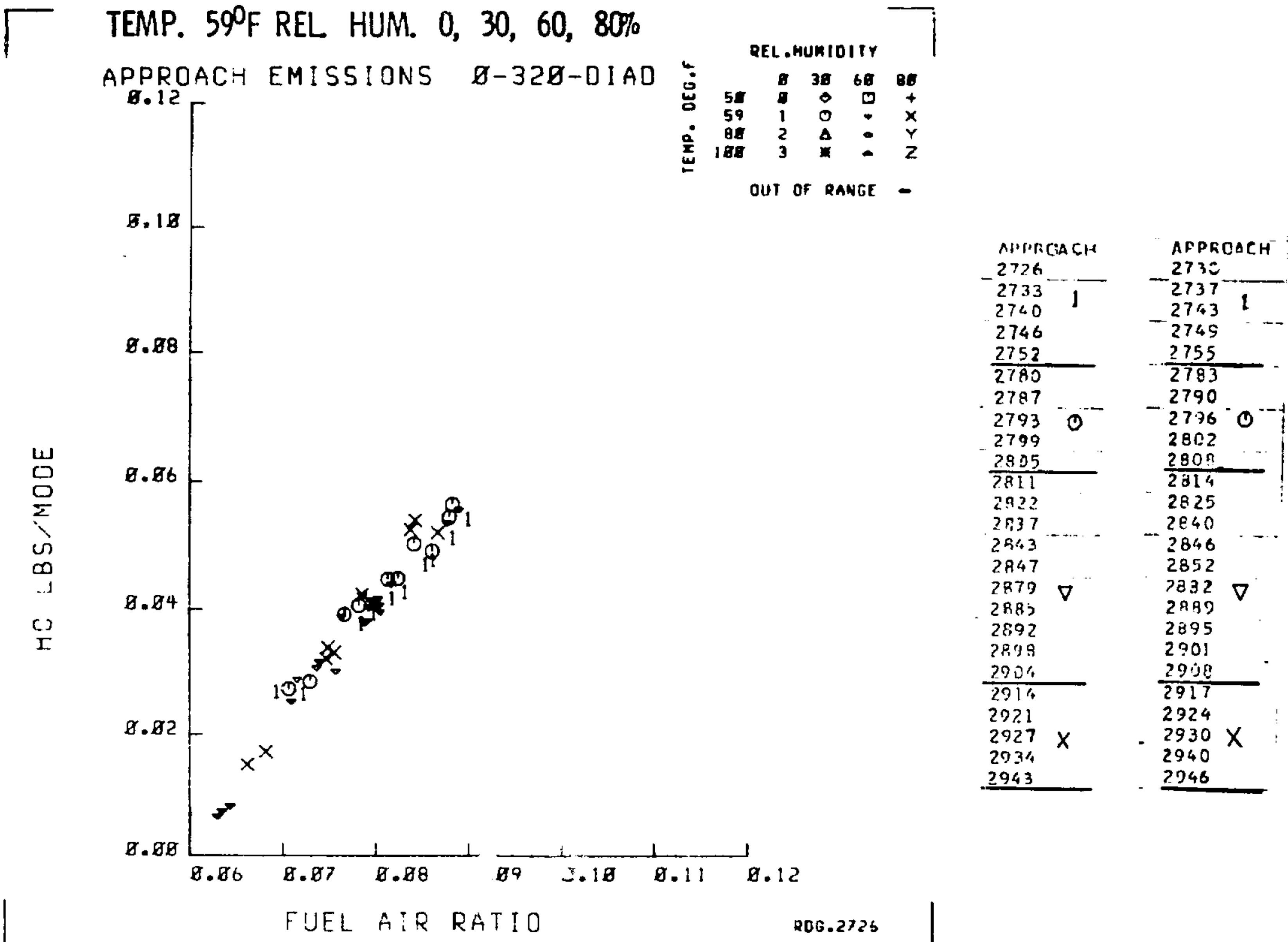

FIGURE 12j

NASA LEAN-OUT DATA

TEMP. 59°F REL. HUM. 0, 30, 60, 80%

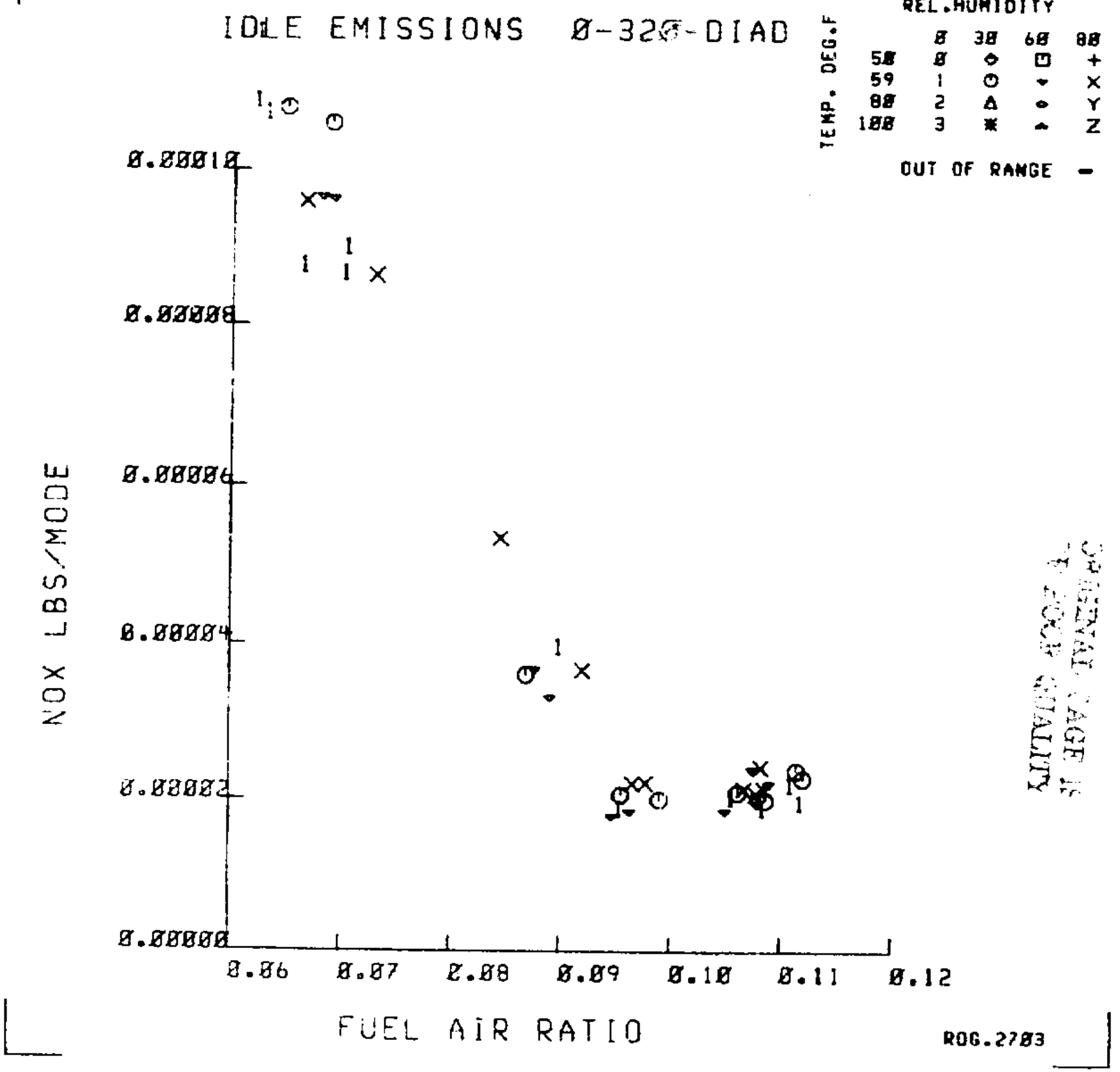

IDLE	
2703	
2708	
2712	1
3542	
3545	
3550	
2757	
2765	
2760	⊙
2773	
2777	
2860	
2864	
2868	▽
2972	
2876	
2963	
2968	
2973	X
2978	
2982	

IDLE	
2705	
2711	1
3541	
3543	
3549	
3551	
2761	
2766	⊙
2769	
2776	
2857	
2861	▽
2865	
2869	
2873	
2959	
2964	
2970	X
2974	
2979	

ORIGINAL PAGE IS OF POOR QUALITY

FIGURE 12k

NASA LEAN-OUT DATA

TEMP 59°F REL. HUM. 0, 30, 60, 80%

TAXI EMISSIONS Ø-320-DIAD

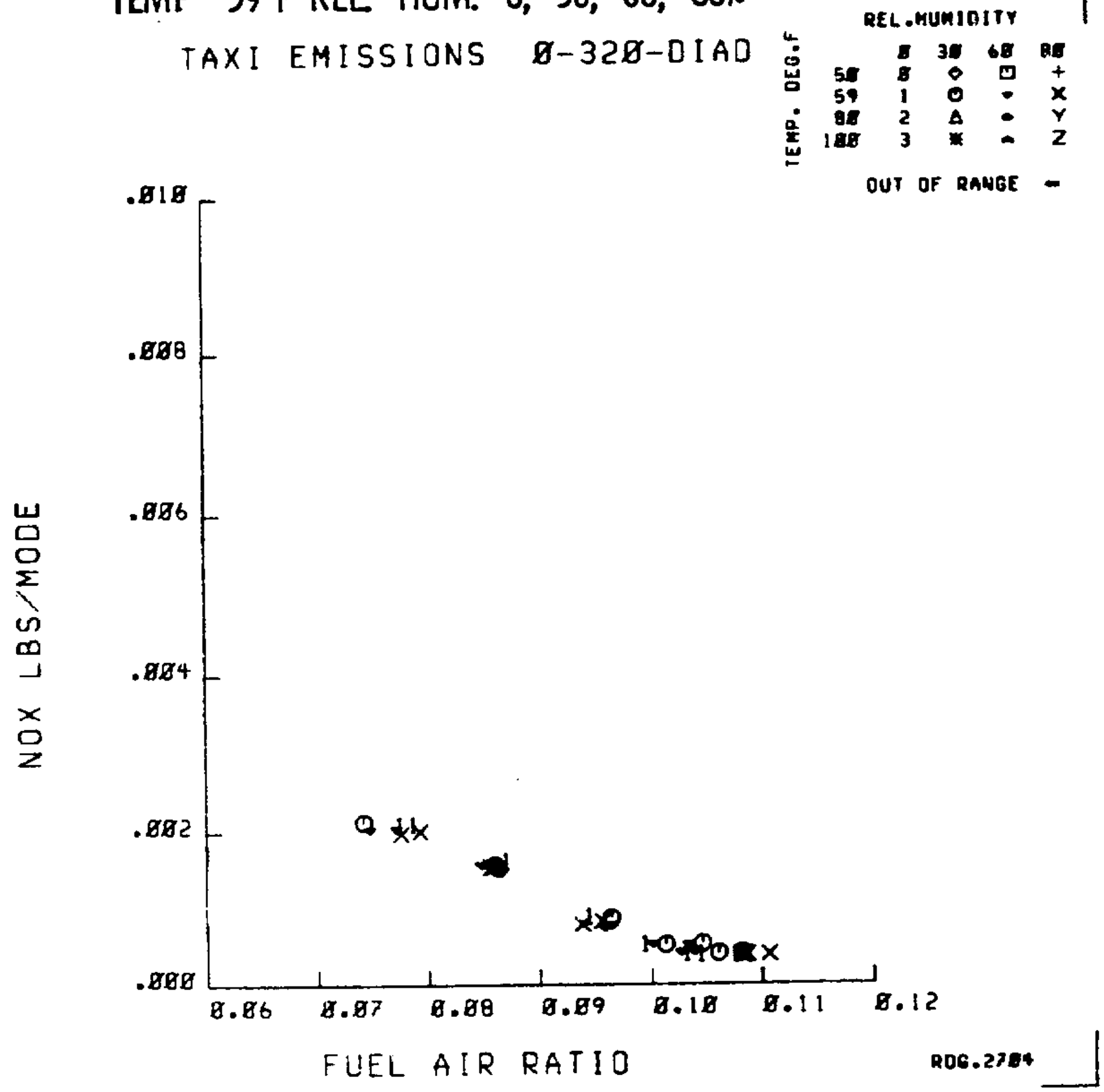

TAXI		TAXI	
2704		2705	
2710	1	2714	1
2717		2718	
2721		2722	
2758		2759	
2763		2764	
2767	O	2770	O
2771		2774	
2775		2858	
2859		2862	
2863		2866	∇
2867	∇	2870	
2871		2874	
2875		2960	
2961		2965	
2967		2971	X
2972	X	2975	
2976		2980	
2981			

FIGURE 121

NASA LEAN-OUT DATA

TEMP. 59°F REL. HUM. 0, 30, 60, 80%

TAKE OFF EMISSIONS Ø-32Ø-DIAD

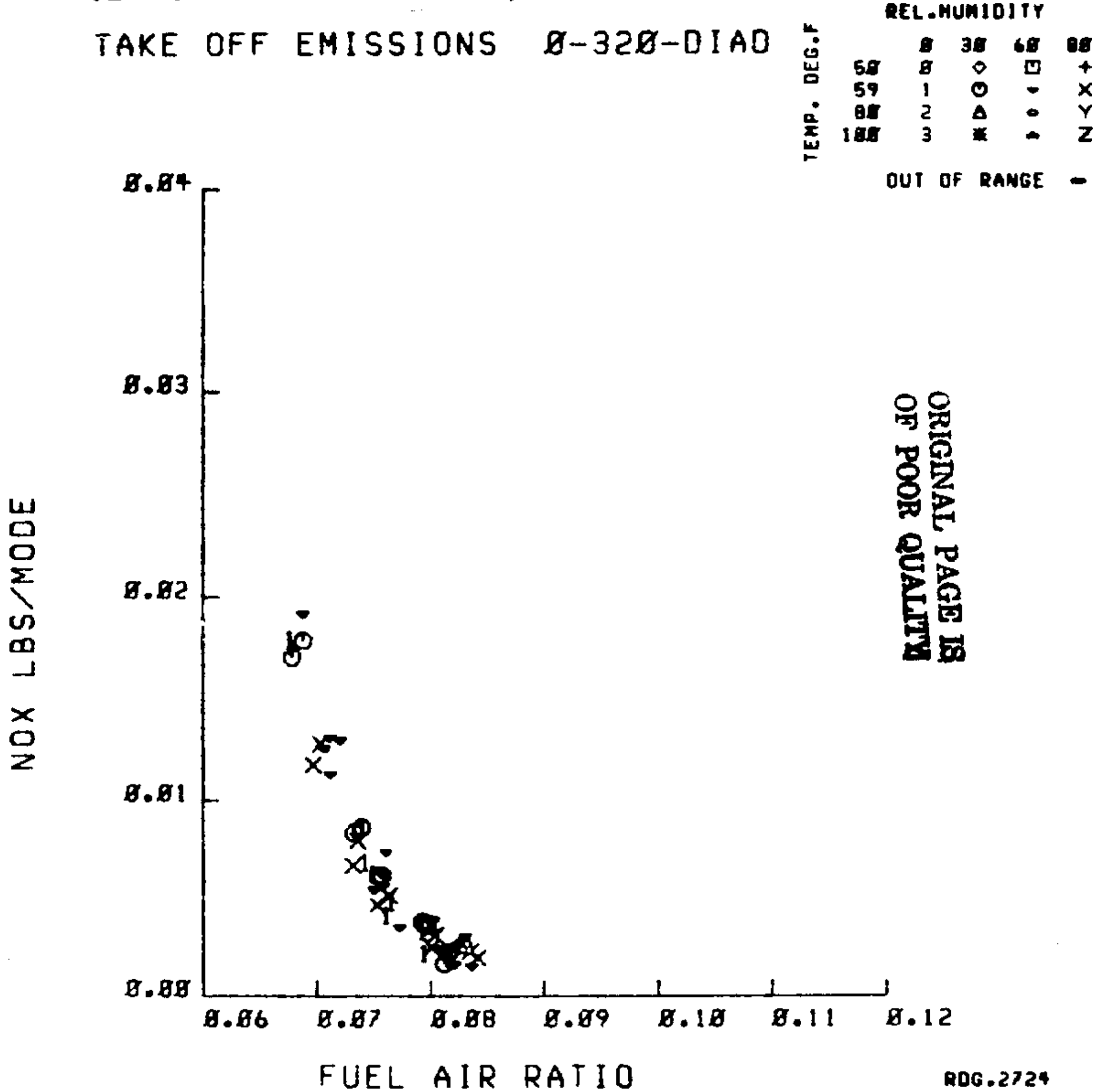

TAKE-OFF		TAKE-OFF	
2724		2729	
2731	1	2735	1
2738		2741	
2744		2747	
2750		2753	
2778		2761	
2784		2785	
2788	⊙	2791	⊙
2794		2797	
2800		2803	
2806		2812	
2819		2823	
2835		2838	
2841		2844	
2848		2850	
2877		2860	▽
2883	▽	2886	
2890		2893	
2896		2899	
2902		2905	
2915		2916	
2919		2922	
2925	X	2928	X
2931		2935	
2941		2944	

FIGURE 12m

NASA LEAN-OUT DATA

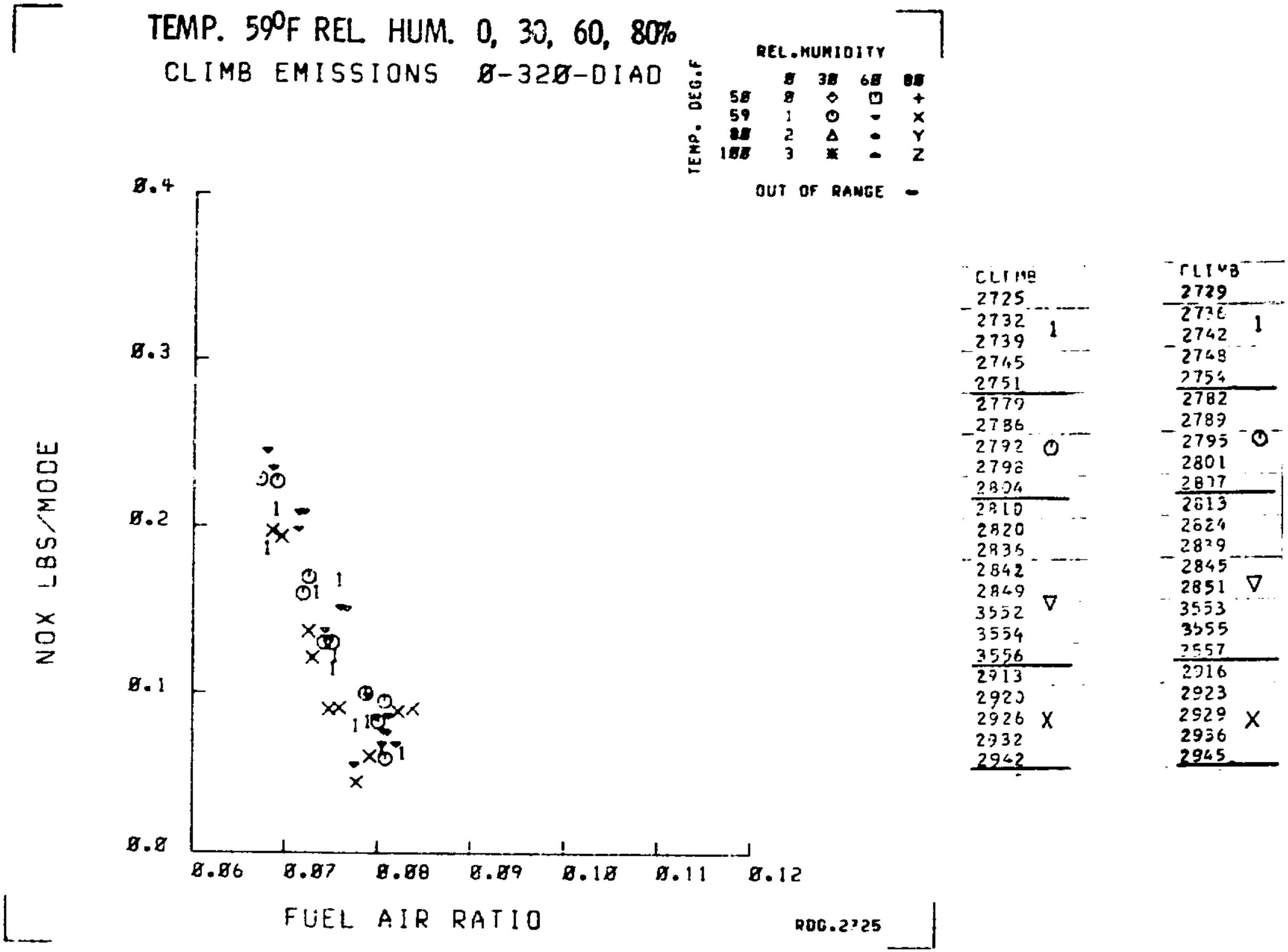

FIGURE 12n

NASA LEAN-OUT DATA

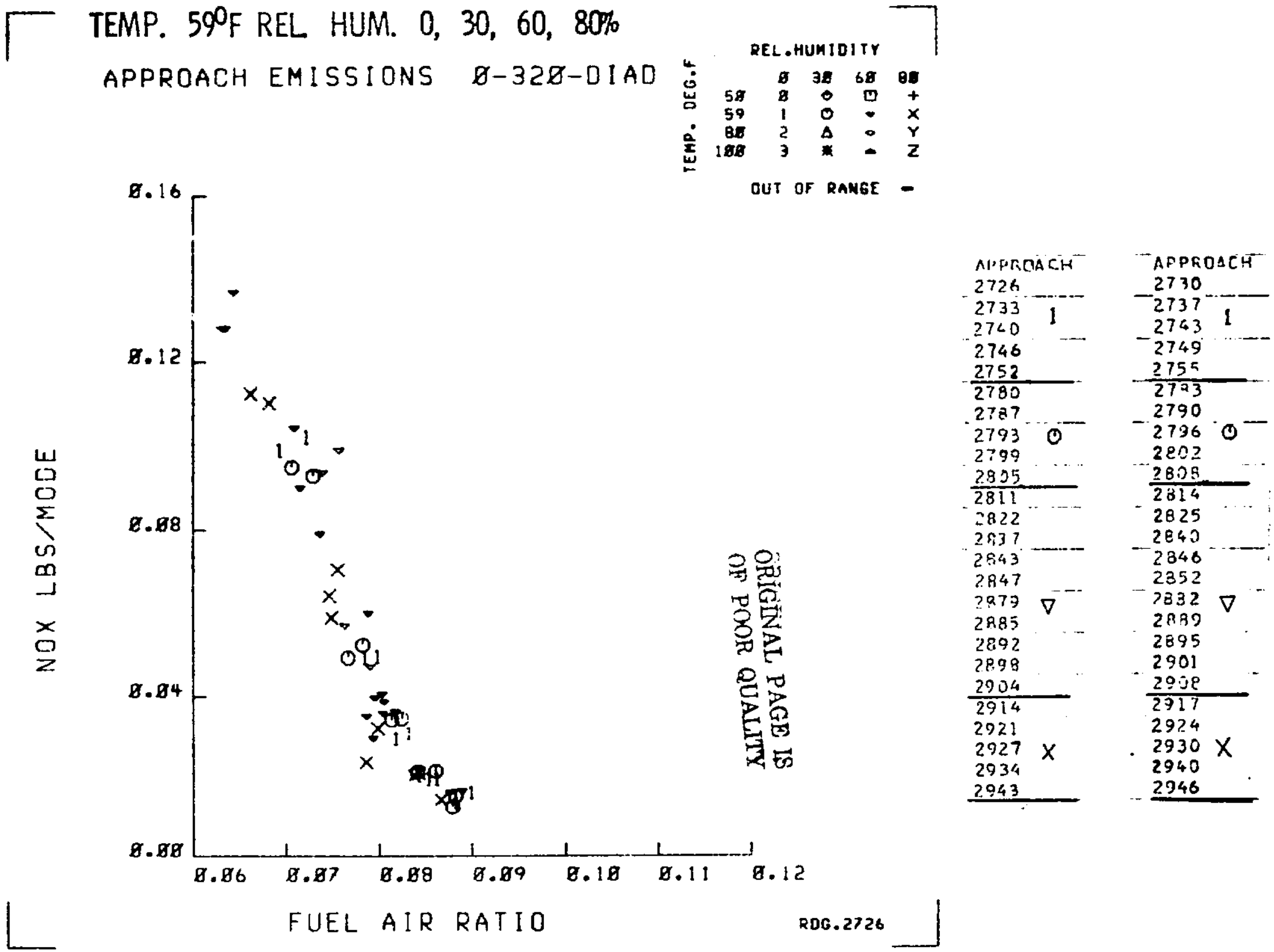

FIGURE 12o

NASA LEAN-OUT DATA

TEMP. 80°F REL. HUM. 0, 30, 60, 80%

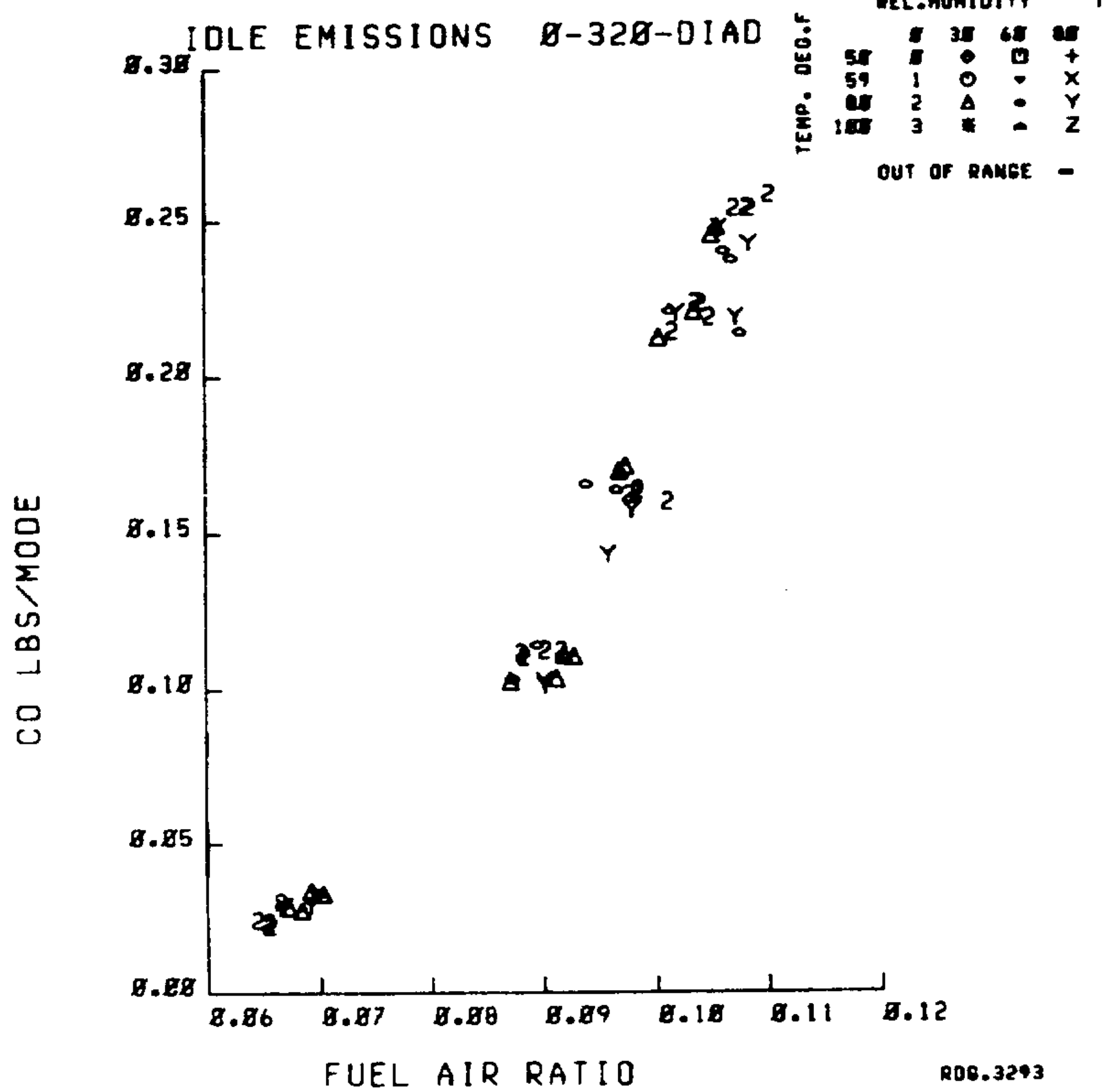

FIGURE 13a

IDLE		IDLE	
3293		3295	
3296		3300	
3301		3304	
3305		3308	
3309		3310	2
[illegible]	2	3314	
[illegible]		3321	
3322		3326	
3328		3331	
3332		3335	
3345		3346	
3348		3349	
3350		3351	
3356	Δ	3358	Δ
3372		3374	
3406		3410	
3411		3414	
3419		3420	
3422		3425	
3431	○	3432	○
3433		3437	
3439		3442	
3446		3447	
3451		3452	
3453	Y	3457	Y
3458		3462	
3463		3466	

NASA LEAN-OUT DATA

TEMP. 80°F REL. HUM. 0, 30, 60, 80%

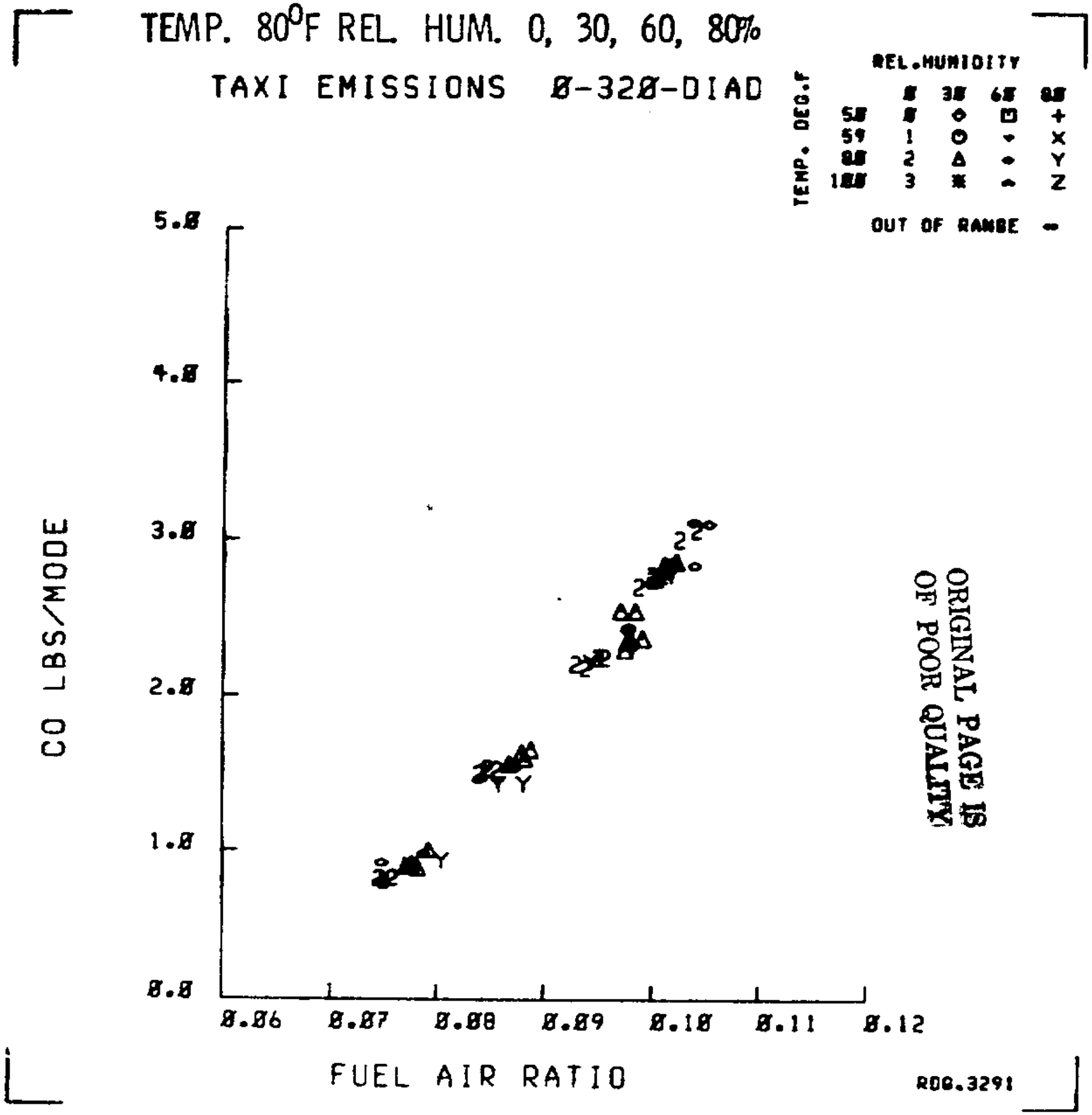

TAXI		TAXI	
3291		3292	
3297		3298	
3302		3303	
3306		3307	
3311		3312	2
3315	2	3316	
3319		3323	
3324		3327	
3329		3330	
3333		3334	
3342		3343	
3344		3347	
3352		3353	
3354	Δ	3355	
3361		3362	Δ
3363		3364	
3407		3408	
3412		3413	
3417		3421	
3423		3424	
3427	o	3429	o
3434		3435	
3440		3441	
3444		3445	
3449		3450	
3455	Y	3456	Y
3459		3460	
3464		3465	

FIGURE 13b

NASA LEAN-OUT DATA

TEMP. 80^0F REL. HUM. 0, 30, 60, 80%

TAKE OFF EMISSIONS Ø-32Ø-DIAD

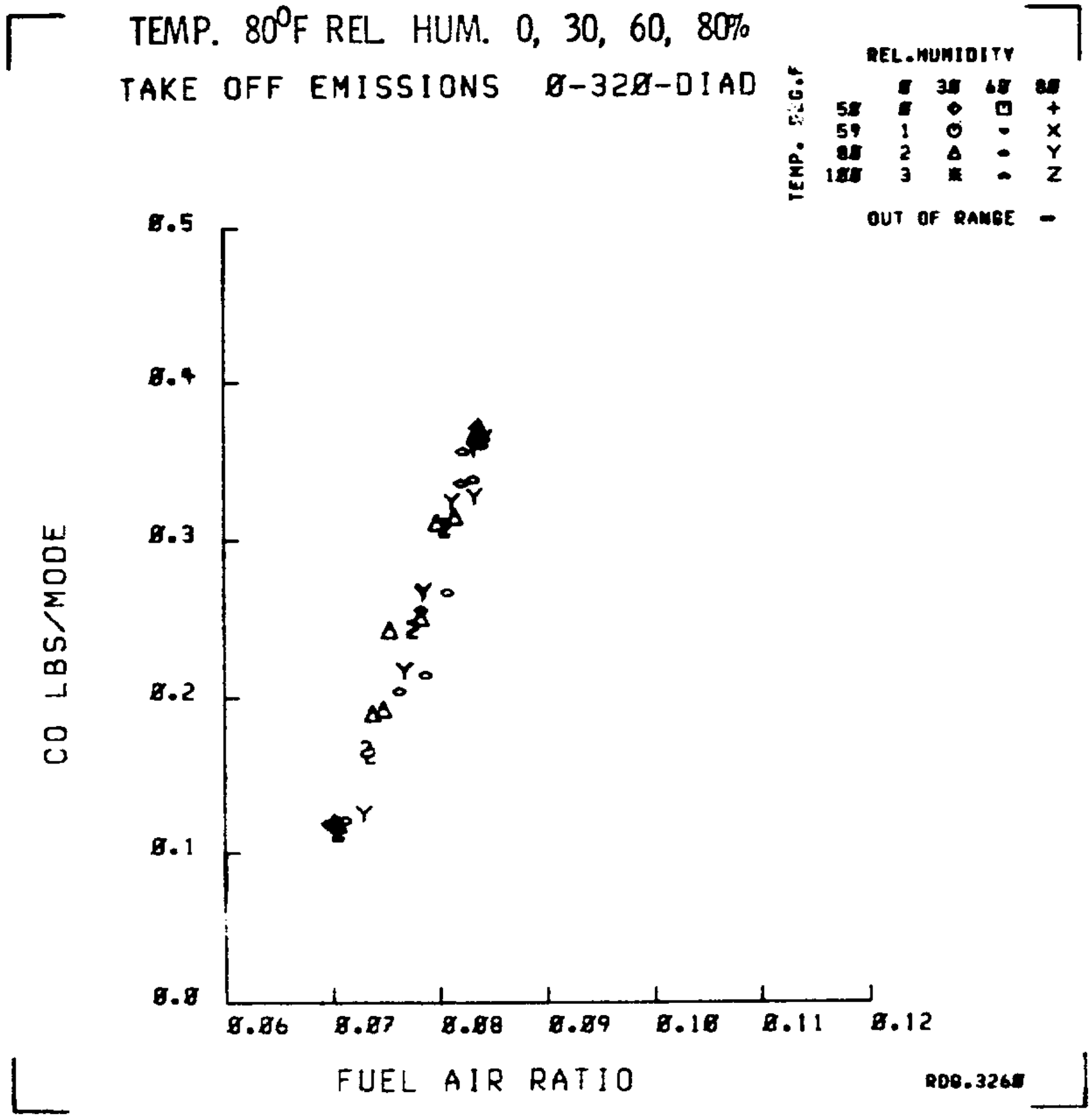

TAKE-OFF		TAKE-OFF	
3260		3263	
3266		3269	
3272	2	3275	2
3278		3281	
3284		3287	
3376		3379	
3382		3385	
3388	Δ	3391	Δ
3394		3397	
3400		3403	
3497		3500	
3503		3506	
3509	⬭	3512	⬭
3515		3518	
3521		3524	
3467		3470	
3473		3476	Y
3479	Y	3482	
3485		3488	
3491			

FIGURE 13c

NASA LEAN-OUT DATA

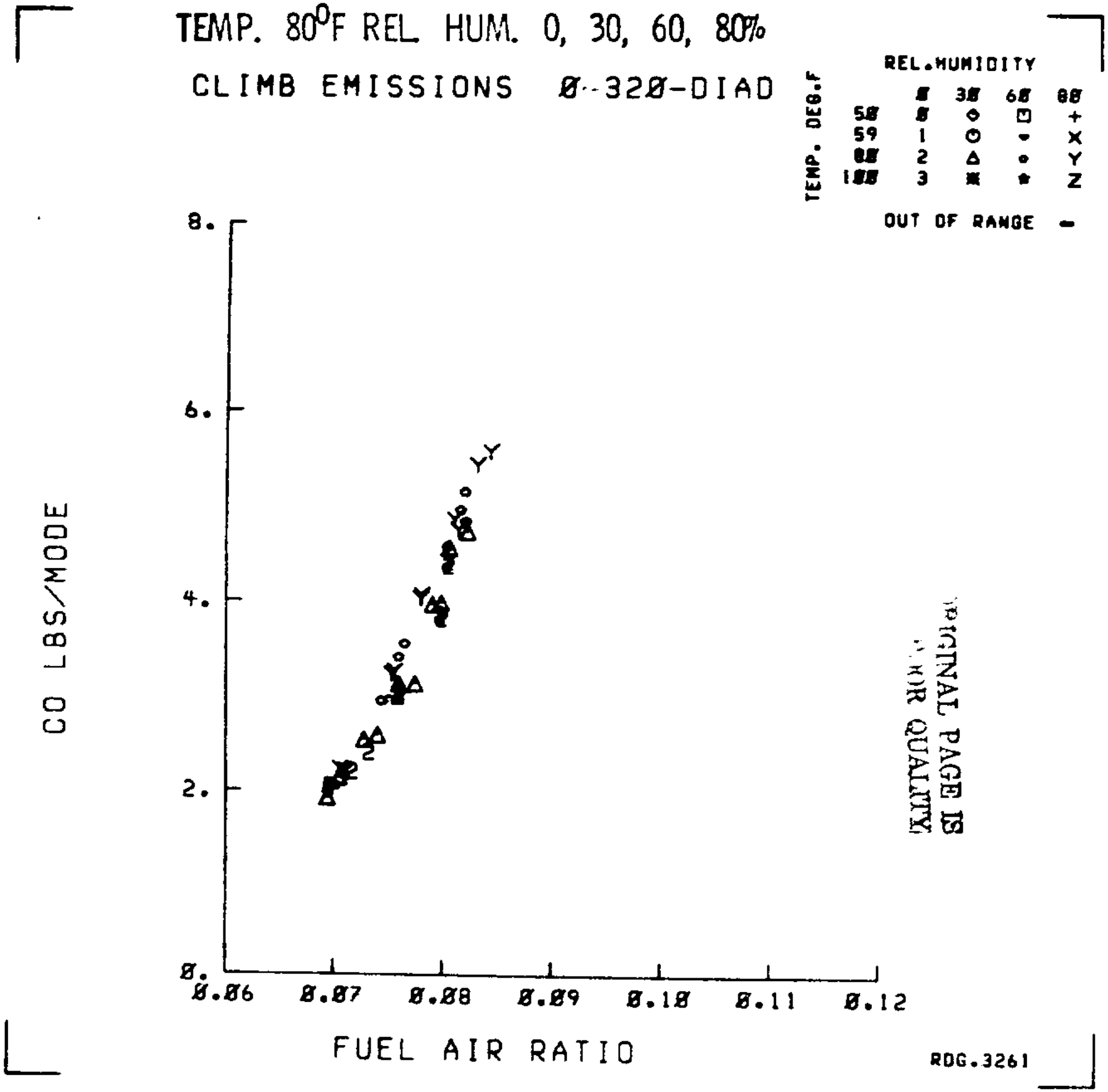

CLIMB		CLIMB	
3261		3264	
3267		3270	
3273	2	3276	2
3279		3282	
3285		3288	
3377		3380	
3383		3386	
3389	Δ	3392	Δ
3395		3398	
3401		3404	
3498		3501	
3504		3507	
3510	○	3513	○
3516		3519	
3525		3526	
3468		3471	
3474		3477	
3480	Y	3483	Y
3486		3489	
3492		3495	

FIGURE 13a

NASA LEAN-OUT DATA

TEMP. 80°F REL. HUM. 0, 30, 60, 80%

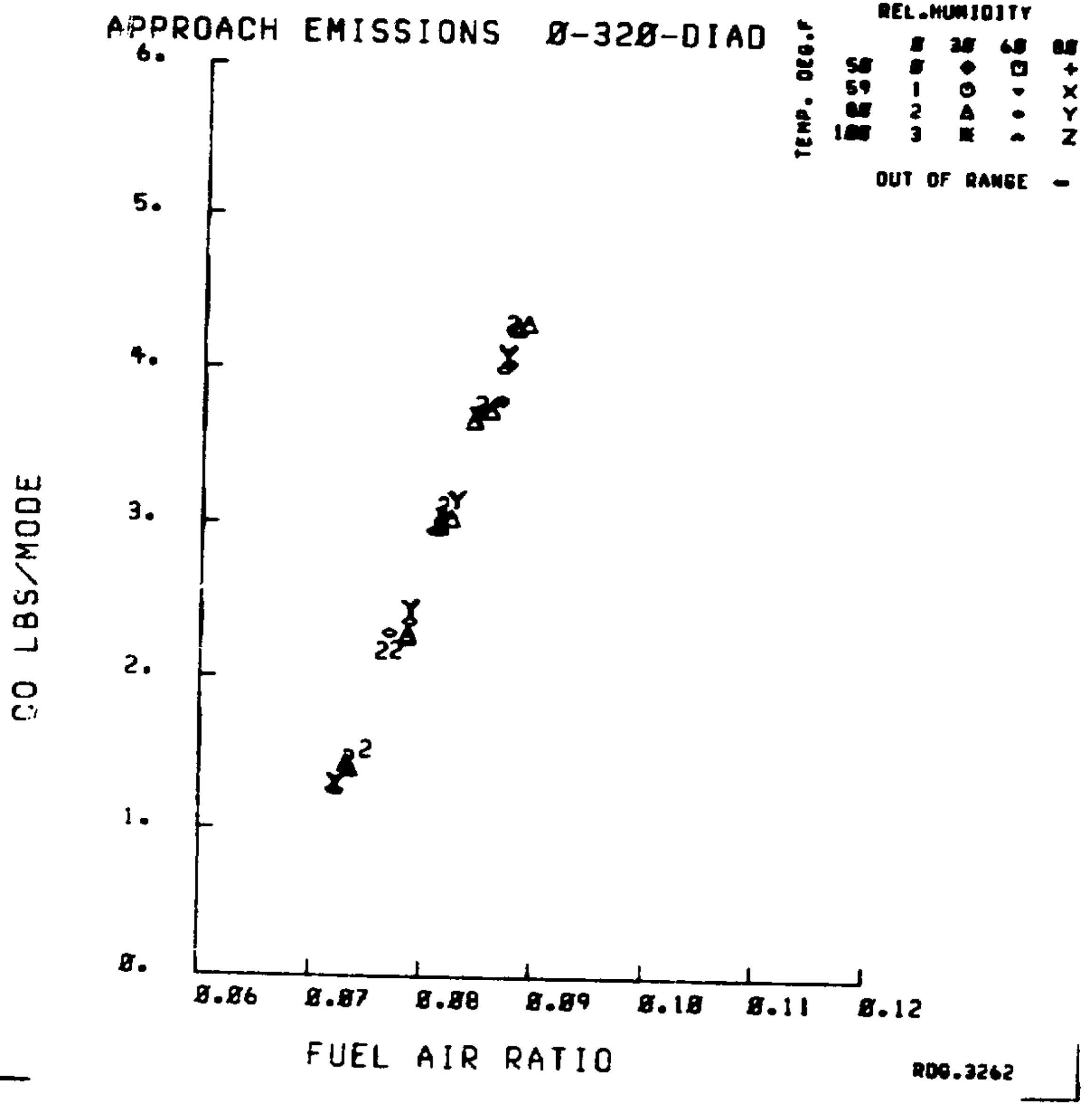

APPROACH	
3262	2
3268	2
3277	2
3283	2
3289	2
3381	Δ
3387	Δ
3393	Δ
3399	Δ
3405	Δ
3502	⬭
3508	⬭
3514	⬭
3520	⬭
3527	⬭
3472	Y
3478	Y
3484	Y
3490	Y
3496	Y

APPROACH	
3265	2
3274	2
3280	2
3286	2
3378	Δ
3384	Δ
3390	Δ
3396	Δ
3402	Δ
3499	⬭
3505	⬭
3511	⬭
3517	⬭
3523	⬭
3469	Y
3475	Y
3481	Y
3487	Y
3493	Y

FIGURE 13e

NASA LEAN-OUT DATA

TEMP. 80°F REL. HUM. 0, 30, 60, 80%

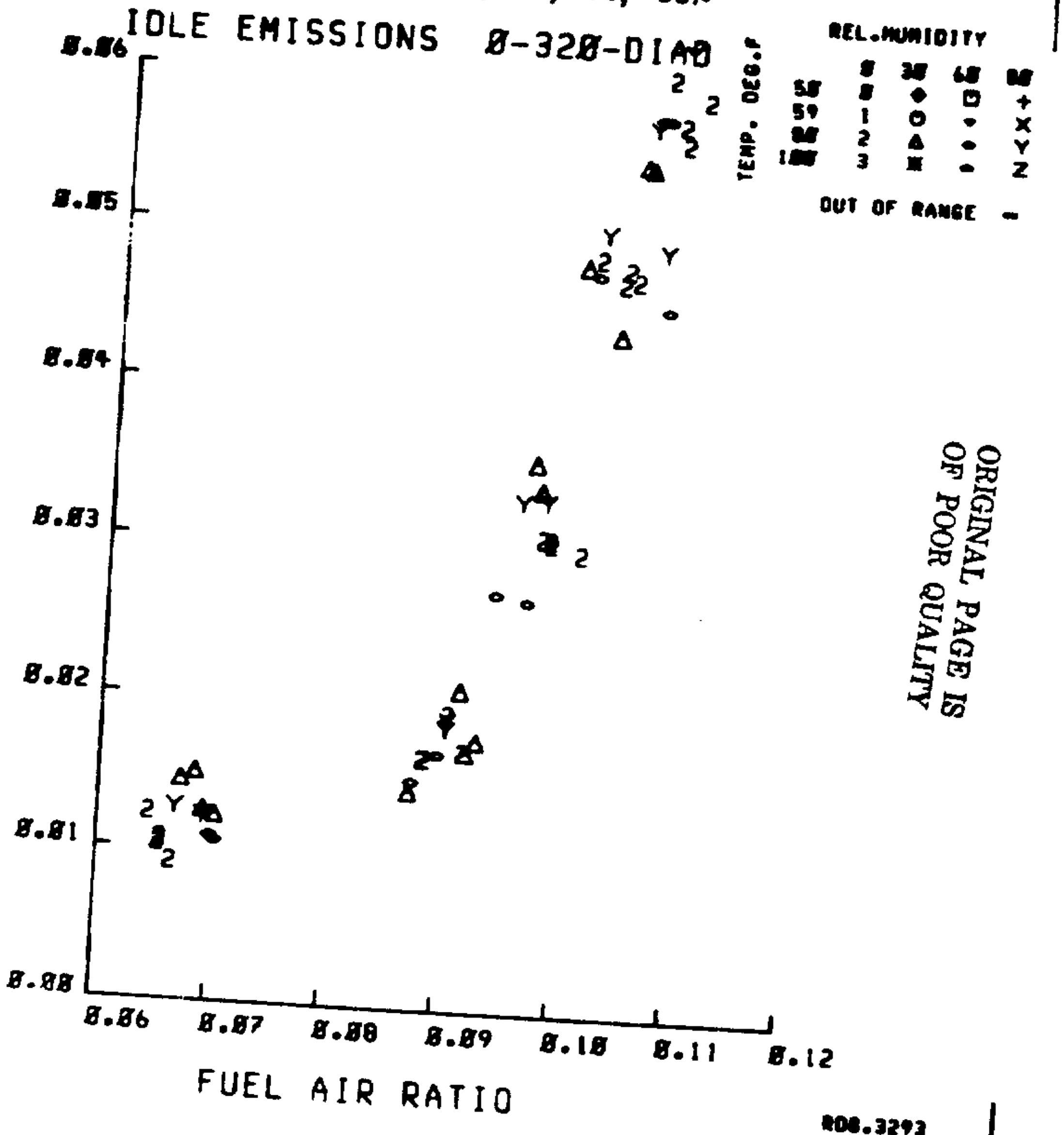

IDLE		IDLE	
3293		3295	
3296		3300	
3301		3304	
3305		3308	
3309		3310	2
3313	2	3314	
3320		3321	
3322		3326	
3328		3331	
3332		3335	
3345		3346	
3348		3349	
3350		3351	
3356	Δ	3358	Δ
3372		3374	
3406		3410	
3411		3414	
3419		3420	
3422		3425	
3431	○	3432	○
3433		3437	
3439		3442	
3446		3447	
3451		3452	
3453	Y	3457	Y
3459		3462	
3463		3466	

ORIGINAL PAGE IS OF POOR QUALITY

FIGURE 13f

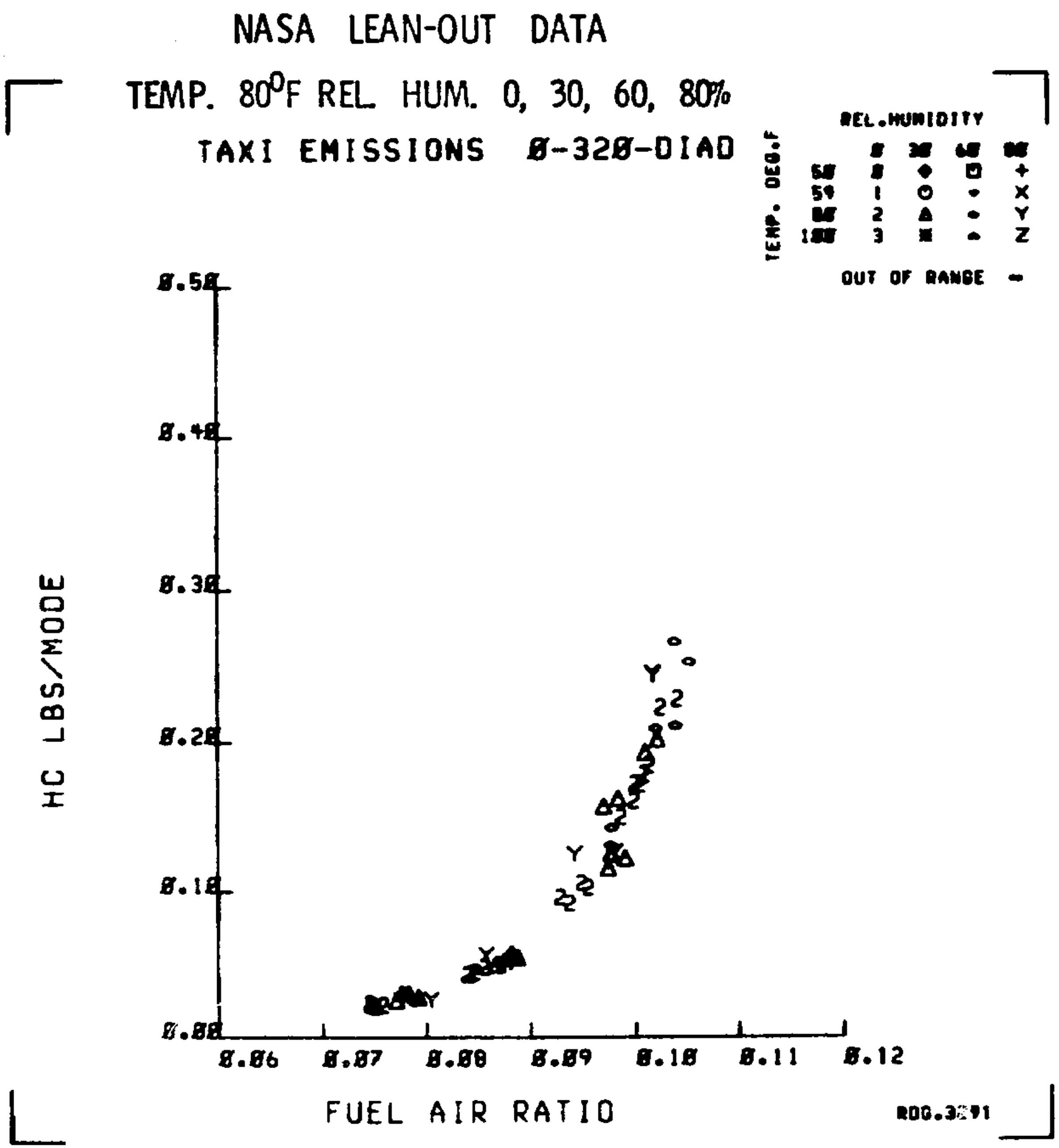

TAXI		TAXI	
3291		3292	
3297		3298	
3302		3303	
3306		3307	
3311		3312	2
3315	2	3316	
3319		3323	
3324		3327	
3329		3330	
3333		3334	
3342		3343	
3344		3347	
3352		3353	
3354	Δ	3355	
3361		3362	Δ
3363		3364	
3407		3408	
3412		3413	
3417		3421	
3423		3424	
3427	◇	3429	◇
3434		3435	
3440		3441	
3444		3445	
3449		3450	
3455	Y	3456	Y
3459		3460	
3464		3465	

FIGURE 13g

NASA LEAN-OUT DATA

TEMP. 80°F REL. HUM. 0, 30, 60, 80%

TAKE OFF EMISSIONS Ø-32Ø-DIAD

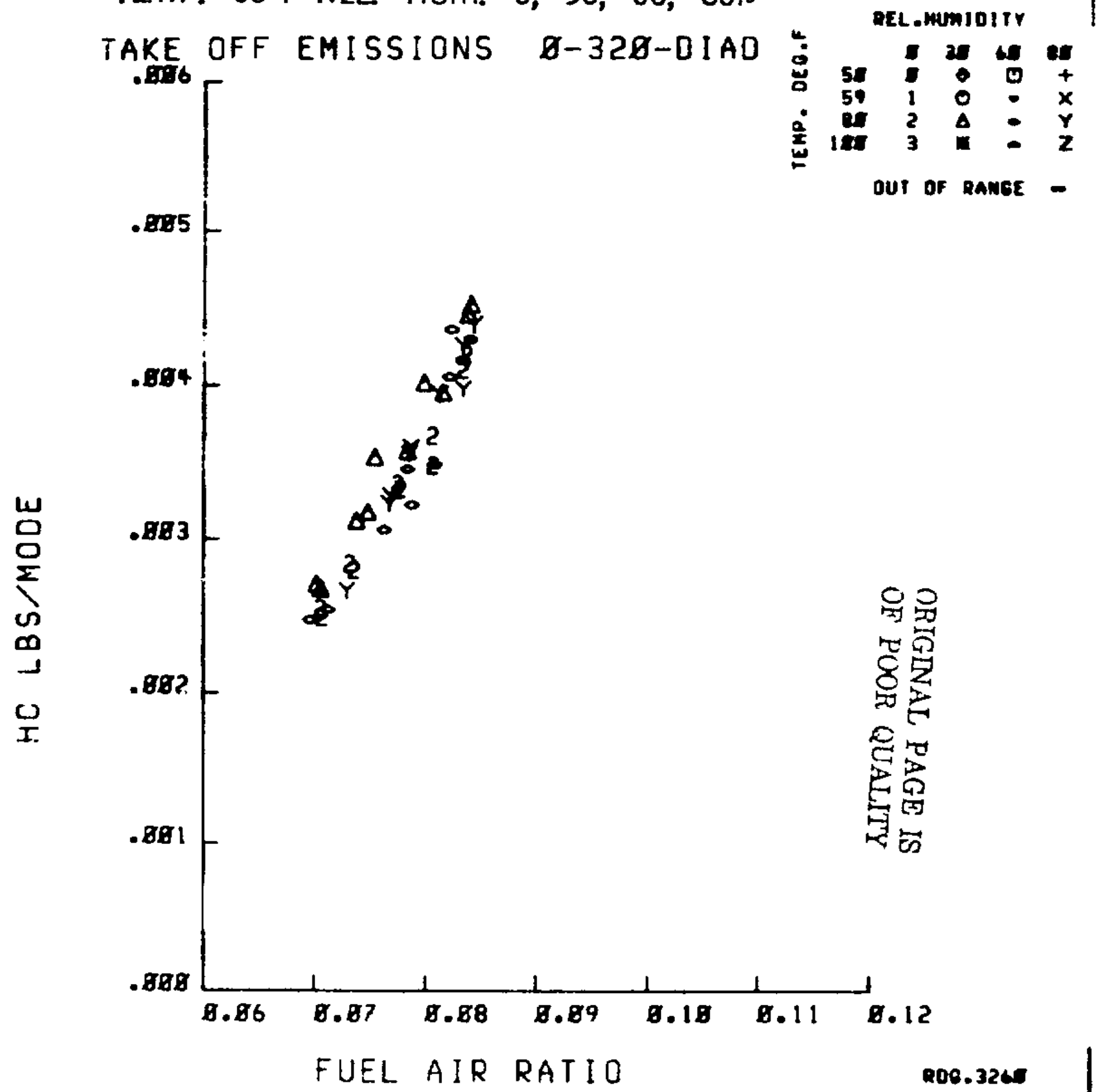

ORIGINAL PAGE IS OF POOR QUALITY

TAKE-OFF		TAKE-OFF	
3260		3263	
3266		3269	
3272	2	3275	2
3278		3281	
3284		3287	
3376		3379	
3382		3385	
3388	Δ	3391	Δ
3394		3397	
3400		3403	
3497		3500	
3503		3506	
3509	o	3512	o
3515		3518	
3521		3524	
3467		3470	
3473		3476	Y
3479	Y	3482	
3485		3488	
3491			

FIGURE 13h

NASA LEAN-OUT DATA

TEMP. 80°F REL. HUM. 0, 30, 60, 80%

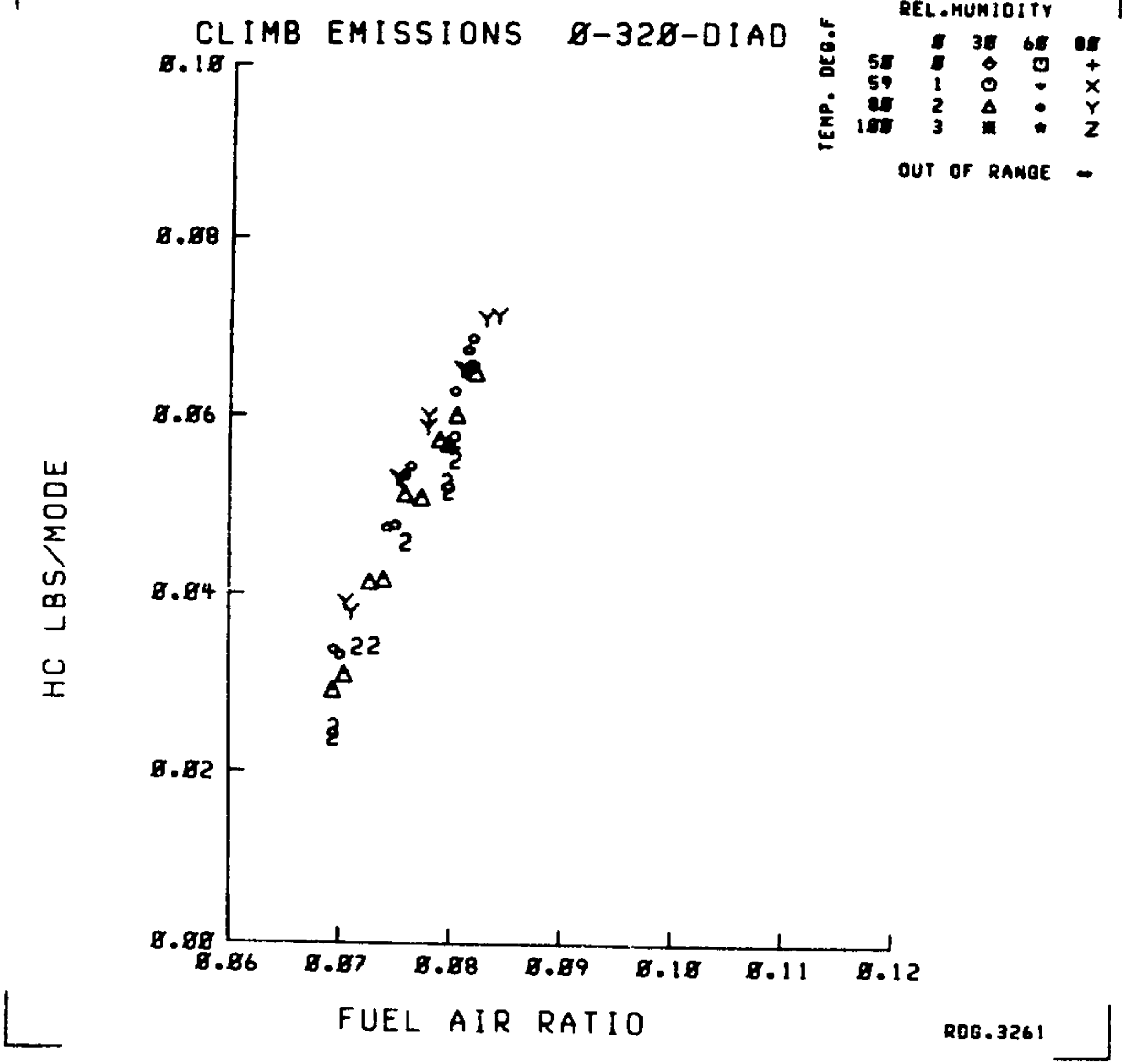

CLIMB		CLIMB	
3261	2	3264	2
3267		3270	
3273		3276	
3279		3282	
3285		3288	
3377	Δ	3380	Δ
3383		3386	
3389		3392	
3395		3398	
3401		3404	
3498	○	3501	○
3504		3507	
3510		3513	
3516		3519	
3525		3526	
3468	Y	3471	Y
3474		3477	
3480		3483	
3486		3489	
3492		3495	

FIGURE 13i

NASA LEAN-OUT DATA

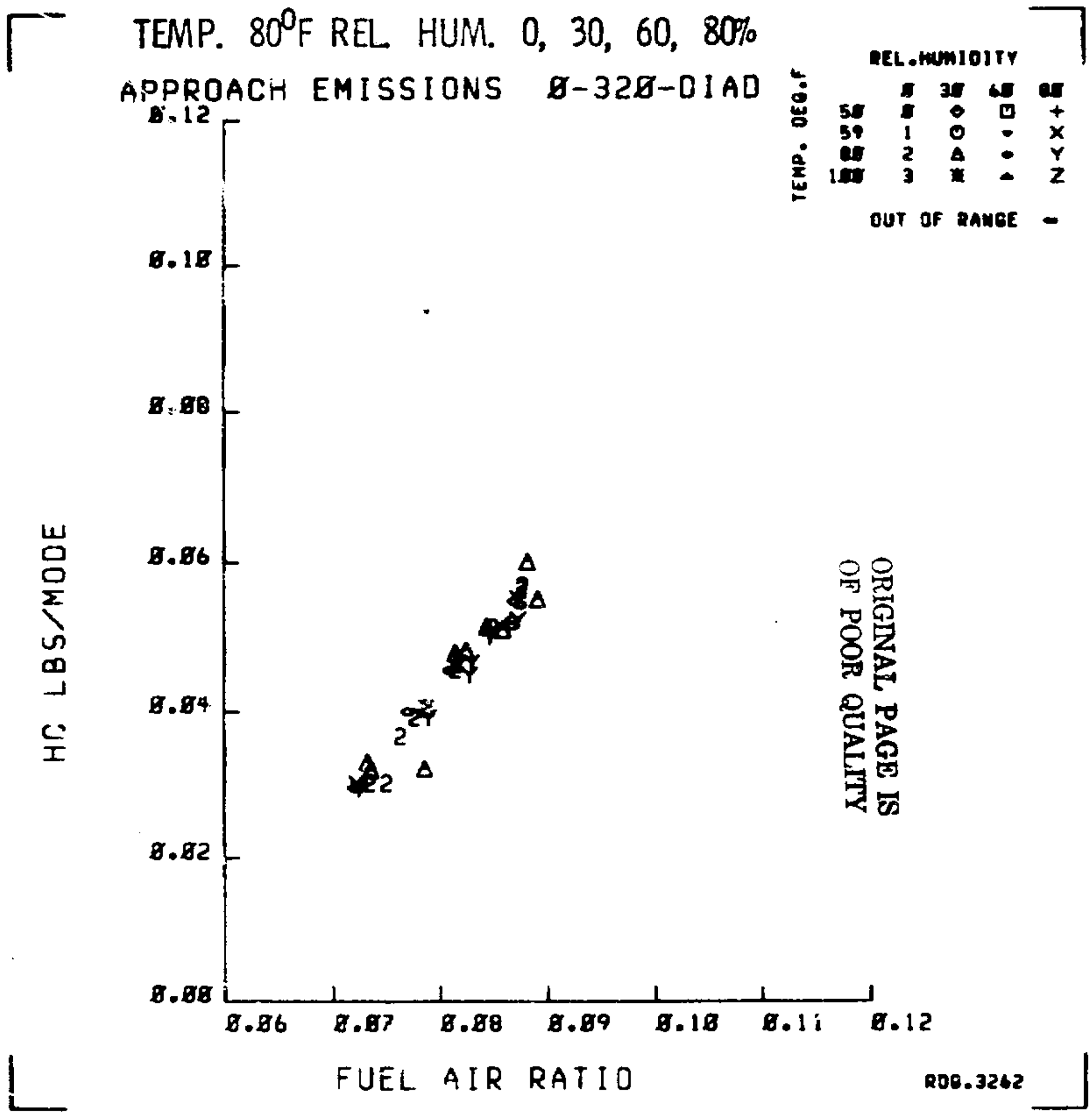

APPROACH		APPROACH	
3262		3265	
3268		3274	
3277	2	3280	2
3283		3286	
3289		3378	
3381		3384	
3387		3390	
3393	Δ	3396	Δ
3399		3402	
3405		3499	
3502		3505	
3508		3511	◇
3514	◇	3517	
3520		3523	
3527		3469	
3472		3475	
3478		3481	Y
3484	Y	3487	
3490		3493	
3496			

FIGURE 13j

NASA LEAN-OUT DATA

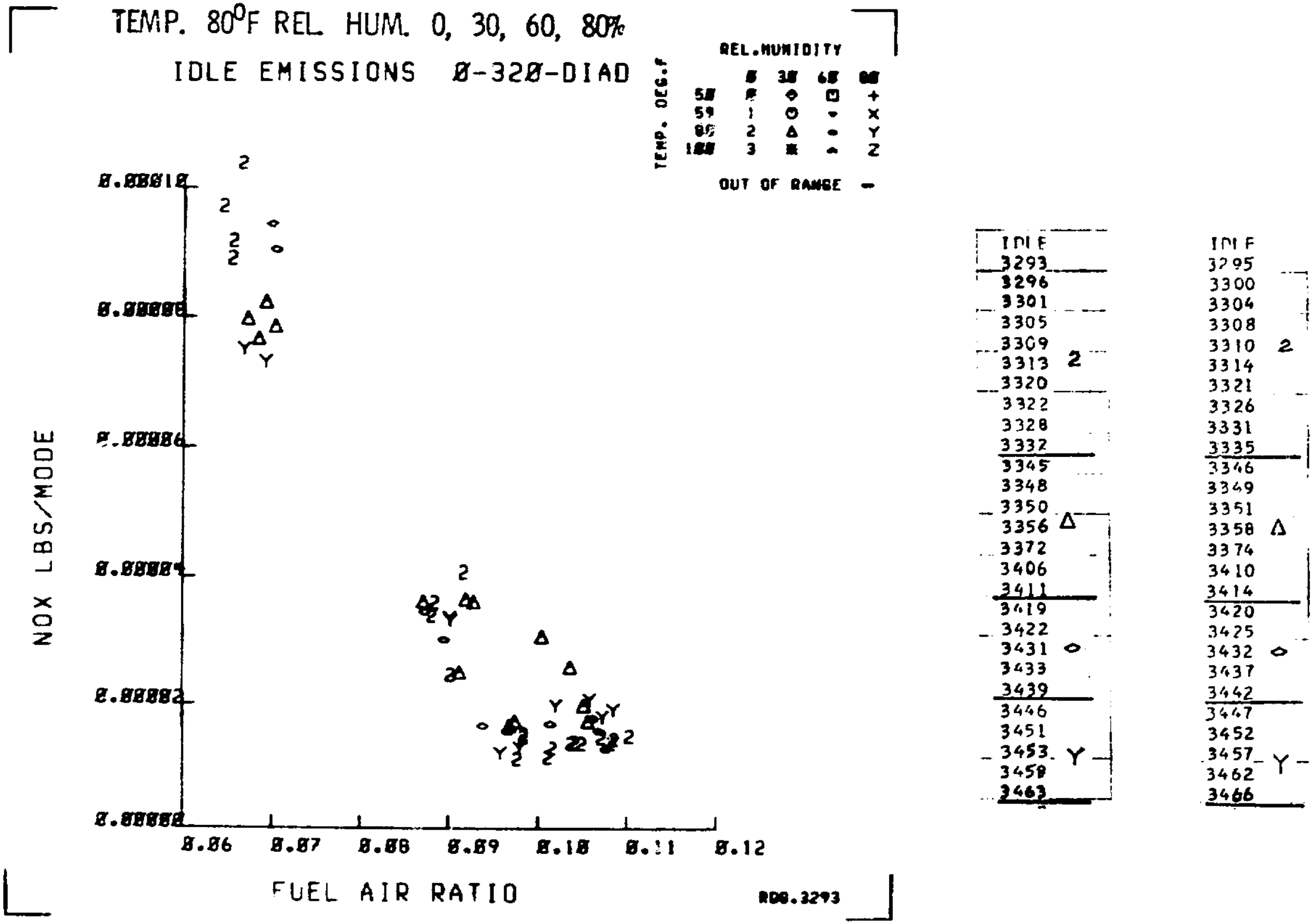

FIGURE 13k

NASA LEAN-OUT DATA

TEMP. 80°F REL. HUM. 0, 30, 60, 80%

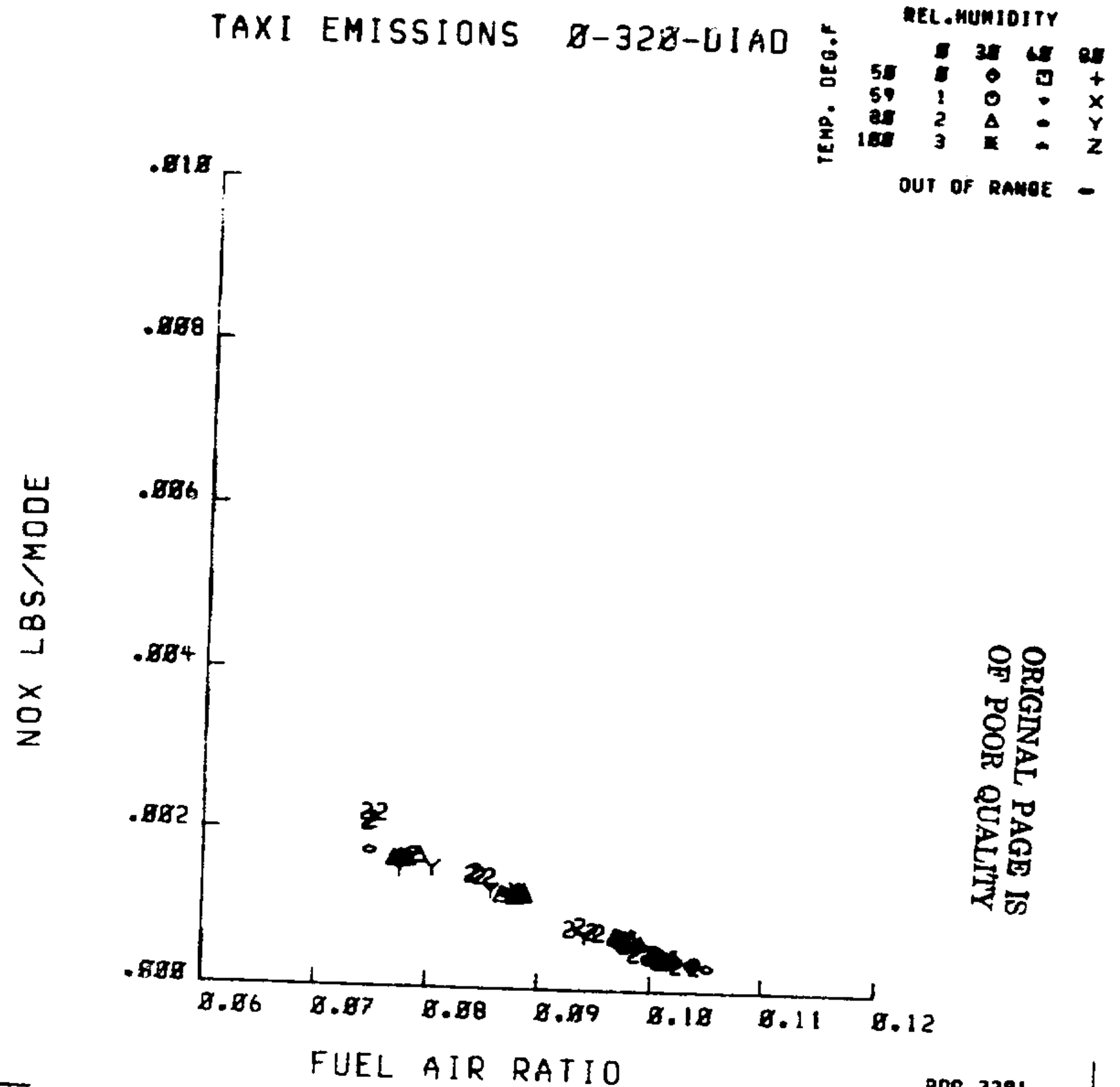

TAXI		TAXI	
3291		3292	
3297		3298	
3302		3303	
3306		3307	
3311		3312	2
3315	2	3316	
3319		3323	
3324		3327	
3329		3330	
3333		3334	
3342		3343	
3344		3347	
3352		3353	
3354	Δ	3355	
3361		3362	Δ
3363		3364	
3407		3408	
3412		3413	
3417		3421	
3423		3424	
3427	⟡	3429	⟡
3434		3435	
3440		3441	
3444		3445	
3449		3450	
3455	Y	3456	Y
3459		3460	
3464		3465	

FIGURE 131

NASA LEAN-OUT DATA

TEMP. 80^{0}F REL. HUM. 0, 30, 60, 80%

TAKE OFF EMISSIONS Ø-32Ø-DIAD

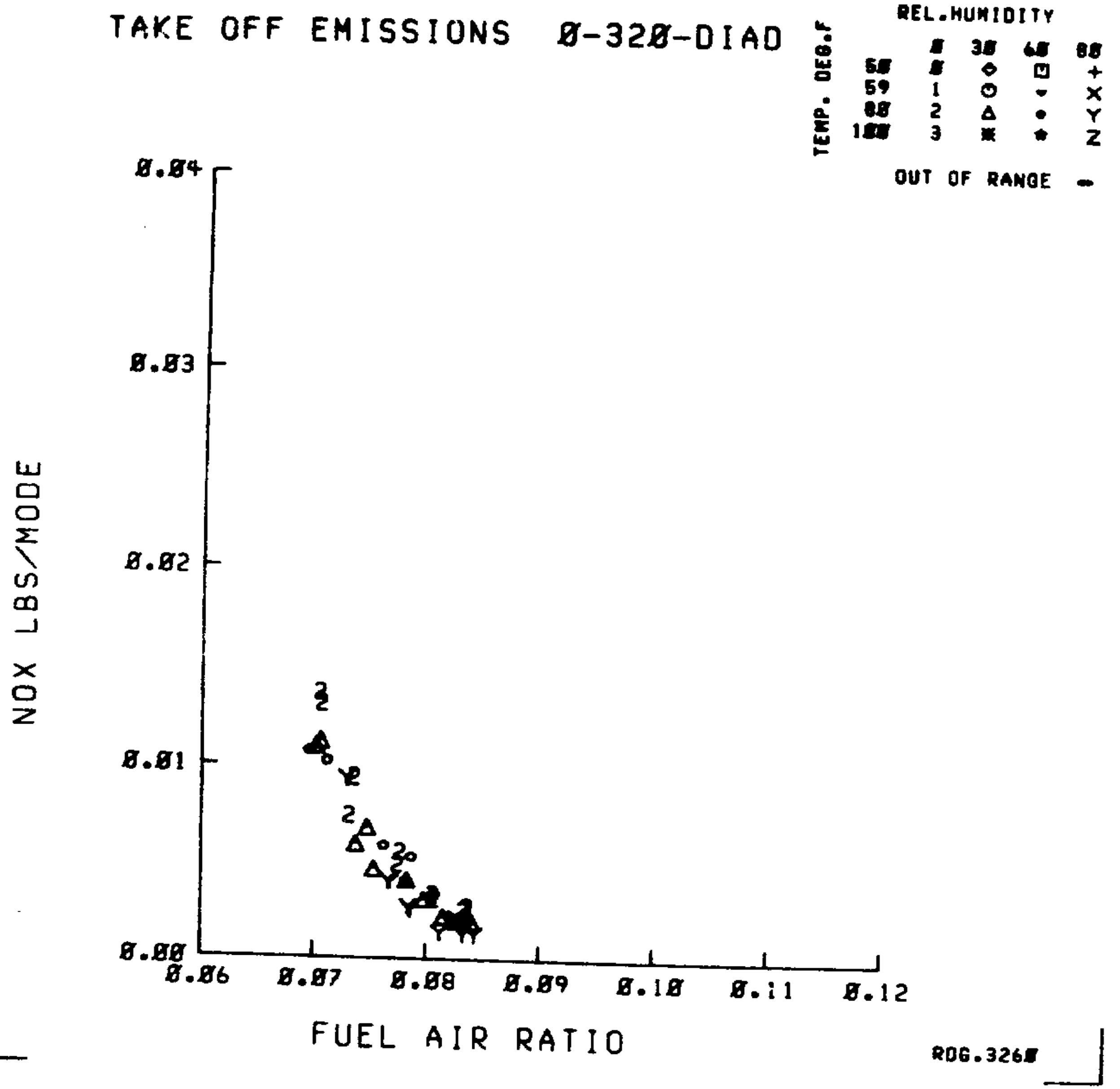

TAKE-OFF		TAKE-OFF	
3260	2	3263	2
3266		3269	
3272		3275	
3278		3281	
3284		3287	
3376	△	3379	△
3382		3385	
3388		3391	
3394		3397	
3400		3403	
3497	◇	3500	◇
3503		3506	
3509		3512	
3515		3518	
3521		3524	
3467	Y	3470	Y
3473		3476	
3479		3482	
3485		3488	
3491			

FIGURE 13m

NASA LEAN-OUT DATA

TEMP. 80^{0}F REL. HUM. 0, 30, 60, 80%

CLIMB EMISSIONS Ø-32Ø-DIAD

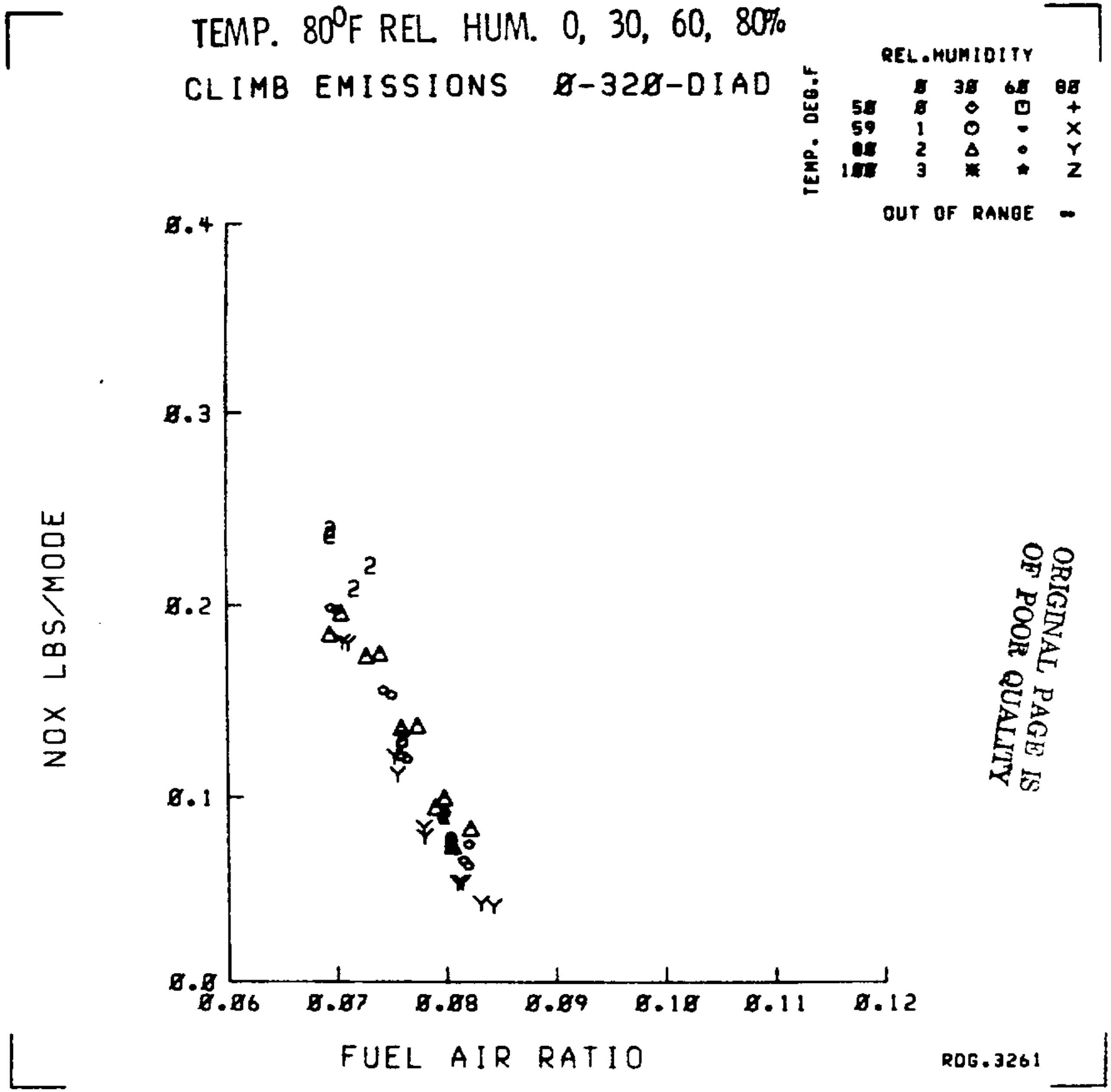

CLIMB		CLIMB	
3261		3264	
3267		3270	
3273	2	3276	2
3279		3282	
3285		3288	
3377		3380	
3383		3386	
3389	Δ	3392	Δ
3395		3398	
3401		3404	
3498		3501	
3504		3507	
3510	◇	3513	◇
3516		3519	
3525		3526	
3468		3471	
3474		3477	
3480	Y	3483	Y
3486		3489	
3492		3495	

ORIGINAL PAGE IS OF POOR QUALITY

FIGURE 13n

NASA LEAN-OUT DATA

TEMP. 80°F REL. HUM. 0, 30, 60, 80%

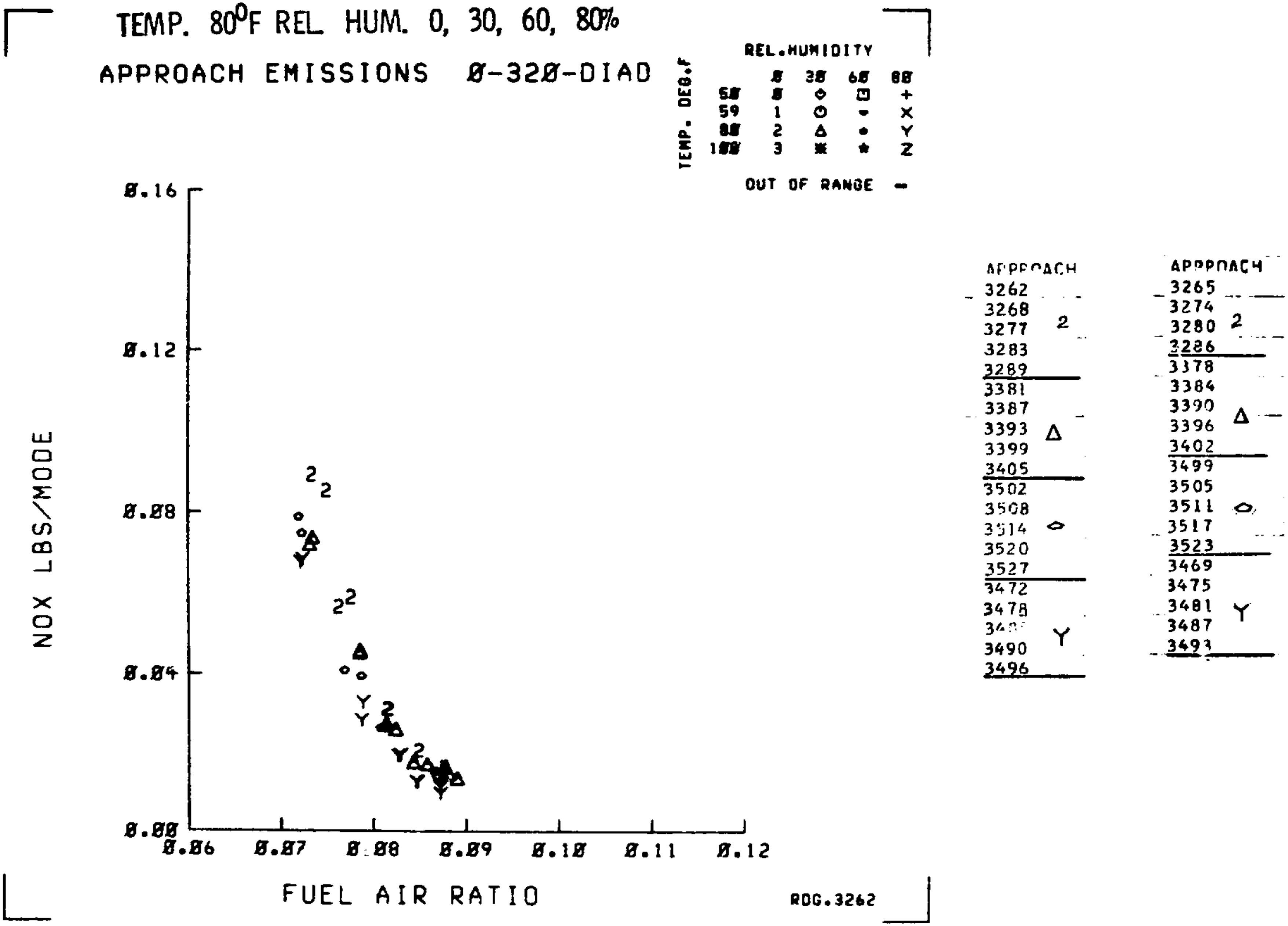

FIGURE 13o

NASA LEAN-OUT DATA

TEMP. 100^0F REL. HUM. 0, 30, 60, 80%

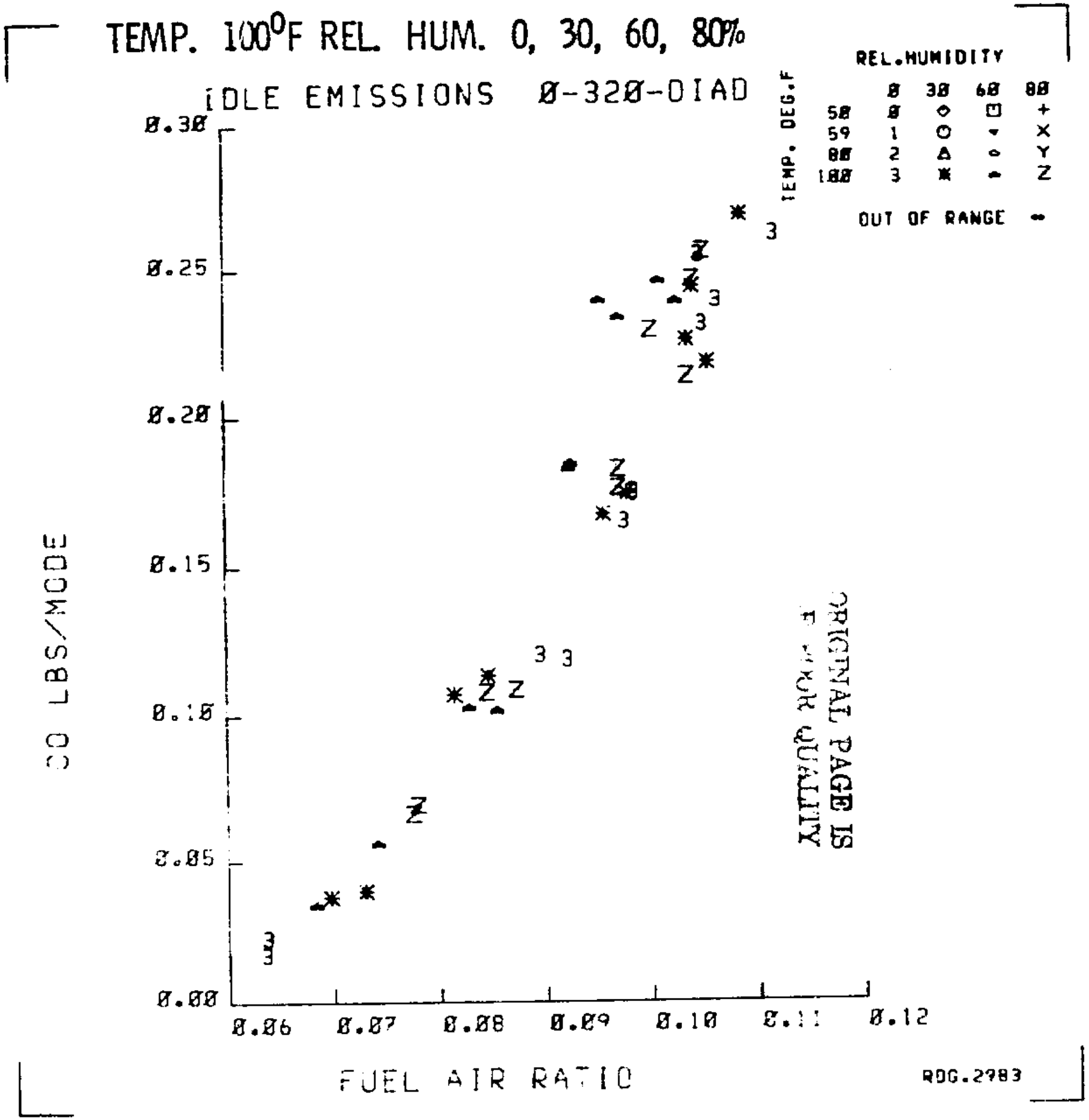

IDLE	
2983	
2990	
2995	3
2999	
3005	
3154	
3158	
3162	*
3166	
3170	
3176	
3184	
3192	▲
3198	
3202	
3053	
3057	
3061	Z
3066	
3071	

IDLE	
2988	
2993	
2998	3
3002	
3008	
3157	
3161	
3165	*
3169	
3173	
3183	
3190	
3195	▲
3201	
3205	
3056	
3060	
3064	Z
3069	
3075	

FIGURE 14a

NASA LEAN-OUT DATA

TEMP. 100°F REL. HUM. 0, 30, 60, 80%

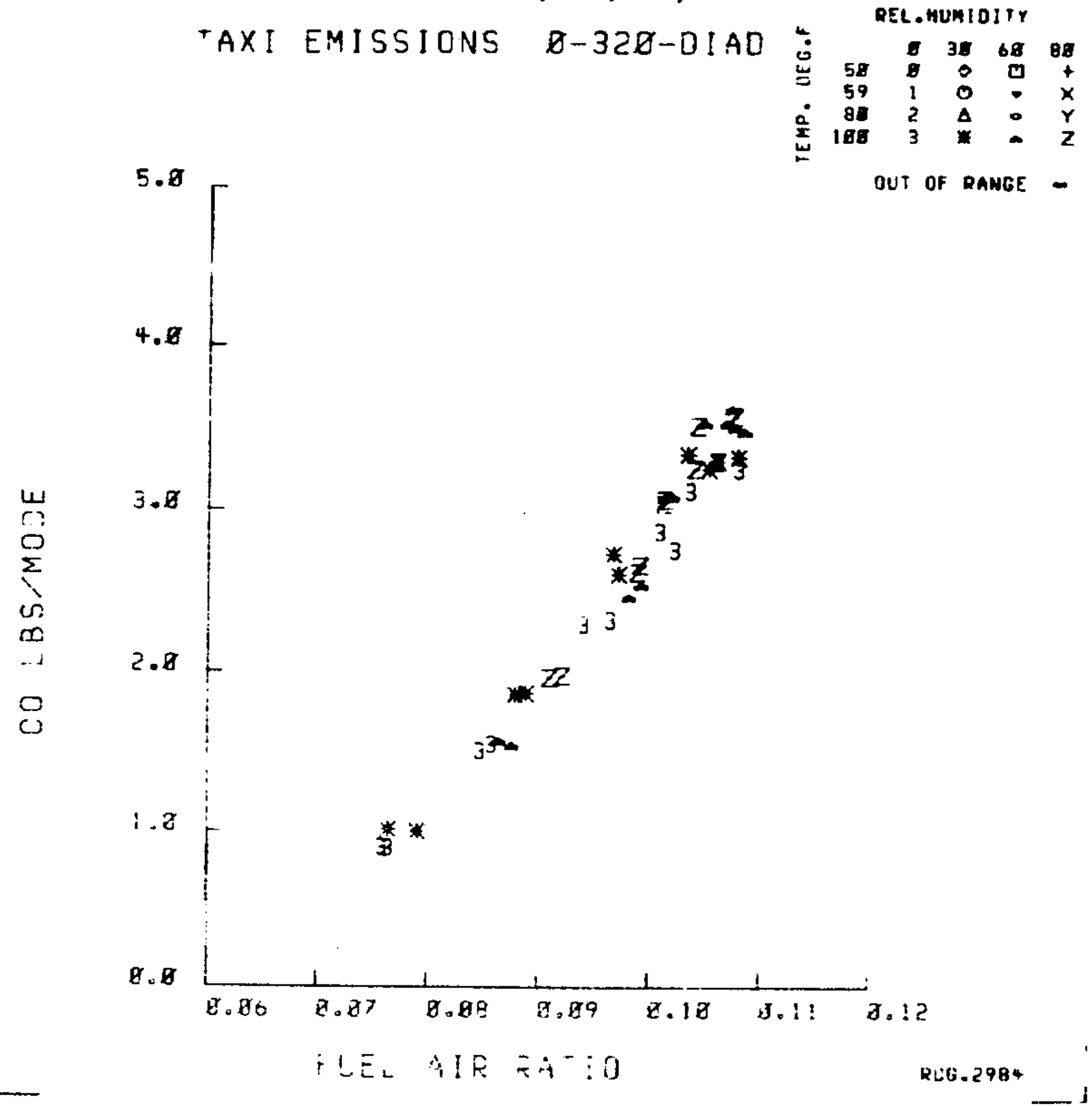

TAXI		TAXI	
2984		2985	
2991		2992	
2996	3	2997	3
3001		3004	
3006		3007	
3155		3156	
3159		3160	
3163	*	316[illegible]	*
3167		3168	
3171		3172	
3177		3180	
3185		3187	
3188	▲	3193	▲
3194		3199	
3200		3203	
3204		3054	
3055		3058	
3059		3062	Z
3063	Z	3067	
3068		3072	
3073			

FIGURE 14b

NASA LEAN-OUT DATA

TEMP. 100°F REL. HUM. 0, 30, 60, 80%

TAKE OFF EMISSIONS Ø-32Ø-JIAD

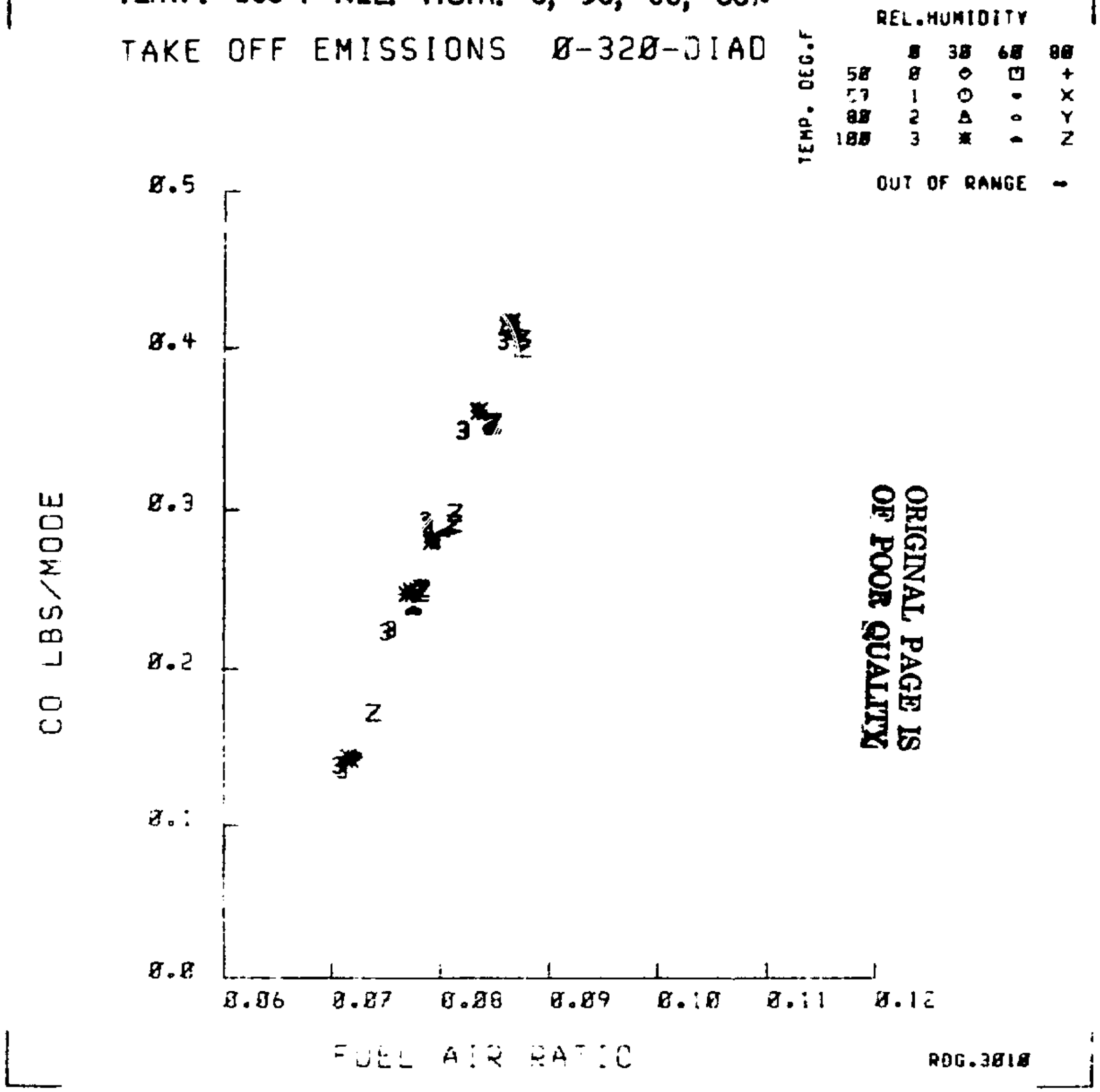

TAKE-OFF		TAKE-OFF	
3010		3014	
3017		3020	
3024	3	3027	3
3032		3035	
3038		3041	
3121		3123	
3126		3129	
3132	*	3135	*
3138		3141	
3144		3147	
3150		3209	
3212		3217	
3220		3224	
3229		3233	
3239		3240	
3247		3076	
3079		3082	
3085		3090	Z
3099	Z	3102	
3105		3110	

FIGURE 14c

NASA LEAN-OUT DATA

TEMP. 100^{0}F REL. HUM. 0, 30, 60, 80%

CLIMB EMISSIONS 0-320-DIAD

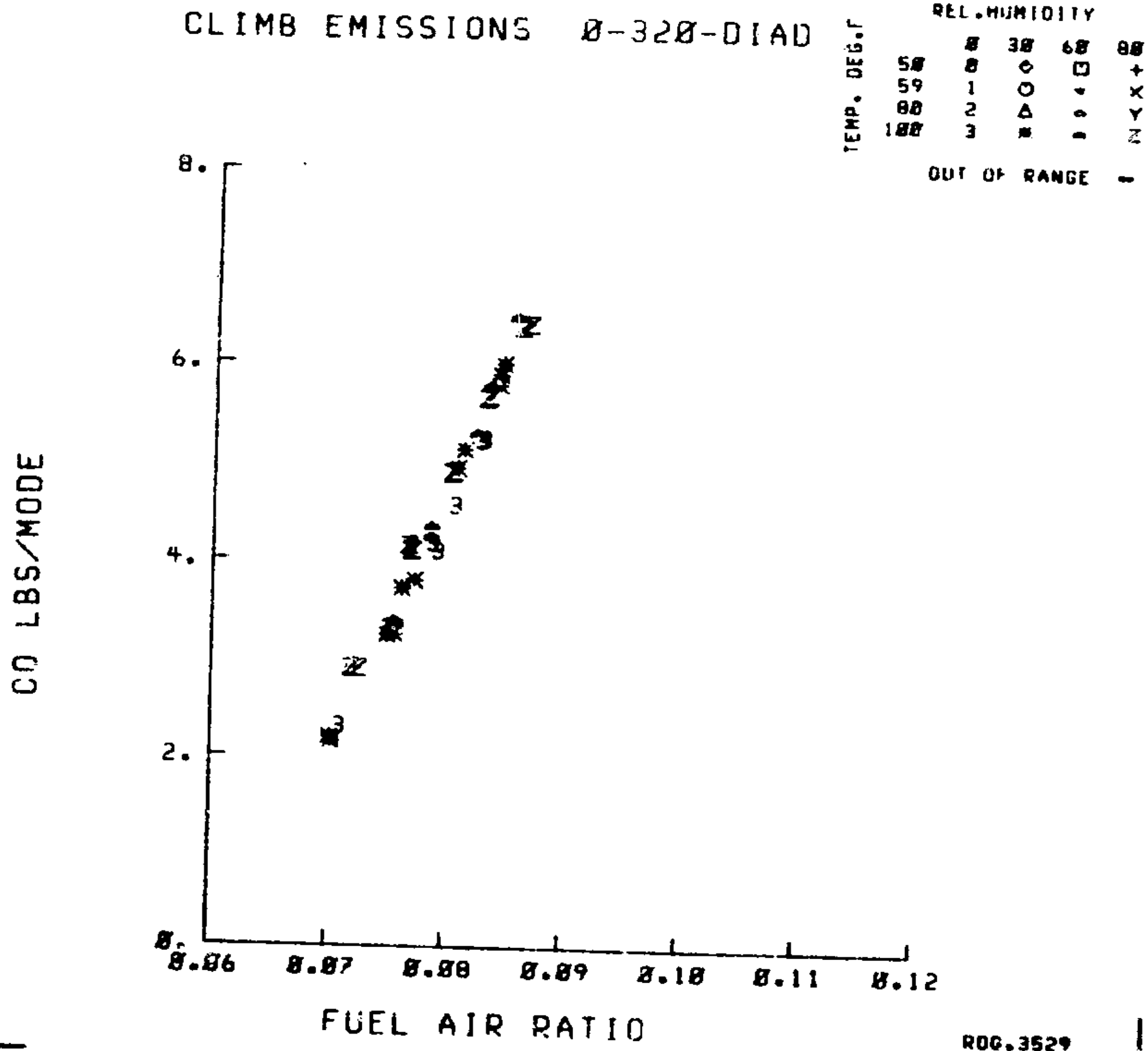

CLIMB	
3529	
3532	
3534	3
3537	
3122	
3127	
3133	
3139	
3145	*
3153	
3216	
3223	
3232	
3237	
3080	
3088	
3100	Z
3108	
3111	

CLIMB	
3531	
3533	
3536	3
3538	
3124	
3130	
3136	*
3142	
3151	
3215	
3218	
3227	
3236	
3077	
3087	
3097	
3106	Z
3109	
3112	

FIGURE 14a

NASA LEAN-OUT DATA

TEMP. 100°F REL. HUM. 0, 30, 60, 80%

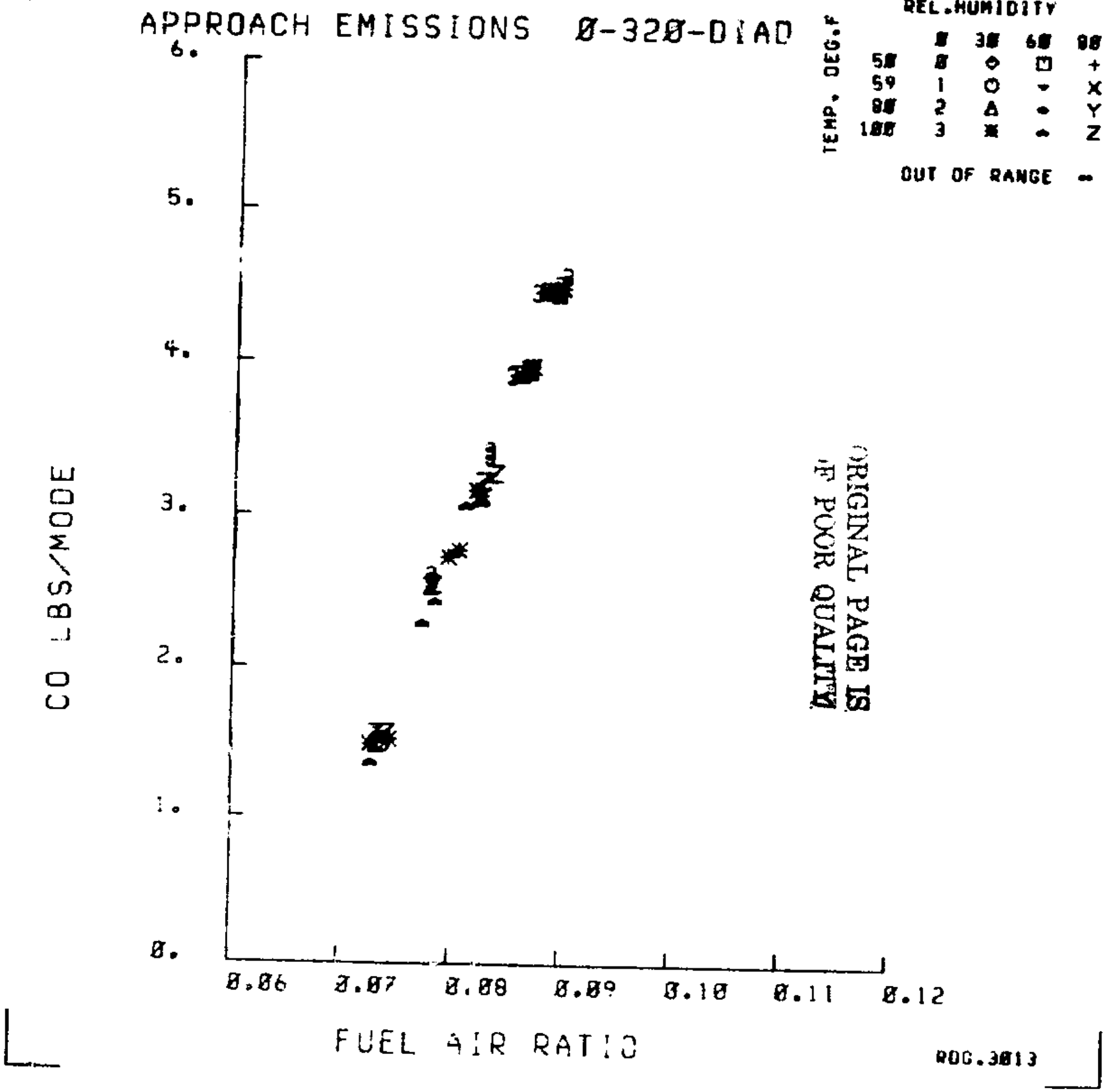

APPROACH		APPROACH	
3013		3016	
3019		3023	
3026	3	3031	3
3034		3037	
3040		3043	
3125		3128	
3131		3134	
3137	*	3140	*
3143		3146	
3149		3152	
3211		3214	
3219		3222	
3226		3231	
3235		3238	
3244		3251	
3078		3081	
3084		3089	
3098	Z	3101	Z
3104		3107	
3113		3116	

FIGURE 14e

NASA LEAN-OUT DATA

TEMP. 100°F REL. HUM. 0, 30, 60, 80%

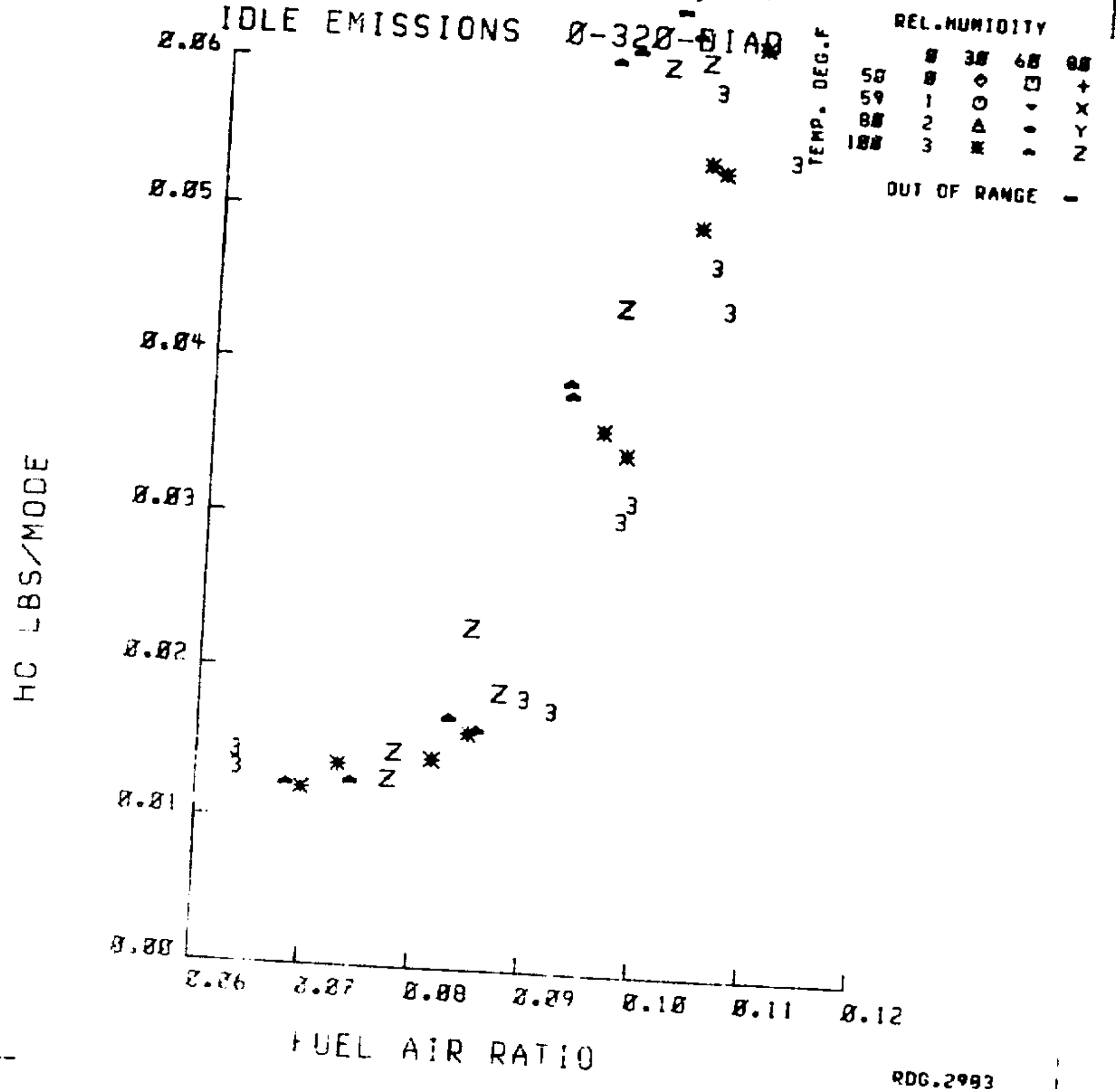

IDLE		IDLE	
2983		2988	
2990		2993	
2995	3	2998	3
2999		3002	
3005		3008	
3154		3157	
3158		3161	
3162	*	3165	*
3166		3169	
3170		3173	
3176		3183	
3184		3190	
3192	^	3195	^
3198		3201	
3202		3205	
3053		3056	
3057		3060	
3061	Z	3064	Z
3066		3069	
3071		3075	

FIGURE 14f

NASA LEAN-OUT DATA

TEMP. 100°F REL. HUM. 0, 30, 60, 80%

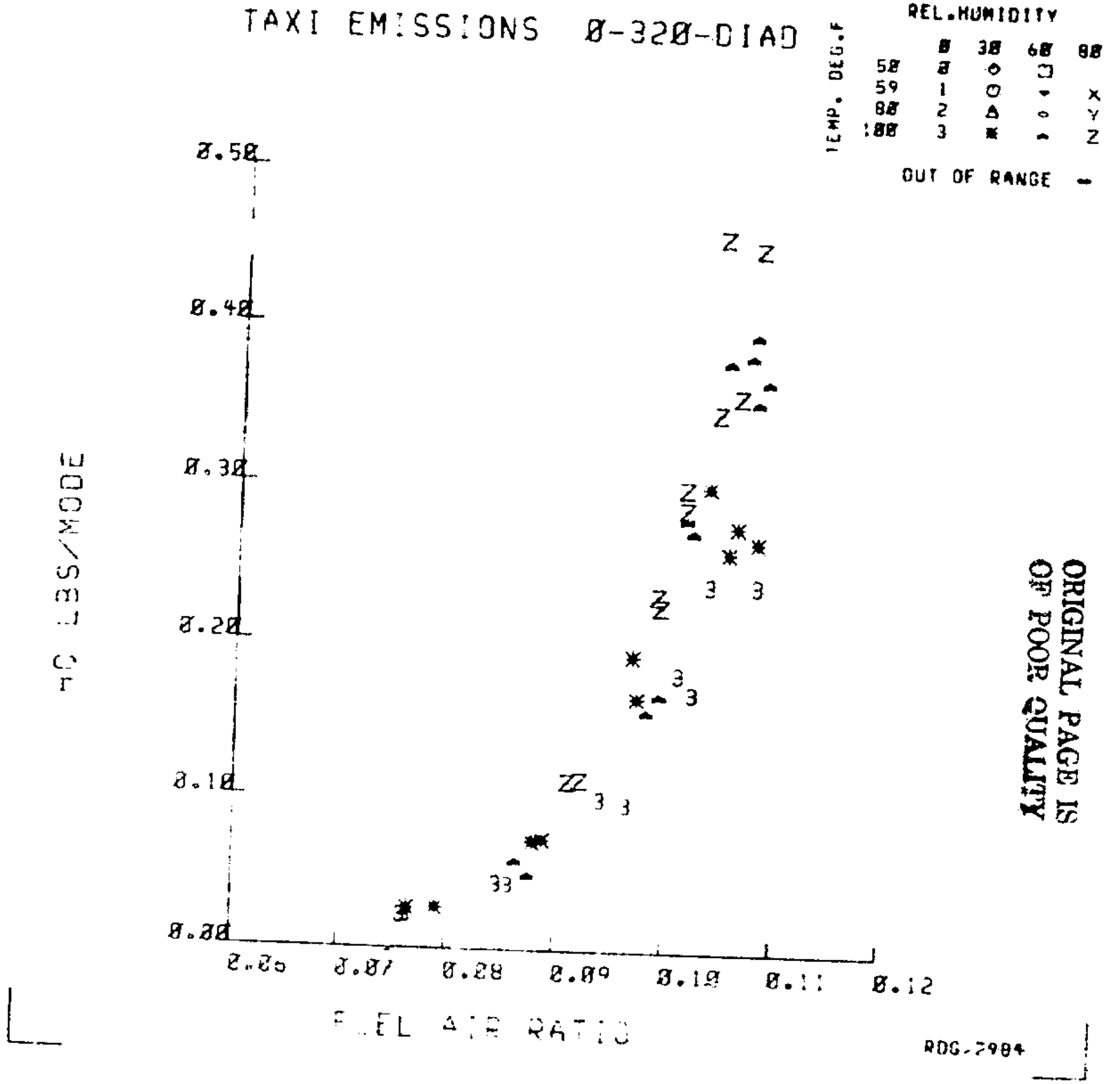

TAXI		TAXI	
2984		2985	
2991		2992	
2996	3	2997	3
3001		3004	
3006		3007	
3155		3156	
3159		3160	
3163	*	3164	*
3167		3168	
3171		3172	
3177		3180	
3185		3187	
3188	▲	3193	▲
3194		3199	
3200		3203	
3204		3054	
3055		3058	
3059		3062	Z
3063	Z	3067	
3068		3072	
3073			

FIGURE 14g

NASA LEAN-OUT DATA

TEMP. 100^0F REL. HUM. 0, 30, 60, 80%

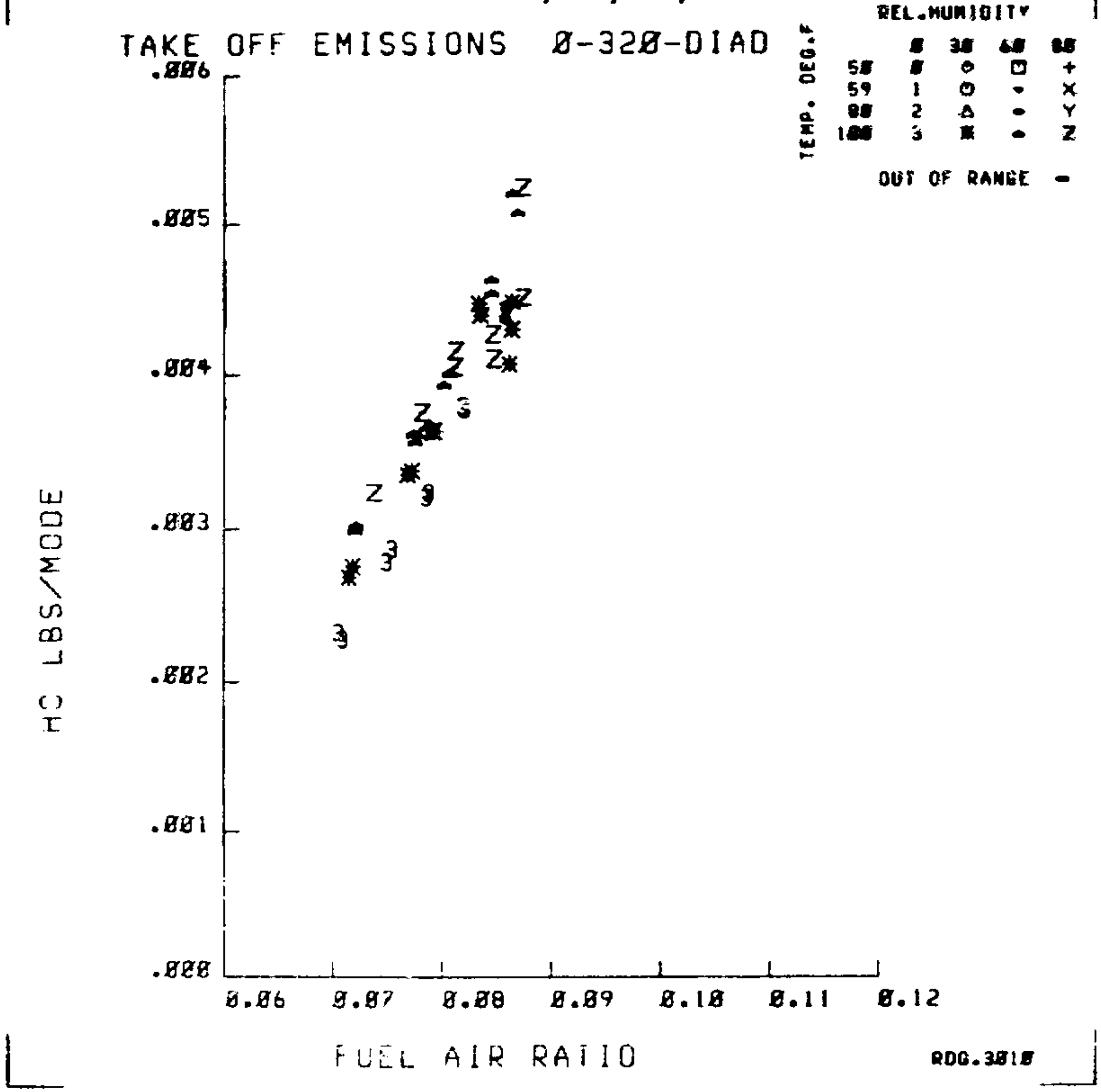

TAKE-OFF	
3010	
3017	
3024	3
3032	
3038	
3121	
3126	
3132	*
3138	
3144	
3150	
3212	
3220	
3229	♠
3239	
3247	
3079	
3085	
3099	Z
3105	

TAKE-OFF	
3014	
3020	
3027	3
3035	
3041	
3123	
3129	
3135	*
3141	
3147	
3209	
3217	
3224	♠
3233	
3240	
3076	
3082	
3090	Z
3102	
3110	

FIGURE 14h

NASA LEAN-OUT DATA

TEMP. 100°F REL. HUM. 0, 30, 60, 80%

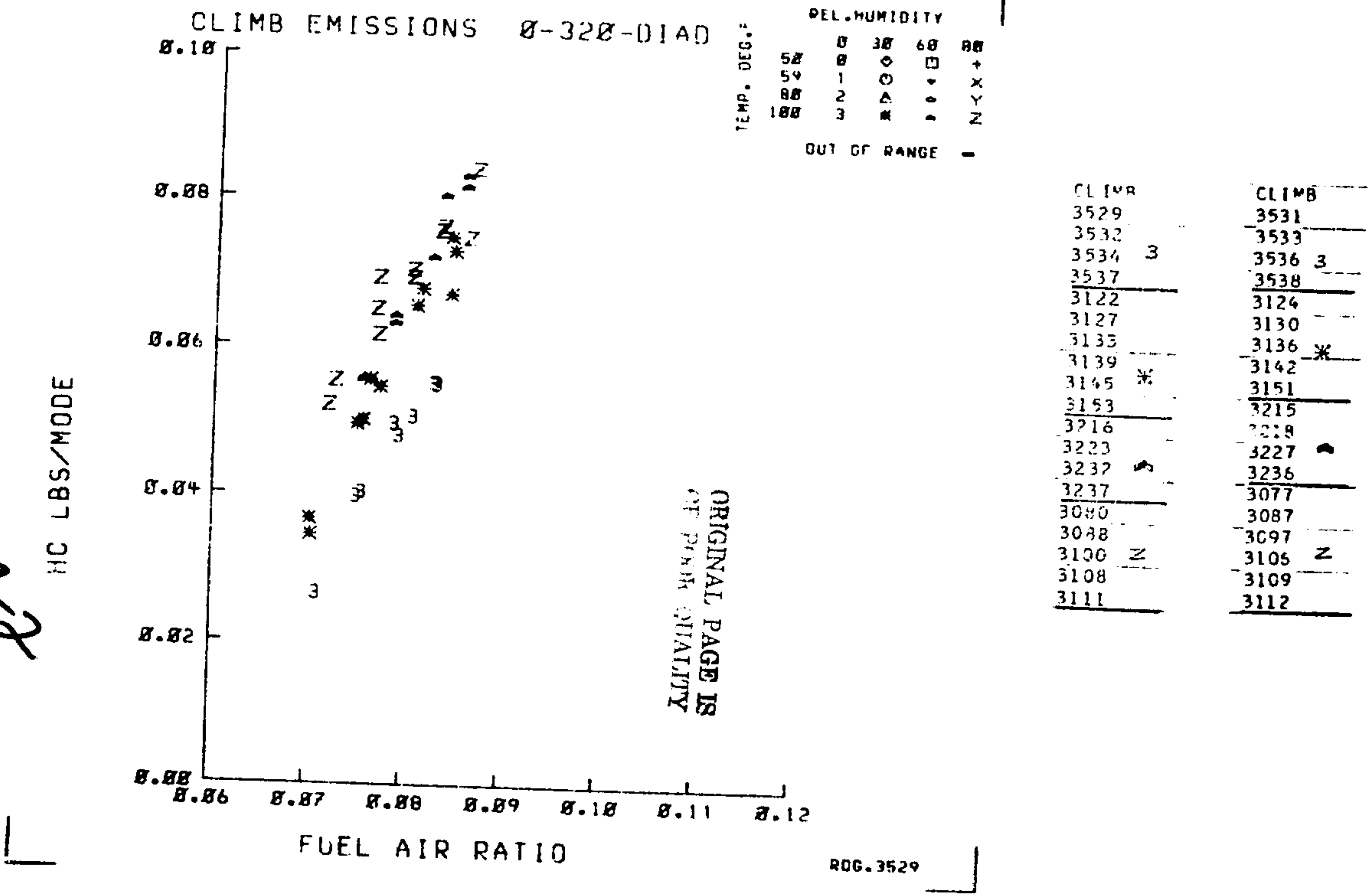

ORIGINAL PAGE IS OF POOR QUALITY

2-

FIGURE 14i

NASA LEAN-OUT DATA

TEMP. 100⁰F REL. HUM. 0, 30, 60, 80%

APPROACH EMISSIONS Ø-32Ø-DIAD

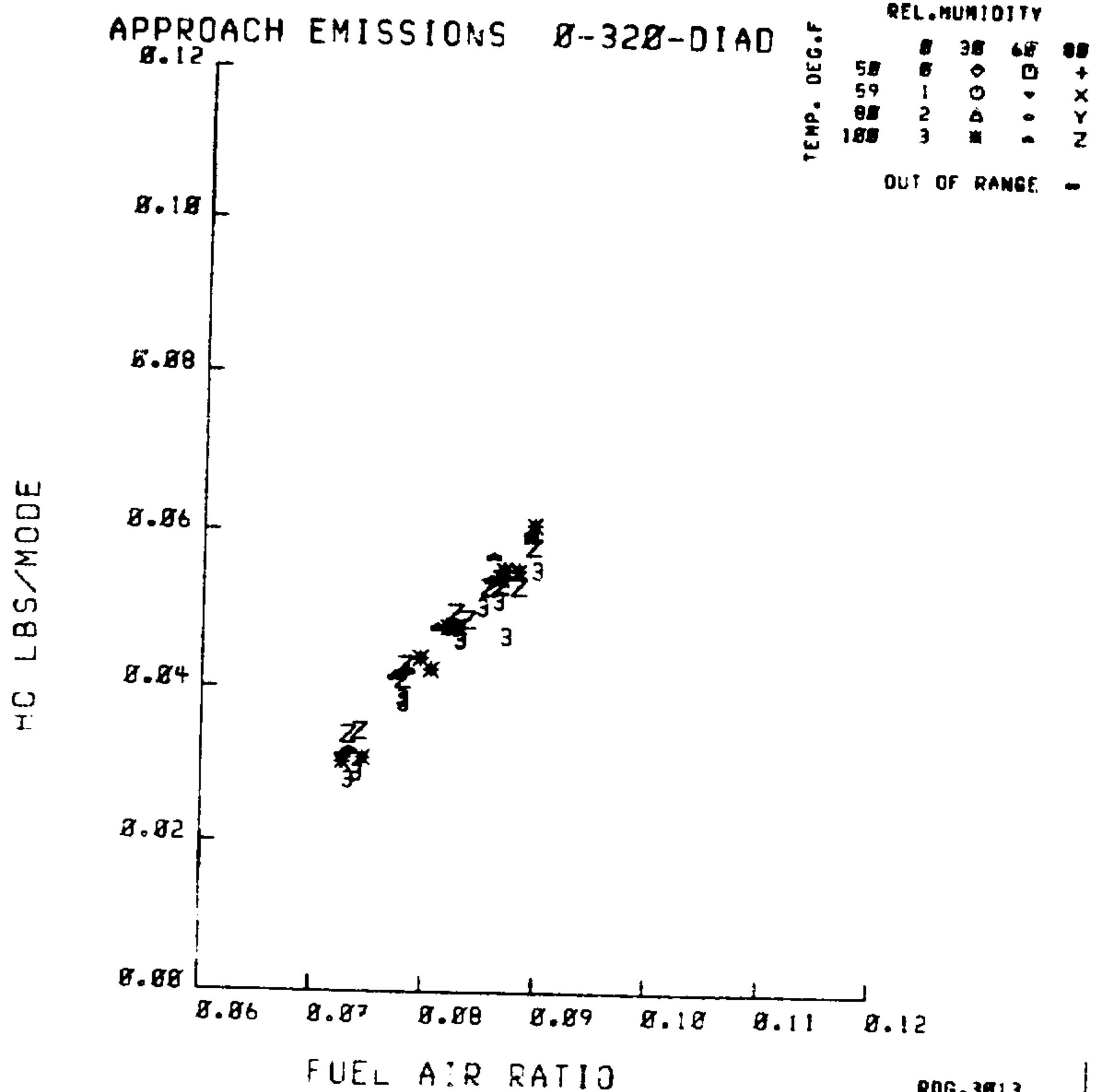

APPROACH		APPROAC	
3013		3016	
3019		3023	
3026	3	3?31	3
3034		30	
3040		30	
3125		3128	
3131		3134	
3137	*	3140	*
3143		3146	
3149		3152	
3211		3214	
3219		3222	
3226		3231	
3235		3238	
3244		3251	
3078		3081	
3084		3089	
3098	Z	3101	Z
3104		3107	
3113		3116	

FIGURE 14j

NASA LEAN-OUT DATA

TEMP. 100°F REL. HUM. 0, 30, 60, 80%

IDLE EMISSIONS 0-320-DIAD

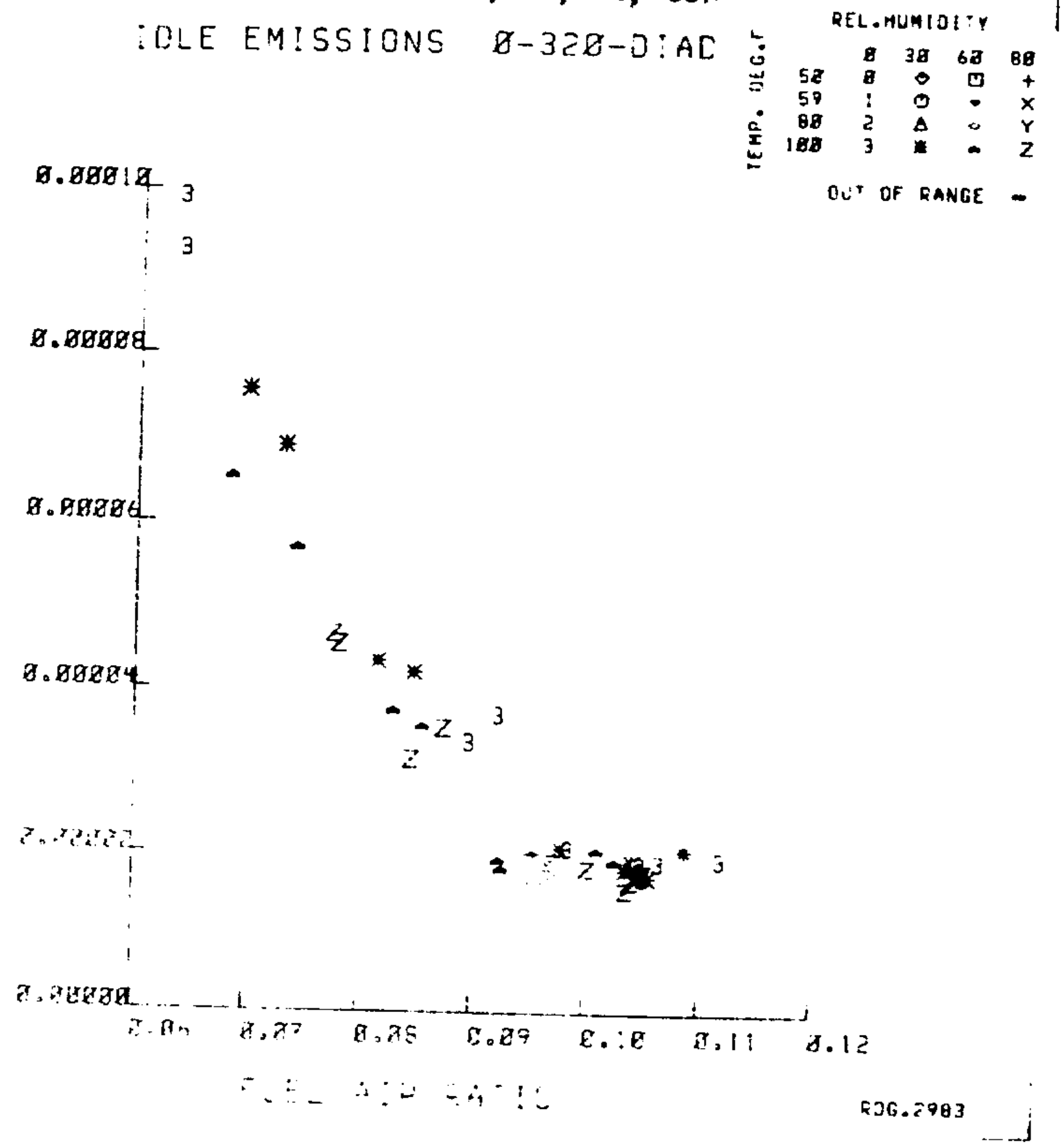

IDLE	
2983	
2990	
2995	3
2999	
3005	
3154	
3158	
3162	*
3166	
3170	
3176	
3184	
3192	▲
3198	
3202	
3053	
3057	
3061	Z
3066	
3071	

IDLE	
2988	
2993	
2998	3
3002	
3008	
3157	
3161	
3165	*
3169	
3173	
3183	
3190	
3195	▲
3201	
3205	
3056	
3060	
3064	Z
3069	
3075	

FIGURE 14k

NASA LEAN-OUT DATA

TEMP. 100^{0}F REL. HUM. 0, 30, 60, 80%

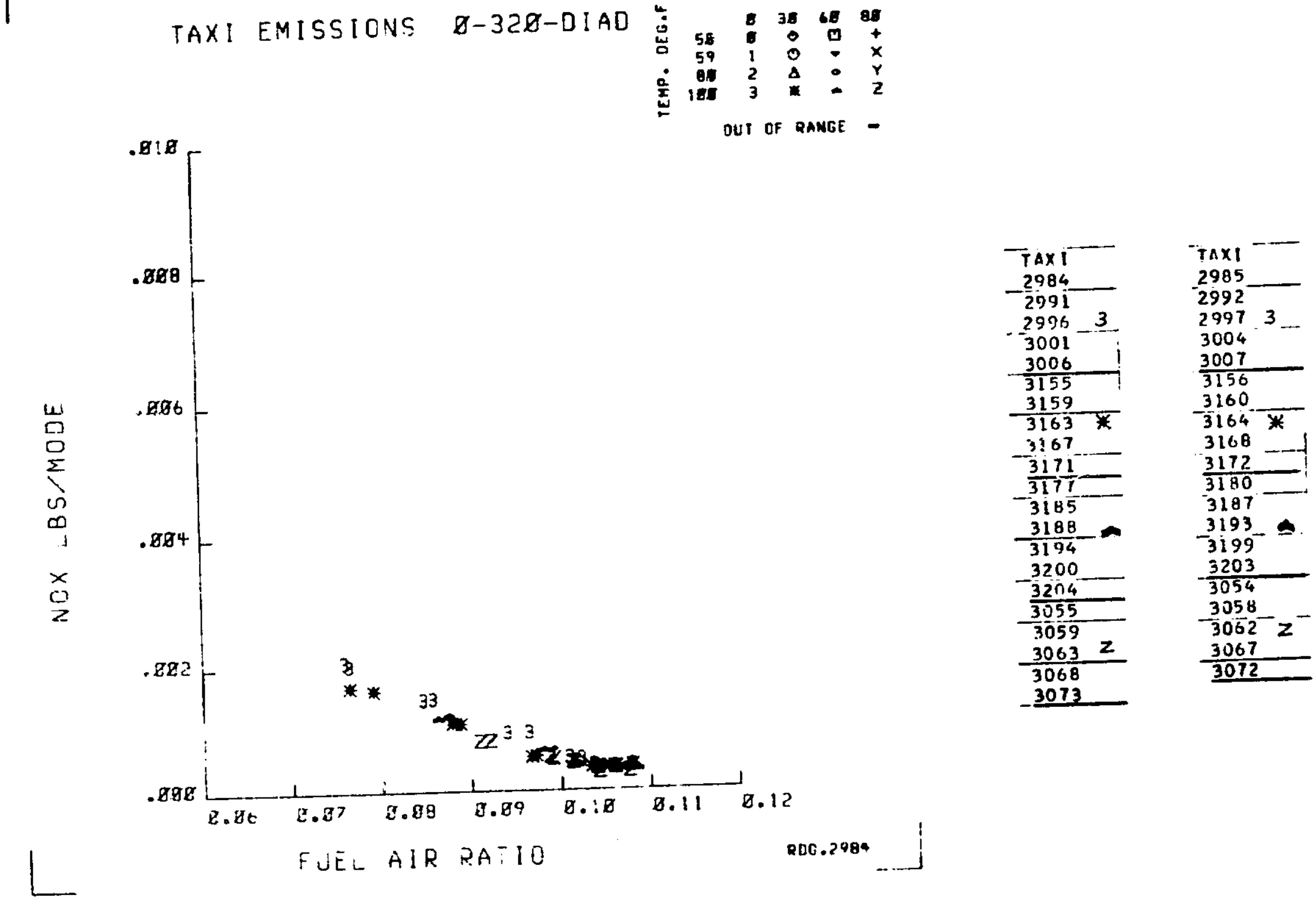

FIGURE 141

NASA LEAN-OUT DATA

TEMP. 100°F REL. HUM. 0, 30, 60, 80%

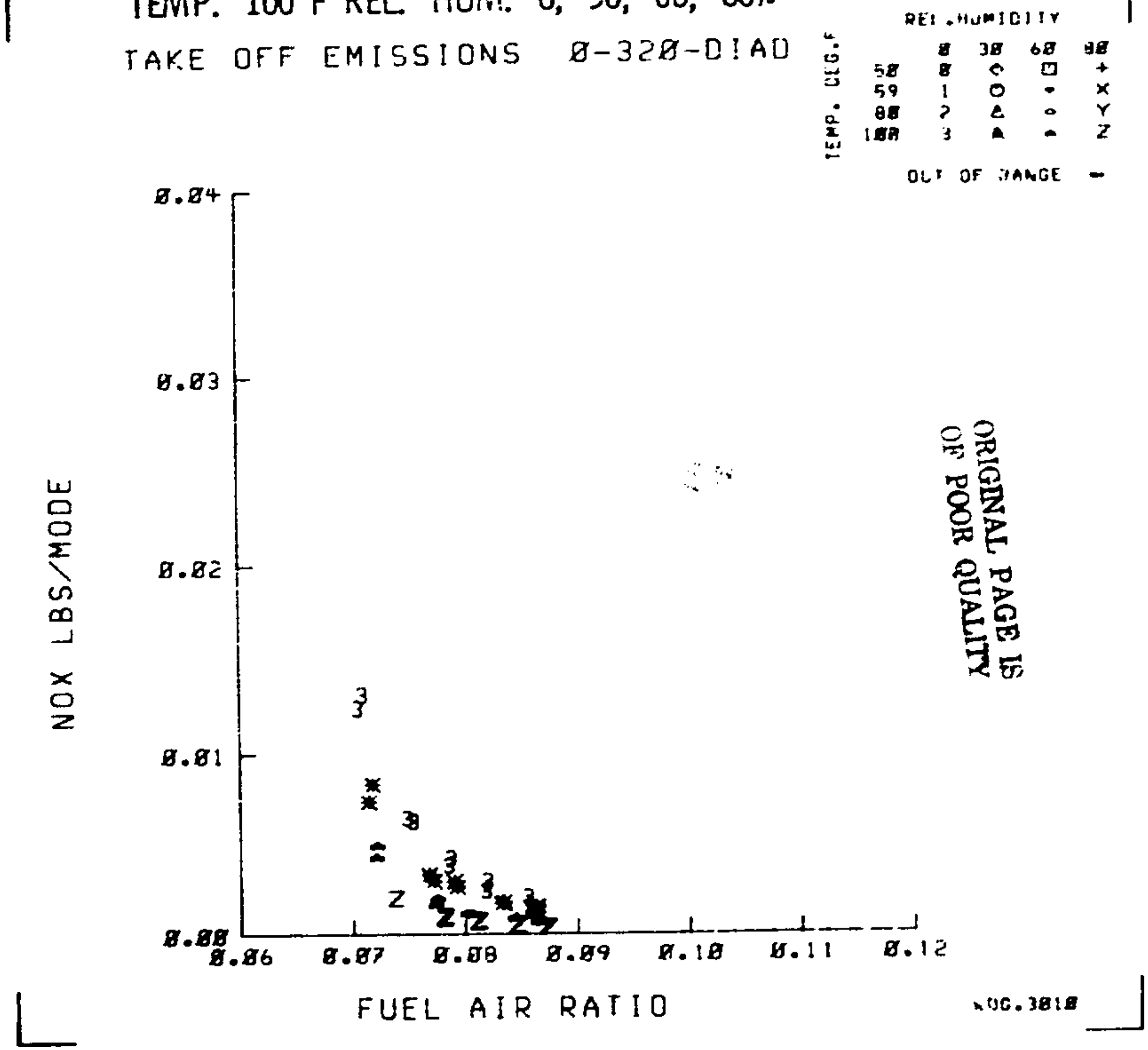

ORIGINAL PAGE IS OF POOR QUALITY

TAKE-OFF		TAKE-OFF	
3010		3014	
3017		3020	
3024	3	3027	3
3032		3035	
3038		3041	
3121		3123	
3126		3129	
3132	*	3135	*
3138		3141	
3144		3147	
3150		3209	
3212		3217	
3220		3224	
3229		3233	
3239		3240	
3247		3076	
3079		3082	
3085	Z	3090	Z
3099		3102	
3105		3110	

FIGURE 14m

NASA LEAN-OUT DATA

TEMP. 100^{0}F REL. HUM. 0, 30, 60, 80%

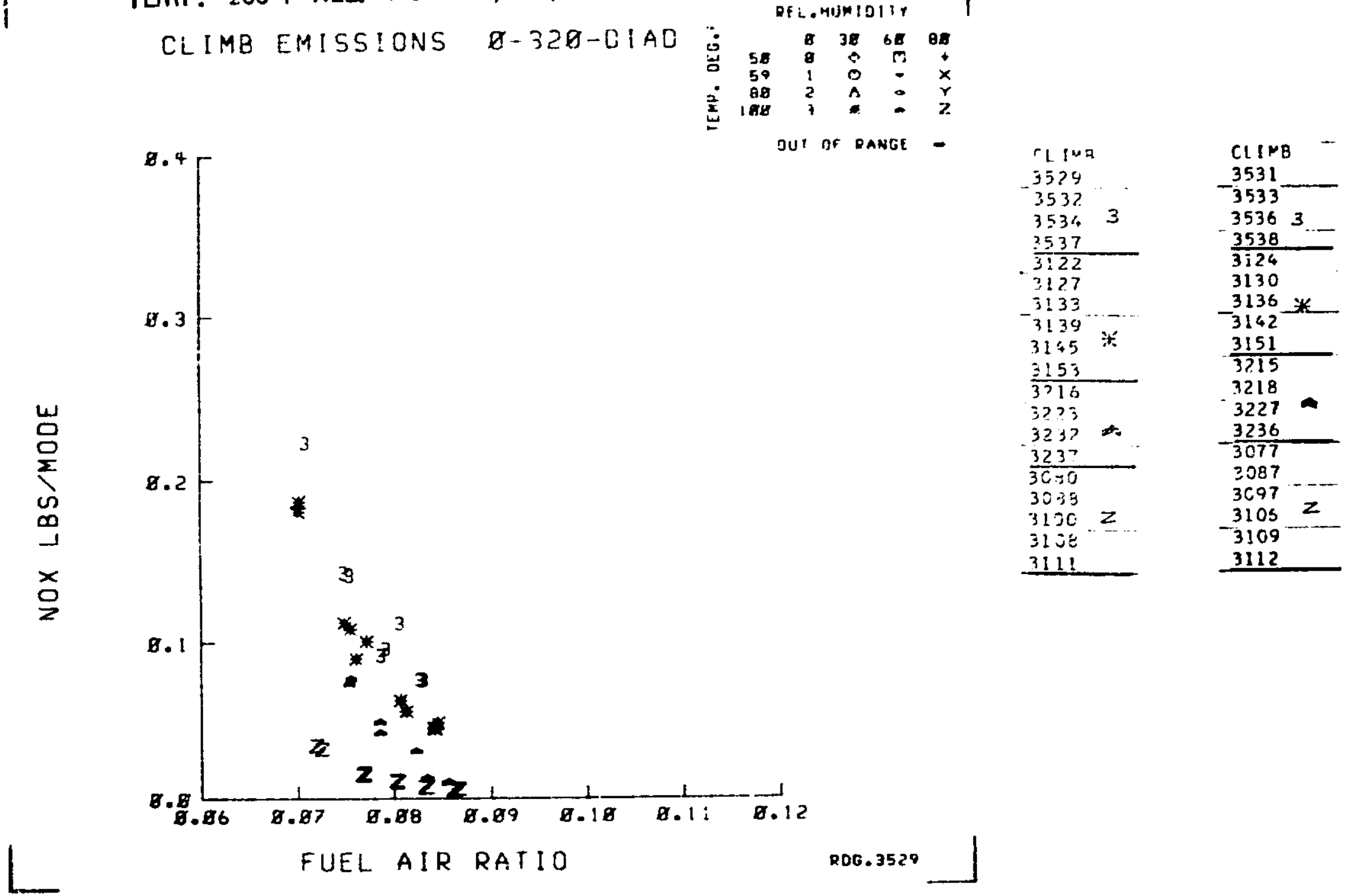

FIGURE 14n

NASA LEAN-OUT DATA

TEMP. 100°F REL. HUM. 0, 30, 60, 80%

APPROACH EMISSIONS 0-320-DIAD

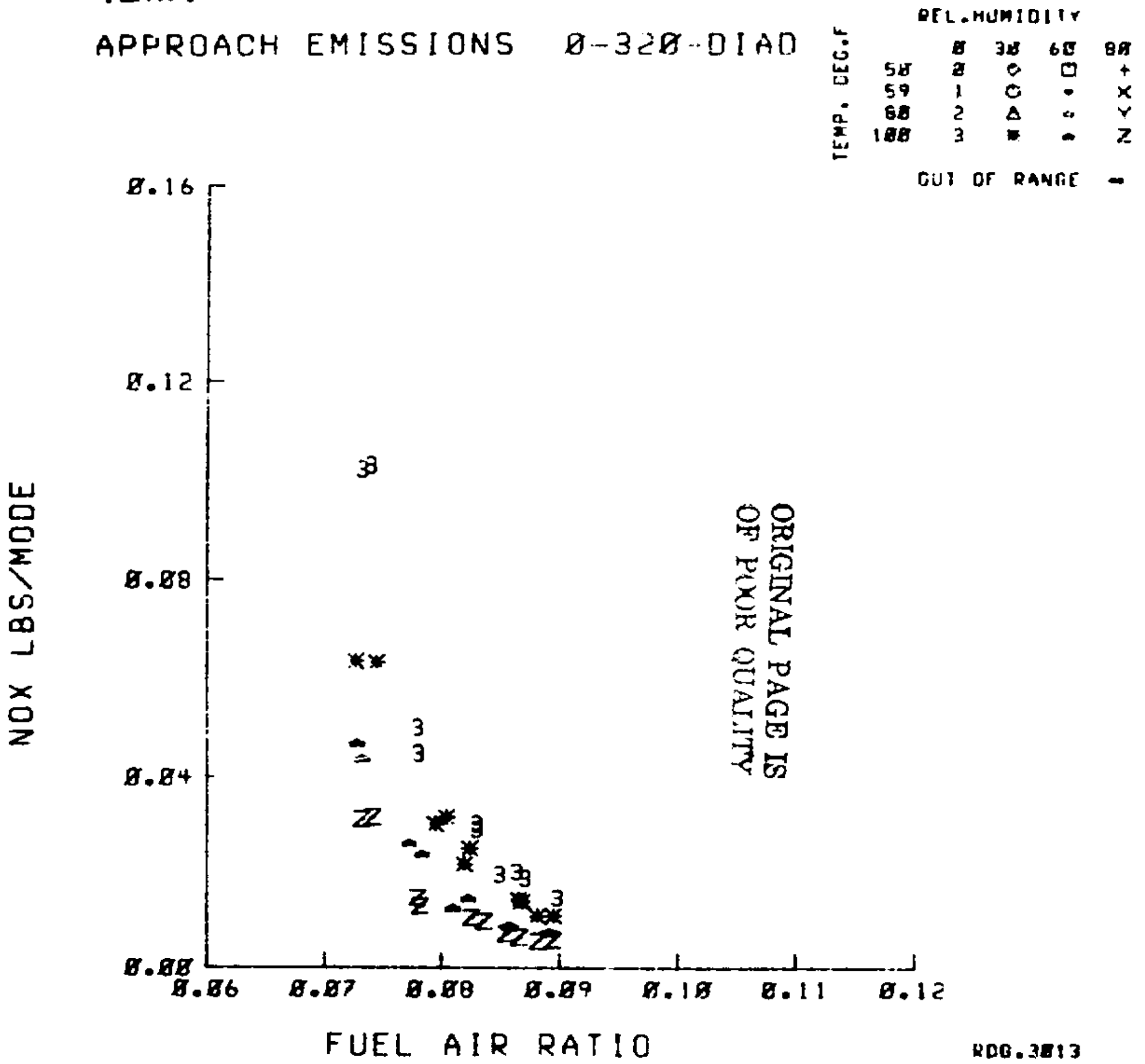

APPROACH		APPROACH	
3013		3016	
3019		3023	
3026	3	3031	3
3034		3037	
3040		3043	
3125		3128	
3131		3134	
3137	*	3140	*
3143		3146	
3149		3152	
3211		3214	
3219		3222	
3224		3231	
3235		3238	
3244		3251	
3078		3081	
3084		3089	
3098	Z	3101	Z
3104		3107	
3113		3116	

FIGURE 140

CO MODAL EMISSIONS VERSUS FUEL-AIR RATIO

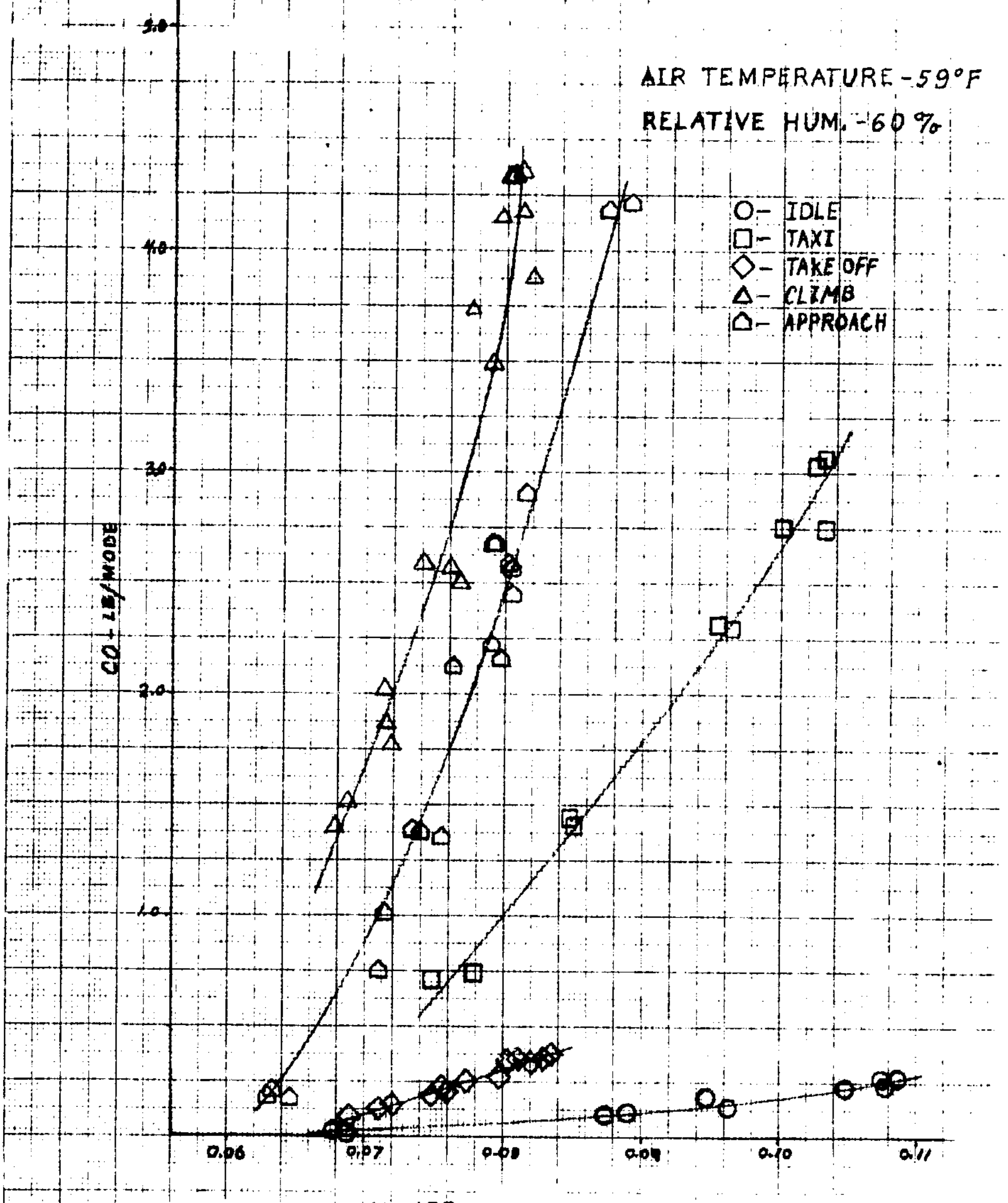

FIGURE 15

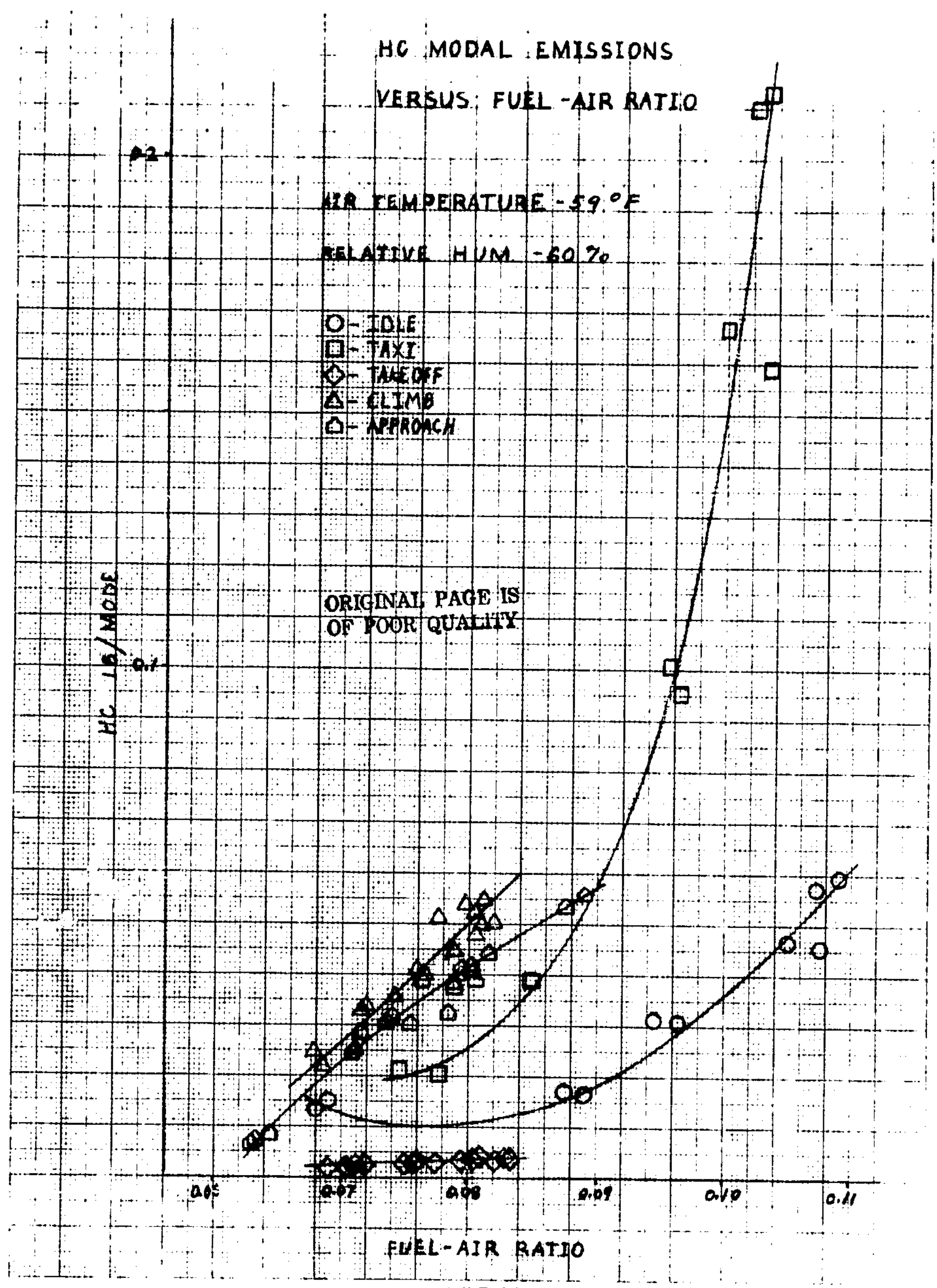

HC MODAL EMISSIONS
VERSUS FUEL-AIR RATIO
AIR TEMPERATURE - 59 °F
RELATIVE HUM. - 60 %
O - IDLE
□ - TAXI
◇ - TAKEOFF
△ - CLIMB
⌂ - APPROACH
ORIGINAL PAGE IS
OF POOR QUALITY
HC lb/MODE
0.2
0.1
0.07
0.08
0.09
0.10
0.11
FUEL-AIR RATIO

FIGURE 16

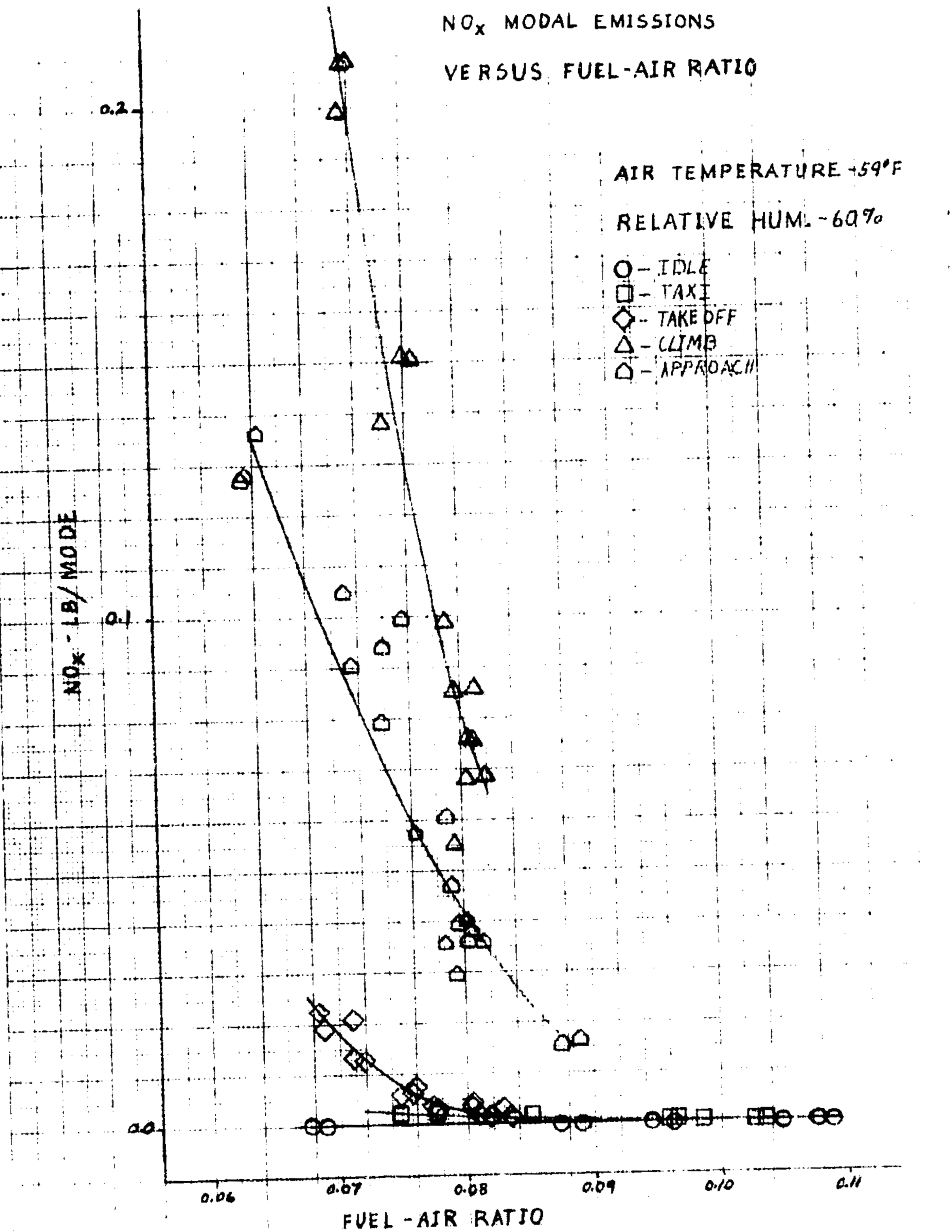

NOx MODAL EMISSIONS
VERSUS FUEL-AIR RATIO
AIR TEMPERATURE -59°F
RELATIVE HUM. -60%
○ - IDLE
□ - TAXI
◇ - TAKE OFF
△ - CLIMB
⌂ - APPROACH
0.2
0.1
0.0
NOx - LB/MODE
0.06
0.07
0.08
0.09
0.10
0.11
FUEL-AIR RATIO

FIGURE 17

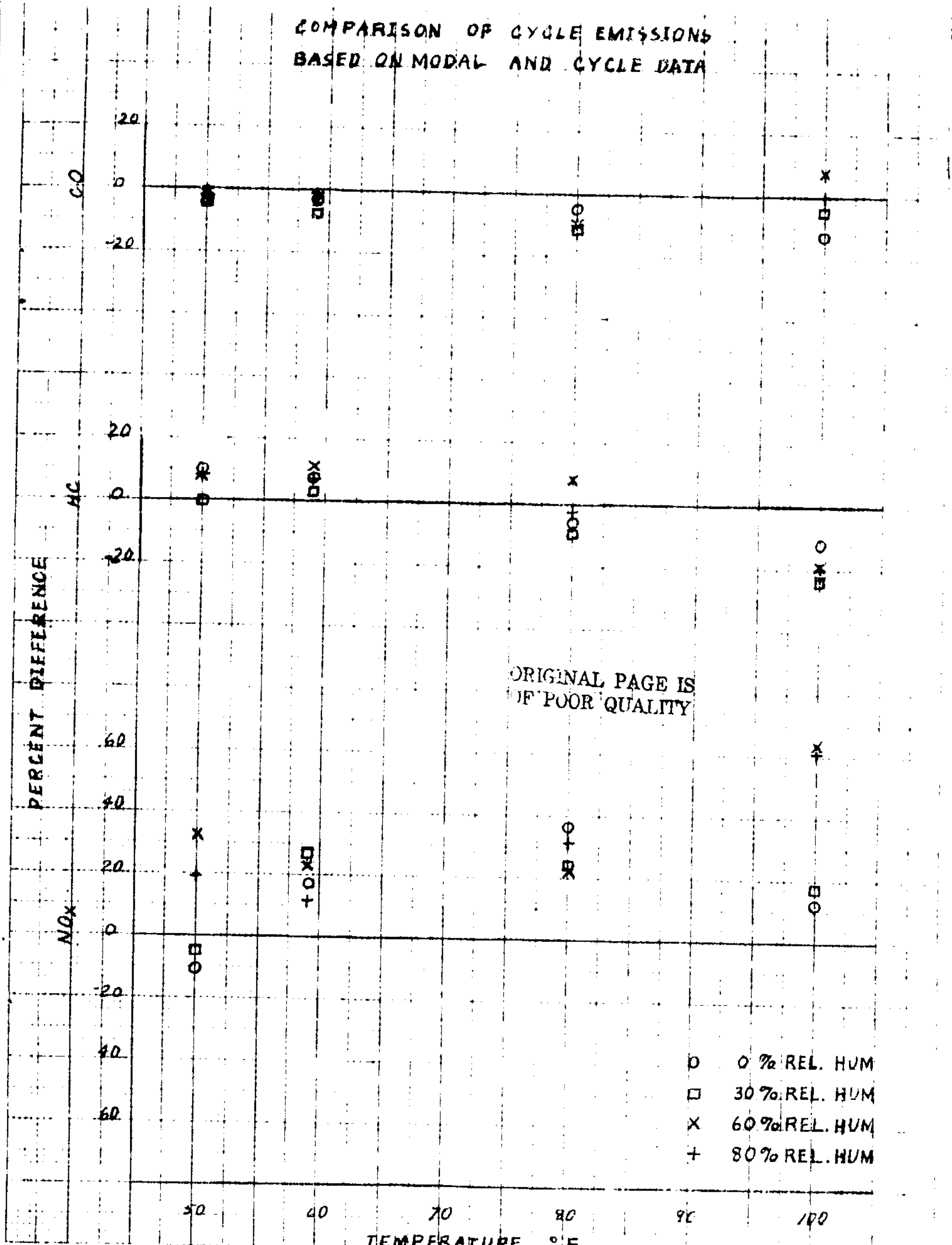

FIG 18

ORIGINAL PAGE IS
OF POOR QUALITY

1. Report No.	2. Government Accession No.	3. Recipient's Catalog No.
NASA TM X-73507, Volume I		

4. Title and Subtitle EFFECT OF AIR TEMPERATURE AND RELATIVE HUMIDITY AT VARIOUS FUEL-AIR RATIOS ON EXHAUST EMISSIONS ON A PER-MODE BASIS OF AN AVCO LYCOMING 0-320 DIAD LIGHT AIRCRAFT ENGINE
VOLUME I - RESULTS AND PLOTTED DATA

5. Report Date

6. Performing Organization Code

7. Author(s)
Michael Skorobatckyi, Donald V. Cosgrove, Phillip R. Meng and Erwin E. Kempke, Jr.

8. Performing Organization Report No.
E-8916-2

9. Performing Organization Name and Address
National Aeronautics and Space Administration
Lewis Research Center
Cleveland, Ohio 44135

10. Work Unit No.

11. Contract or Grant No.

12. Sponsoring Agency Name and Address
National Aeronautics and Space Administration
Washington, D.C. 20546

13. Type of Report and Period Covered
Technical Memorandum

14. Sponsoring Agency Code

15. Supplementary Notes

16. Abstract
A carbureted four-cylinder air-cooled 0-320 DIAD Lycoming aircraft engine was tested to establish the effects of air temperature and humidity at various fuel-air ratios on the exhaust emissions on a per-mode basis. The test conditions included carburetor lean-out at air temperatures of 50^{o}, 59^{o}, 80^{o}, and 100^{o} F at relative humidities of 0, 30, 60, and 80 percent. Temperature-humidity effects at the higher values of air temperature and relative humidity tested indicated that the HC and CO emissions increased significantly, while the NO_x emissions decreased. Even at a fixed fuel-air ratio, the HC emissions increase and the NO_x emissions decrease at the higher values of air temperature and humidity. The report is divided in two volumes: Volume I contains the results and plotted data, and Volume II contains the data taken at each of the individual test points. (The data of Volume II are included on microfilm in a pocket at the back of Volume I.)

17. Key Words (Suggested by Author(s))	18. Distribution Statement
Aircraft piston engine Exhaust emissions Ambient condition effects	Unclassified - unlimited STAR Category 07

19. Security Classif. (of this report)	20. Security Classif. (of this page)	21. No. of Pages	22. Price*
Unclassified	Unclassified		

* For sale by the National Technical Information Service, Springfield, Virginia 22161